Seafloor analysis based on multibeam bathymetry and backscatter data

Meeresbodenanalyse auf Basis von Bathymetrie und akustischer Rückstreuung

---

Andreas Beyer

Ber. Polarforsch. Meeresforsch. 540 (2006)
ISSN 1618 - 3193

Andreas Beyer

Alfred Wegener Institute for Polar and Marine Research
P.O.B. 12 0161
27515 Bremerhaven
Germany

Die vorliegende Arbeit ist die inhaltlich unveränderte Fassung einer Dissertation zur Erlangung des Doktorgrades der Naturwissenschaften im Fachbereich Geowissenschaften der Universität Bremen.

Die elektronische Version dieses Dokumentes enthält Farbabbildungen und kann bezogen werden unter:
http://www.awi-bremerhaven.de • Publikationen

Content

List of Figures and Tables

Abstract

Large areas of the world's oceans are still unexplored. Previously unknown structures and ecosystems are discovered due to the increasing exploration of the oceans, in particular at the continental margin and the continental shelf. Research is essential to understand these structures and to analyze their potential and importance for human society and the ecosystem. This PhD thesis is one part of multidisciplinary research at the European continental margin. Hydroacustic methods were applied in order to identify and distinguish different seabed structures and facies.

Hydroacustic techniques are an established approach to analyze the seafloor. Echo intensity was used in this study for interpretation in addition to the travel time of the acoustic signal. The ship-borne multibeam system Hydrosweep DS-2 and the sub-bottom profiler Parasound were used for data recording.

The investigation areas of this study comprise the Håkon Mosby mud volcano situated at the Norwegian-Barents-Svalbard continental margin and the carbonate mounds in the Belgica mound province together with adjacent channels situated in the Porcupine Seabight at the Irish continental margin. Mud volcanoes and carbonate mounds are characterized by active sediment and transport processes and are related to the existence of subsurface hydrocarbon, mainly methane. Seafloor channels indicate sediment transport in lateral and vertical direction. These structures are focus of recent research due to the contribution of methane to the carbon cycle.

A terrain model of the Håkon Mosby mud volcano was created providing the basis for detailed studies which require precise positioning for sampling and observation devices. The fine structure of the mud volcano was mapped by dense survey lines and overlapping swathes. The Håkon Mosby mud volcano is located at a water depth of about 1270 m and can be separated into three morphological segments: weak, crater-like center (950 m diameter, 12 m height), circular embankment (1350 m diameter, 100 m breadth, 2 m height) and the area influenced by mud volcanism which is characterized by a reduced surface slope compared to the general margin (2500 m diameter).

Investigations of the Belgica mound province show that the carbonate mounds occur in a depth range between 1000 m and 700 m. They are aligned along the margin and show heights of about 50 m up to 100 m maximum. Their morphology resembles ellipses with axes ranging from 0.5 km to 1.0 km and from 1.0 km to 1.5 km, respectively, ridge-like mounds or terrace-like structures. Other morphological properties comprise steep surface slopes of about 20° and depressions at the foot of some mounds having variable depths up to 50 m. This morphology is different from other mound provinces in the Porcupine Seabight. Carbonate mounds proposed south of the Belgica province in the Gollum Channel System were not evidenced by this study.

In addition to the morphology of the seabed structures, acoustic backscatter data were analyzed in the study areas. The Håkon Mosby mud volcano shows strong backscatter at the central area in contrast to reduced backscatter at the surrounding, circular depression. This might be due to gas occurrence in the sediment and high surface roughness at the central crater. Soft and homogeneous sediments with low

surface roughness are expected at the surrounding moat. The eastern part of the mud volcano, however, shows spatially different variability of morphology and backscatter data.

Angular backscatter data of the individual depth measurements were analyzed in the Porcupine Seabight area. Segments of the seafloor of different acoustical properties were separated based on morphology and angular backscatter data. These segments were studied with respect to the parameters mean angular response, slope and variation of the angular backscatter data. Seabed facies like surface mounds, buried mounds, channels and inter-channel areas were characterized and distinguished. First information on the seabed variability is now available to select specific sample locations.

The maps showing the spatial distribution of the backscatter data indicate sediment transport at the seabed by lineated structures. These structures occur in the vicinity of the carbonate mounds in the Porcupine Seabight and point to seabed currents with an oblique direction to the continental slope. Backscatter data at the Håkon Mosby mud volcano show that the outflowing material is transported down slope, probably by bottom currents or gravity.

Zusammenfassung

Weite Teile des Meeresbodens sind noch unerforscht und beherbergen unbekannte Strukturen und Ökosysteme. Mit fortschreitender Nutzung der Ozeane und speziell der Schelfgebiete und Kontinentalränder werden diese Strukturen entdeckt. Um deren Bedeutung und Potential für Ökosystem und Menschheit ableiten zu können, ist es notwendig, diese Strukturen zu erforschen. Die vorliegende Arbeit liefert einen Beitrag im Rahmen multidisziplinärer Forschung am europäischen Kontinentalhang. Es wurden hydroakustische Methoden verwendet, um unterschiedliche Strukturen am Meeresboden und sedimentologische Fazien abzugrenzen und zu unterscheiden.

Die Verwendung von hydroakustischen Daten für die Analyse des Meeresbodens ist ein etabliertes Verfahren. Neben der Laufzeit des akustischen Signals wurde in dieser Arbeit die Echointensität für die Interpretation verwendet. Das schiffsgebundene Fächerecholot-System Hydrosweep DS-2 und das Sedimentecholot Parasound dienten dabei als Erfassungsgeräte.

Die Untersuchungsgebiete dieser Arbeit sind der Håkon Mosby Schlammvulkan am Norwegen-Spitzbergen-Kontinentalhang in der Barentssee sowie die Karbonathügel der Belgica Provinz und Kanäle am irischen Kontinentalhang in der Porcupine Bucht. Schlammvulkane und Karbonathügel sind durch aktive Sedimentations- und Transportprozesse gekennzeichnet und stehen im Zusammenhang mit Kohlenwasserstoffvorkommen, hauptsächlich Methan. Kanalstrukturen weisen auf Transportprozesse hin, die Sediment am Kontinentalhang in horizontaler und vertikaler Richtung umlagern. Aufgrund des Beitrags von Methan zum Kohlenstoffkreislauf sind diese Strukturen Blickpunkt aktueller Forschung.

Am Håkon Mosby Schlammvulkan wurde ein Geländemodell generiert, das die Grundlage für detaillierte multidisziplinäre Forschung liefert und die genaue Positionierung von Beprobungs- und Beobachtungseinrichtungen ermöglicht. Durch mehrfach überlappende Vermessungslinien und eine sorgfältige Datenanalyse wurde

die flache und kleinräumige Struktur des Schlammvulkans kartiert. Er befindet sich in einer Wassertiefe von etwa 1270 m und lässt sich in drei morphologische Zonen unterteilen: ein flaches, kraterartiges Zentrum von 950 m Durchmesser und 12 m Höhe, ein ringförmiger Damm von 1350 m Durchmesser, 100 m Weite und 2 m Höhe sowie das Einflussgebiet des Håkon Mosby Schlammvulkans mit einem Durchmesser von 2500 m, dass durch eine geringere Bodenneigung im Vergleich zum Kontinentalhang gekennzeichnet ist.

Untersuchungen der Belgica-Provinz zeigen, dass die Karbonathügel in einem Tiefenbereich zwischen 1000 m und 700 m vorkommen. Sie sind entlang des Kontinentalhanges ausgerichtet und weisen Höhen um 50 m bis maximal 100 m auf. Die morphologische Ausprägung variiert zwischen einzelnen, ellipsoidischen Hügeln mit Achsenlängen von 0,5-1,0 km und 1,0-1,5 km, rückenartigen sowie terrassenförmig angeordneten Hügeln. Gräben am Fuß einiger Hügel mit Tiefen von einigen Metern bis maximal 50 m sowie steile Hangneigungen um 20° sind weitere morphologische Eigenschaften. Damit steht die Morphologie der Belgica-Provinz im Gegensatz zu anderen Hügelprovinzen in der Porcupine Bucht. Karbonathügel, die im Gollum-Kanalsystem südlich der Belgica-Provinz vermutet wurden, konnten in dieser Studie nicht bestätigt werden.

Neben der Analyse der Morphologie der betrachteten Strukturen wurden die akustischen Rückstreudaten der Untersuchungsgebiete ausgewertet. Der Håkon Mosby Schlammvulkan weist eine sehr starke Rückstreuung im Zentralbereich auf, im Gegensatz zu deutlich verringerter Rückstreuung der umgebenden, ringförmigen Mulde. Ursachen hierfür können im vorhandenen Gas im Sediment des Kraterzentrums sowie in erhöhter Oberflächenrauhigkeit liegen. In der Mulde werden hingegen weiche, homogene Sedimente mit geringer Oberflächenrauhigkeit erwartet. Allerdings zeigt sich im östlichen Teil des Schlammvulkans, dass Morphologie und Rückstreuung eine unterschiedliche räumliche Variabilität aufweisen.

Im Bereich der Porcupine Bucht wurden die einfallswinkelabhängigen Rückstreuwerte der einzelnen Tiefenmessungen analysiert. Auf Basis von Morphologie und akustischer Rückstreuung ließen sich Meeresbodensegmente mit unterschiedlichen Rückstreueigenschaften abgrenzen. Diese wurden anhand der Parameter Stärke, Neigung und Variabilität der einfallswinkelabhängigen Rückstreudaten quantifiziert. Sedimentologische Fazien wie Oberflächenhügel, zusedimentierte Hügel, Kanäle und Zwischen-Kanalgebiete wurden daraufhin charakterisiert und abgegrenzt. Damit stehen erste Informationen über die Variabilität des Meeresbodens und die Sedimentbeschaffenheit zur Verfügung, um gezielt Beprobungsstationen auszuwählen.

In der flächenhaften Darstellung der akustischen Rückstreuung beider Gebiete sind linienhafte Strukturen abgebildet, die auf Transportprozesse hinweisen. In der Porcupine Bucht verlaufen diese Strukturen in direkter Umgebung der Karbonathügel und deuten auf Bodenströmungen mit schrägem Winkel zum Kontinentalhang hin. Am Håkon Mosby Schlammvulkan zeigen die Rückstreudaten ausgeflossenes Material an, das durch Bodenströmung oder Gravitation hangabwärts transportiert wurde.

INTRODUCTION

1 Introduction

This thesis concentrates on the description of morphological features and sedimentary facies at two different locations at the slope of passive continental margins in the Atlantic and the Arctic Ocean: (i) the Håkon Mosby mud volcano located at the Norwegian-Barents-Svalbard continental margin (Figure 1-1), and (ii) the carbonate mounds in the Belgica province together with adjacent channels at the eastern slope of the Porcupine Seabight, west of Ireland (Figure 1-2). The data analyzed in this study were acquired during the RV *Polarstern* expeditions ANT XVII/4 and ARK XIX/3 (Kuhn, in preparation; Klages et al., 2004).

Both locations, i.e. mud volcanoes and carbonate mounds, are related to fluid migration and hydrocarbon occurrence in seabed sediments. They are a major focus of international multidisciplinary research investigating the development and structure of these features (e.g. Henriet et al., 1998; Vogt et al., 1999b). However, for the Håkon Mosby mud volcano, the existence of gas hydrates and free gas is evident, whereas for

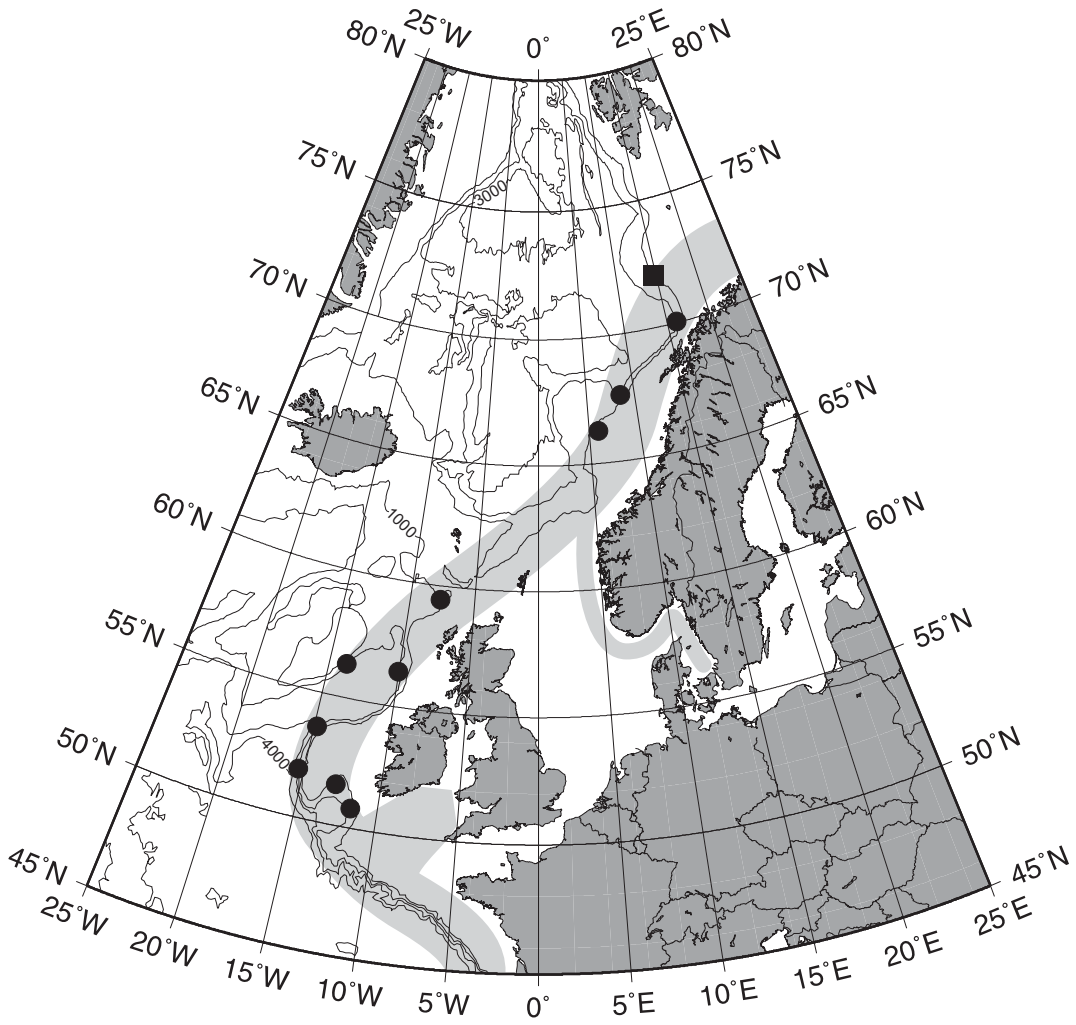

Figure 1-1. Distribution of carbonate mounds (solid black) and cold water coral reefs (light gray) at the European continental margin (after Freiwald and Roberts, 2005). The location of the Håkon Mosby mud volcano is given as square. Bathymetry is indicated by 1000 m contour lines (GEBCO, 1997).

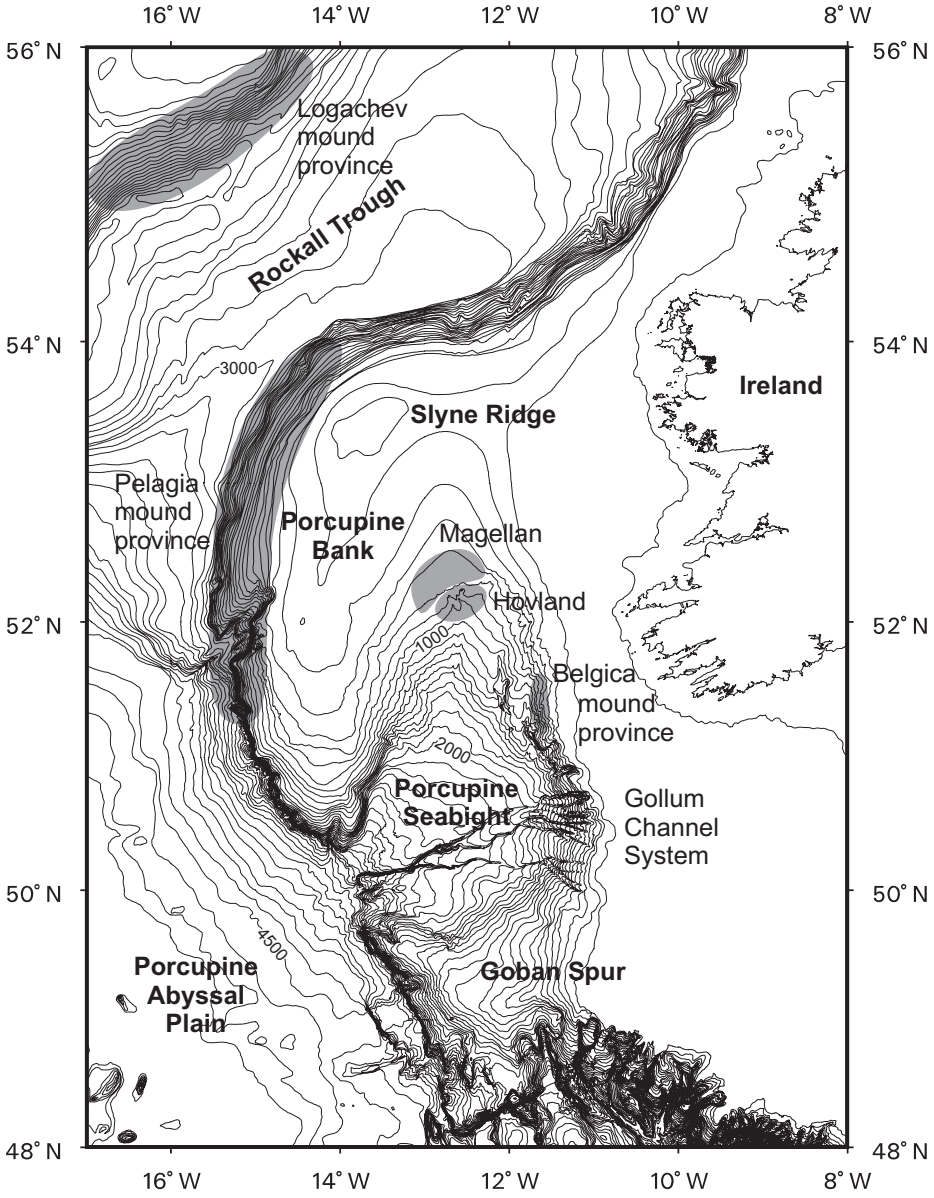

Figure 1-2. Regional settings and locations of carbonate mound provinces west off Ireland (after Freiwald and Roberts, 2005). Bathymetry is indicated by 100 m contour lines (GEBCO, 1997).

the Belgica province the relation between gas occurrence and the development of carbonate mounds is under discussion (Van Weering et al., 2003a).

Seeping gas, mainly methane, contributes to the global carbon cycle. Structures correlated with methane seepage have, thus, attracted attention of a broad scientific community, and intense research has been carried out during recent years (e.g. Hovland and Judd, 1988; Hovland and Thomsen, 1997; Milkov et al., 2003 and references therein). Furthermore, very specialized species and communities have been discovered which feed on migrating gas (e.g. Pimenov et al., 1999; Boetius et al., 2000; Gebruk et al., 2003; Levin et al., 2003).

Processes initiated during sediment accumulation, transport, redistribution, and fluid migration create distinct seabed structures. These structures can be observed and in turn indicate sediment transport. They also help to obtain insight into the internal structure of the sediments.

The study sites for this thesis are focal locations for researchers from several scientific disciplines. Scientists working in the fields of geology, biology, geochemistry, geophysics and oceanography combine their results to obtain comprehensive data sets and interpretations of the area. Detailed recording and mapping of surface structures is essential for the multidisciplinary scientific community to establish and integrate data. The most common limitation for comprehensive interpretation is the lack of this type of coordinated data effort.

Global available bathymetric data show a spatial resolution that is too coarse to show the small scale seabed structures analyzed in this study. Bathymetric data determined from satellite altimetry (resembling gravity anomalies) typically provide 2 arc-minutes horizontal resolution (ETOPO-2 based on Smith and Sandwell, 1997). In contrast, the GEBCO global data set is based on bathymetric measurements (GEBCO, 1997). The vertical resolution of the available depth contours in deep water is 100 m. However, depth information may be doubtful in areas occasionally visited by survey vessels due to large distances between the survey lines. For scientific demands detailed bathymetric data need to be acquired which result in a homogenous high resolution data set. Global and previously available data of lower resolution are used in this study to narrow the area of investigation and to adjust the planning of the bathymetric surveys (GEBCO, 1997; Ginsburg et al., 1999; Lemke, 2003).

The seafloor studies of this thesis are based on hydroacoustic techniques. The data analyzed represent acoustic measurements of the ship-borne hull mounted multibeam echo sounding system Hydrosweep DS-2 and the sub-bottom profiler Parasound (Gutberlet and Schenke, 1989; Grant and Schreiber, 1990). These data consist of depth and echo intensity data as well as sediment stratigraphy information.

1.1 Aims of this thesis

The locations studied in this thesis represent areas related to gas discharge and gas hydrate occurrence at the Norwegian-Barents-Svalbard continental margin, i.e. the Håkon Mosby mud volcano (Figure 1-1), and at the eastern slope of the Porcupine Seabight (Irish shelf), i.e. the carbonate mounds in the Belgica province and adjacent channels (Gollum Channel System) (Figure 1-2). Detailed bathymetric information of such carbonate mounds and gas related mud volcano structures are of fundamental interest to a broad interdisciplinary research community, forming the basis for geological, geophysical, biological, biogeochemical and ecological studies. Mapping and analyzing seabed structures forms the basis for investigating sedimentary processes. The recent status of research related to carbonate mounds and mud volcanoes was the motivation for studying the key locations analyzed in this thesis.

The aims of this thesis are:

- to provide detailed bathymetric terrain models and charts of the study areas that allow mapping of geological and ecological provinces and function as background maps against which future changes in these areas can be tested,
- to evaluate the performance of multibeam data to determine seabed sediment characteristics with special emphasis on sedimentological interpretation of hydrocarbon related seabed structures,

- to estimate the applicability of multibeam bathymetry and backscatter data to determine spatial and temporal variability of surface seabed matter at different regional scales,
- to evaluate the quality of multibeam angular backscatter data as a means of mapping geological provinces continuously and more efficiently than can be done using sample information of surface sediments only.

The results of these issues are important for future experiments and studies which need precise information about the seabed and its surface variability.

1.2 Outline and structure of this thesis

This first chapter of this thesis gives a general introduction to the aims and purpose of this study.

Chapter two gives a short introduction into the regional settings of passive continental margins and focuses on geology and ecosystem of the seabed structures analyzed in this study, i.e. the Håkon Mosby mud volcano and carbonate mounds in the Porcupine Seabight.

The methods of seabed investigations by means of acoustic sensors as used in this study are described in chapter three with special emphasis on bathymetric depth measurement (section 3.2) and multibeam angular backscatter data (section 3.3). This chapter also provides the background of the necessity of bathymetric investigations as basic information for marine sciences.

Chapter four describes the bathymetric structure of the Håkon Mosby mud volcano. It concentrates on the morphological setting of this relatively small feature which became a major focus to study processes related to deep water mud volcanism. The data set provides detailed depth information for various scientific studies that need accurate position information within the study area. Morphology and echo intensity data are discussed in relation to the structure of the mud volcano.

Chapter five analyses the eastern slope of the Porcupine Seabight situated on the Irish shelf. It focuses on the occurrence of carbonate mounds in the Belgica mound province in the northern part of the study area and on the Gollum Channel System in the south. It describes the morphology of the mounds and channels, their variability and spatial occurrence. Mounds rising from the seabed and buried mounds are distinguished and described in detail. Data of another mound province in the area of the Porcupine Seabight provides information for comparison. It also contains a map that shows the bathymetry of the area in detail. The map is scaled down in this thesis due to reproduction issues (Figure 5-6), but it can be found in full size in Beyer et al. (2003b).

Chapter six focuses on acoustic multibeam angular backscatter data and provides methods for seabed analysis. It discusses the echo intensity of the multibeam sonar signal that was acquired during the survey described in chapter four. The backscatter data is used for seafloor investigations and gives details on the seabed surface. Seabed segmentation is proposed for the study area and cannot be done based solely on bathymetry. The mound and channel areas at the eastern slope of the Porcupine Seabight are target areas for segmentation. A major focus lies on submarine channels

that were recorded south of the Belgica mound province.

Chapter seven gives a general summary of chapters three to five and focuses on answering the points raised in section 1.1. It furthermore gives an overview of outstanding problems and questions that could form the focus of future research.

This thesis contains the original text, figures and tables of three articles that were submitted to international peer-reviewed journals. The first manuscript (printed in chapter four) was published by Marine Geophysical Researches (Springer, The Netherlands; Beyer et al., 2005b). The second manuscript (chapter five) was published by Marine Geology (Elsevier, The Netherlands; Beyer et al., 2003b). The article printed in chapter six was published by the International Journal of Earth Sciences (Geologische Rundschau, Springer, Germany; Beyer et al., 2005a). Due to the cumulative form of this thesis, repetitions within the text cannot completely be avoided.

2 Regional settings of the study areas

The continental margins adjacent to the Atlantic and Arctic Ocean are characterized as passive continental margins. During the last decades, passive continental margins have become more and more important for the human society due to their ecological and economical potential. Passive continental margins represent the transition zone from continental to oceanic crust and are normally characterized by thick stratified sediments. Tectonic activity is low because of the absence of collisional, subductive or transform plate boundary plate motions.

Passive continental margins play a key role in the world's sedimentary cycle being one of the major depositional areas for both lithogenic and organic material. Riverine sedimentary material accumulates at the continental margin and is, partially, redistributed and transported further to the deep sea, for example by bottom currents. Mass flows (e.g. turbidity currents, gravity flows) are another major process that transports sedimentary matter from the continental shelf down to the deep sea exemplifying lateral and vertical transport processes. Their activity can result in the formation of submarine channels. Fluid migration within the sediment can also contribute to the sediment redistribution.

Nutrients brought by the rivers allow enhanced primary productivity at passive continental margins, leading to highly developed, rich ecosystems that are nowadays exploited for example by the fishery industry. Enhanced primary productivity also leads to enhanced burial of organic matter in the sediment. Early diagenetic processes at the sediment-water interface and within the sediment result in alteration of the accumulated material. Due to the accumulation and burying of terrigeneous and biogenic material, hydrocarbons can develop in different depths of the sediment (e.g. thermogenic and biogenic hydrocarbon formation). Parts of the hydrocarbon can migrate and seep through the seabed surface. The occurrence and various types of seepage at passive continental margins and at other locations have been documented (e.g. Hovland and Judd, 1988).

The co-occurrence of migration and sediment accumulation gives therefore first indications of underlying reservoirs. Today, understanding of the development and related processes of large hydrocarbon reservoirs is improving (e.g. Tissot and Welte,

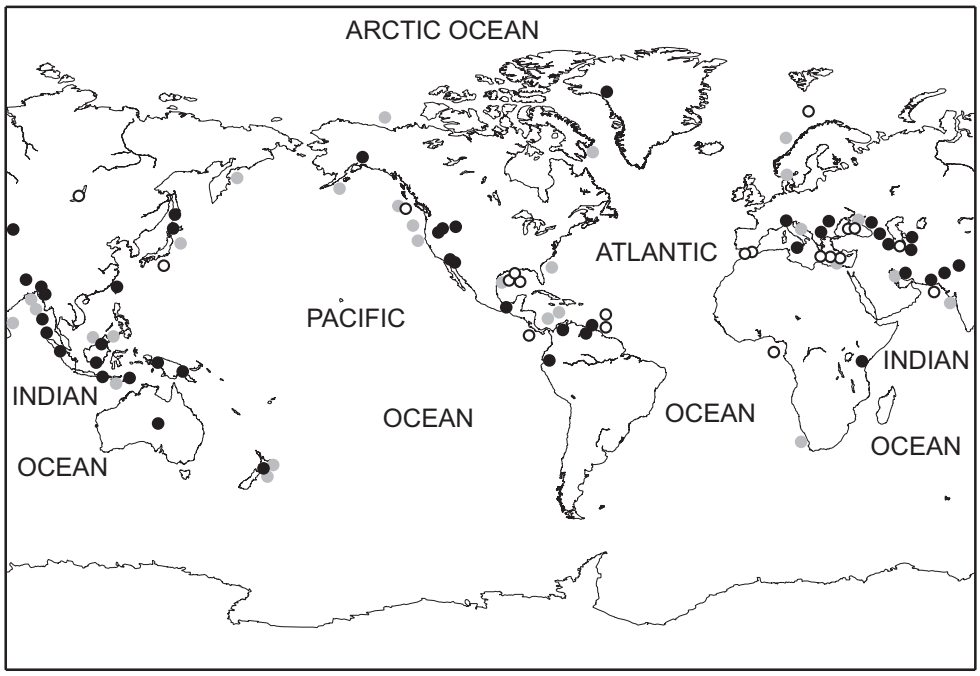

Figure 2-1. Worldwide distribution of known onshore (solid black), offshore (black circles) and inferred offshore (solid gray) mud volcanoes (after Milkov et al., 2003).

1984; Welte et al., 1996). However, small scale structures are not clearly understood yet. For example the development and processes in conjunction with carbonate mounds and mud volcanoes are still topics of scientific research. Figures 1-1 and 2-1 show the occurrence of carbonate mounds and associated cold water corals at European continental margins and the distribution of mud volcanoes in the world, respectively. Both phenomena are widespread and have global importance.

2.1 General settings of mud volcanoes

One example of methane related structures are mud volcanoes. Mud volcanoes which are characterized by fluid, mud, and gas expulsion are ideal opportunities to study the hydrocarbon seepage from sources in the sediments (e.g. Dimitrov, 2002; Bohrmann et al., 2003; Klages et al., 2004). Submarine mud volcanoes mainly form either on top of a shale diapir that reaches the seafloor or due to the rise of fluidized sediments along faults (Milkov et al., 2000). They typically show a circular shape with low relief (Huguen et al., 2004). The existence of mud volcanoes is widespread over the world comprising onshore and offshore regions, active and passive continental margins and abyssal parts of inland seas (Milkov et al., 2000; Kopf et al., 2002) (Figure 1-3). The migration of deep-seated sediments to the seabed creates mixed sediments whose interpretation becomes challenging when information about the existence of a mud volcano is not available (Kohl and Roberts, 1994).

Mud volcanoes are a significant source emitting methane into the ocean and the atmosphere and are not yet considered in models of atmospheric methane (Milkov et al., 2004). However, it is assumed that methane discharged from deep water mud volcanoes is rapidly dissolved and oxidized in the water column and only marginally contributes to the atmospheric carbon cycle (Milkov et al., 2003). Furthermore, mud

volcanoes are considered to contain gas hydrates (provided that temperature and pressure conditions allow the formation of gas hydrates). Gas hydrates have been studied intensely during the last years and have potential as future energy resource (e.g. Hovland, 2000; Clennell, 2000). However, gas hydrates should not be considered as passive reservoir, because a sudden dissolution of gas hydrate may cause slope instabilities and result in massive land slides causing geo-hazards (Mienert et al., 2003).

Mud volcanoes and other hydrocarbon cold seeps are characterized by specialized chemosynthetic communities (Hovland and Judd, 1988). They are covered with methanotrophic bacteria and benthic communities that feed on the migrating methane (e.g. Kulm et al., 1986; MacDonald et al., 1989; Sibuet and Olu, 1998; Suess et al., 1999; Pimenov et al., 2000). Bacteria mats subsist by sulphate reduction and methane oxidation which takes place in the upper part of the sediments under both anaerobic and aerobic conditions (Pimenov et al., 1999). However, anaerobic oxidation of methane appears to be the more important process (Boetius et al., 2000). Microbial and benthic communities around seep locations can give information about the development of the region and the ecosystem. Due to the separation of such ecosystems from the atmosphere it can also be considered representative for a certain period of time during the history of life in general.

2.2 Håkon Mosby mud volcano

The Håkon Mosby mud volcano is the only mud volcano in polar regions that has been studied in great detail (Klages et al., 2004). It is situated at the Norwegian-Barents-Svalbard continental margin between Norway and Svalbard in a water depth of about 1270 m, within a slide scar on the Bear Island glacial submarine fan (Figures 1-1 and 3-1). The bedrock consists of oceanic crust with an age of about 33 to 37 million years at this location (Hjelstuen et al., 1999), and is overlain by Cenozoic sediments that are divided into a lower preglacial and an upper glacial unit (about 6.1 km total thickness). Multichannel seismic profiles show a 1 to 2 km wide disturbed zone below the Håkon Mosby mud volcano which is related to the presence of free gas in the sediment. This is further supported by relatively low seismic velocities in this area (Hjelstuen et al., 1999). Disturbed and disrupted seismic reflectors below the mud volcano in depths of about 2.5 km suggest that the gas has its source in the terrigeneous Late Pliocene sediments (Milkov et al., 2004). It is assumed that the Håkon Mosby mud volcano is the result of a sediment slide that was triggered by an earthquake causing side wall collapse and sediment destabilization (Vogt et al., 1999a). The observation of gas hydrates in sediment cores and gas escape at the seafloor confirms that the Håkon Mosby mud volcano is an active gas seep (Vogt et al., 1997; Klages et al., 2004; Sauter et al., 2006).

First data of this mud volcano were recorded during a 1989-1990 sidescan and bathymetric survey initiating scientific interest (Vogt et al., 1999b and references therein). Following investigations reported gas hydrates and associated chemo-synthesis related benthic fauna (Pimenov et al., 1999). Multidisciplinary studies around the Håkon Mosby mud volcano focus both on the ecosystem that exists around the gas discharge locations, on the question how this mud volcano developed, and on the kind

of force that drives the mud expulsion (Hjelstuen et al., 1999; Vogt et al., 1999b).

At the Håkon Mosby mud volcano, methane-consuming bacteria mats and tubeworms dominate the ecosystem. The high biomass of benthic organisms marks the basis of the food chain at this mud volcano (Pimenov et al., 1999; Vogt et al., 1999b). A high activity of microbial processes was found in the outside zone of the Håkon Mosby mud volcano exceeding the rates of the central area enormously (Pimenov et al., 1999). The abundance of pogonophorans in this area is therefore related to the higher activity of the methanotrophic bacteria. Methanotrophic bacteria and pogonophorans form a symbiosis with the bacteria living inside the tubeworms (Vogt et al., 1999b). Additionally, gastropods and demersal fishes that feed on the tubeworms have been observed (Milkov et al., 1999; Gebruk et al, 2003; Bergmann, 2004).

2.3 General settings of carbonate mounds

Other seabed features that are related to gas migration are carbonate mounds. The aim of investigating carbonate mounds is to better understand the relation between the deep geosphere and the biosphere and how the mounds are related to ancient geological mound structures (Van Weering et al., 2003a).

The carbonate mounds are built up of a framework of cold-water corals (mainly *Lophelia pertusa* and *Madrepora oculata*), fine grained sediments with biogenic calcareous rubble and coral fragments (De Mol et al., 2002). Cold water coral reefs and carbonate mounds have been discovered all along the European North Atlantic continental margin in depths of about 50 m to 2000 m (De Mol et al., 2002; Freiwald and Roberts, 2005) (Figure 1-1). They have become a major focus of research because they form rich ecosystems independent from the photic zone and are endangered by the exploitation and fishery industry for example due to the heavy deep sea trawl equipment (Anonymous, 1999; Kozachenko et al., 2002).

The corals exhibit a mound building potential. While the corals are growing, sediment accumulates stabilizing the coral framework finally resulting in coral banks and mound structures (De Mol et al., 2002; Henriet et al., 2003). A hard substratum is needed for the corals to start growing (De Mol et al., 2002). The accumulation of organisms and their skeletons together with the local precipitation of carbonates form hardgrounds where the corals can settle (Hovland et al., 1994; Hovland, 2002; Henriet et al., 2003).

Strong bottom currents are necessary to supply enough nutrients for the corals and to prevent sediment burial (Van Rooij et al., 2003). Based on the balance of sedimentation and nutrient supply, the corals continue growing or they are buried in the sediment. Buried mounds have been discovered in association with outcropping mounds in the Porcupine Seabight (Henriet et al., 1998; De Mol et al., 2002).

A connection of cold-water coral reefs to seeping pore water and hydrocarbons is suggested by Hovland et al. (1994) and Hovland and Thomsen (1997) and references therein. Gas hydrates may be another source of hydrocarbon seepage (Henriet et al., 1998). Hydrocarbons provide nutrients to bacteria which are at the lower end of the food chain (Hovland et al., 1994). Although numerous indicators exist which point to a close link between fluid seepage and the occurrence of carbonate mounds and deep water corals, there is no proof of direct dependence (Hovland and Risk, 2003).

2.4 Porcupine Seabight

The Porcupine Seabight is situated in the North Atlantic off western Ireland and bounded by the Porcupine Bank, the Slyne Ridge, the Irish shelf and the Goban Spur (Figure 1-2). It overlies the Porcupine Basin which is one of a number of sedimentary basins on the European continental margin. The Porcupine Basin is a north-south shaped basin that formed during an east-west extension in the Mid Jurassic prior to the opening of the North Atlantic in the Late Cretaceous (Shannon, 1991a). Rifting and subsequent thermal subsidence of the underlying thinned continental crust has resulted in accumulation of thick (up to 8 km) Cretaceous and younger sediments (Masson and Miles, 1986; Croker and Klemperer, 1989). These strata unconformably overlie faulted Jurassic rocks (Shannon, 1991b). Proven and potential hydrocarbon reservoirs are present in the Porcupine Basin (Crocker and Shannon, 1987). Cretaceous and Jurassic source rocks provide the richest potential for hydrocarbon reservoirs and flows of oil and/or gas have been reported for a number of wells (Shannon, 1991b).

Water depths of the Porcupine Seabight range from 200 m at the shelf edge down to more than 3500 m at the mouth of the Seabight (Figure 1-2). Channel systems at the northern and eastern slopes of the Seabight indicate significant long-term transport of sediment from the shelf down towards the basin (Kenyon et al., 1978; Rice et al., 1991). Drift sediments observed along the European margin give evidence of transport by along slope northward flowing currents (Rice et al., 1991). Drift deposits characterize the sedimentary environment of the Porcupine Seabight (Van Rooij et al., 2003).

The first description of corals in the Porcupine Seabight was made by Thomson et al. in 1873 (Huvenne et al., 2003) and research on deep water corals and carbonate mounds was initiated with the first publication by Hovland et al. (1994) who imaged and described the mounds based on seismic profiles. Further studies were carried out during cruises 7 and 8 of the Training-through-Research programme of the Inter-governmental Oceanographic Commission of UNESCO (Kenyon et al., 1998 and 1999). Recent studies within the European Union's 5th framework program, i.e. Aces (Atlantic Coral Ecology Studies), Ecomound (External Controls on Mound Formation) and Geomound (Geological Controls of Mound Formation) focus on geological and ecological aspects of carbonate mounds and associated coral reefs driven by the challenge to preserve valuable deep sea ecosystems while exploring for new energy resources (Anonymous, 1999).

A number of recent mound provinces have been discovered on the Irish shelf in the area of the Porcupine Seabight and Rockall Trough (Hovland et al., 1994; Croker and O'Loughlin, 1998; Henriet et al., 1998; Kenyon et al., 2003) (Figure 1-2). Three provinces of carbonate mounds (Magellan, Hovland and Belgica mound province) were discovered in the Porcupine Seabight (Figure 1-2). The Belgica province is situated at the eastern slope of the Seabight, whereas the two others are found in the north. They are target of recent scientific activity and are linked to hydrocarbon seepage probably related to dissolution of a shallow layer of gas hydrates initiating the growth of the overlying biological community (Hovland et al., 1994; Henriet et al., 1998).

The top of the mounds is associated with corals and a diverse deep-water benthic fauna comprising mainly suspension feeders (Sumida and Kennedy, 1998; Van

Weering et al., 2003b). The principal structure of the mounds is characterized by living coral colonies at the top with an open spaced zone of dead coral framework and debris underneath (De Mol et al., 2002). The coral framework is filled with sediment in the lower part. Seismic profiles image the mounds as acoustically transparent structures with parabolic outline and no internal reflections (Van Rooij et al., 2003). The mounds of the Belgica province are underlain by a continuous erosional surface of Miocene age which indicates an older age compared to the other mound provinces in the Porcupine Seabight, and observations indicate a short period of initial mound growth (De Mol et al., 2002).

Recent investigations suggest that the major development of the coral banks in the Porcupine Seabight is related to ocean circulation and internal waves, generated at the boundary of different water masses, and associated nutrient supply (De Mol et al., 2002). The present-day pathways of bottom currents are closely related to the position of the mounds (Van Rooij et al., 2003). First data about the structure and basement of one mound in the Porcupine Seabight was recently obtained during the expedition 307 of the Integrated Ocean Drilling Program (Expedition Scientists, 2005). Evidence for carbonate hardgrounds at the mound base and hydrocarbon influence on the mound development was not found. However, a photograph showing bacteria mats within a *Lophelia* colony is described in Hovland (2005) and underlines the link between mound building corals and methane consuming bacteria.

The southern part of the study area is represented by the Gollum Channel System. It consists of six channels that feed into one single channel at about 3000 m depth. The channel system had dominant activity during glacial stages and limited activity in recent times (Wheeler et al., 2003). Sediments might still be transported by tidal currents (Tudhope and Scoffin, 1995).

3 Methods of seafloor analysis

Geophysical methods can help to detect structures that indicate sedimentary processes. In contrast to terrestrial investigations in the field, mapping of structures at the seabed surface requires adapted methods and equipment. Marine studies need much more effort and are characterized by restricted access to the study areas, which has to be realized using vessels, difficult sampling conditions and absence of direct overview observations. These constraints have led to the development of marine geophysical techniques. Classical geophysical mapping techniques in the marine environment consist of hydroacoustic and seismic systems. Hydroacoustic systems comprise sediment profilers and seabed surface mapping systems, i.e. multibeam and sidescan systems. These techniques give detailed information about the stratigraphy of the upper tens to hundreds of meters of the seabed sediments and about morphology and sediment structure of the seabed surface in terms of depth and acoustic backscatter strength. Seismic investigations provide deeper penetration and obtain information about the internal structure of the marine sediments and the underlying bedrock.

Different scales of the investigation targets require adjusted types of equipment for data recording. Due to the frequency-dependent characteristics of the acoustic pulse, penetration into the sediment and spatial resolution of the acquired data varies.

Penetration into the sediments decreases whereas the ability to resolve smaller structures increases with increasing frequency. Low frequencies of tens to hundreds of Hertz are used for deep penetration during seismic investigations. Sediment profilers use frequencies of a few Kilohertz and deep water multibeam echo sounders typically operate at about twelve Kilohertz.

Multibeam echo sounder systems have become standard for precise depth recording. The main principle of bathymetric measurements is to measure travel times of transmitted acoustic pulses that propagated through the water column in different, known, directions and were returned at the water seabed interface. This information provides a detailed picture of the seabed surface topography and the corresponding echo strength. Channels, slopes, seabed structures (e.g. sediment waves, ripples), mounds, and flat plains are detectable using bathymetry. Bathymetry is also used to trace subsurface structures visible in seismic profiles. Acoustic echo intensity provides information about the variation of the echo strength in the study areas. Local variations can be linked to changing seabed properties and indicate promising sampling locations.

A variety of methods were developed to investigate the seafloor and its diversity based on the energy of the acoustic signal of multibeam systems (see section 3.3). The echo intensity information comprises sidescan and angular backscatter data and is related to the geometry and the characteristics of the surface sediments. The angular backscatter analysis focuses on acoustical parameters to classify the mapped seabed (see section 7). Based on known parameter sets in combination with seafloor samples the seabed can be characterized. New seabed types can be identified when the parameter sets differ significantly from known seabed types. Other approaches try to model the backscattering process and to determine a number of model parameters (Lurton, 2002).

3.1 Hydroacoustic methods

Bathymetry provides critical information to investigate seafloor processes and genesis. It is of essential importance for marine science because it shows the result of processes both below the seabed surface (e.g. outcropping of subsurface structures) and at the seafloor. Detailed bathymetric data are required to map seabed structures with complete coverage to obtain an inventory of seabed features at one moment and to establish a basis for monitoring tasks to acquire data about the variability of the seafloor (see sections 4 and 5). Geological, biological and chemical processes and interrelations can only be fully understood if bathymetric data of sufficient resolution are available.

To derive further information of the seabed, recorded sub-bottom profiles of the sediment complement the bathymetry and are used to extend the applicability of bathymetric interpretation. The subsurface geology can be explored on the basis of stratigraphy which becomes visible by different reflections of the acoustic pulse that penetrated the seafloor. The stratigraphy provides additional information at locations which are not clearly interpretable based on bathymetry (e.g. detection of buried mounds in section 5.3.4). The acoustic pulse can penetrate the seabed up to 200 m depending on the sediment type (Dr. G. Kuhn, AWI Bremerhaven, personal

communication). However, the interpretation of sub-bottom profiles is limited to a qualitative analysis because the velocity of sound propagation in the sediment is not fully documented.

3.2 Introduction into bathymetric methods

The development of analyzing underwater sound dates back to 1490 when Leonardo da Vinci described the first example of a passive underwater listening device: “If you cause your ship to stop, and place the head of a long tube in the water and place the outer extremity to your ear, you will hear ships at great distance from you.” (in Caruthers, 1979). However, the main development began almost four centuries later at the end of the 19th and continued in the 20th century.

In 1880, Jacques and Pierre Curie discovered the piezoelectricity. Certain crystals have the ability to produce electric charge across certain pairs of their faces when pressurized which is the basis of the acoustic transducers (Urick, 1983). However, it was not before 1913 when Alexander Behm received the patent for the invention of an acoustic echo sounder to detect ranges and direction of ships or obstacles and depths by reflected sonar waves. First commercial echo sounders for ships were available in 1925 (Urick, 1983). Fishery sounders were developed designed to detect fish shoals and process the echoes coming from the entire water column. Sidescan sonar systems were invented in the early 1960s and are used to obtain acoustic intensity images of the seabed (Lurton, 2002). To this day they are a major tool for seafloor mapping in marine geology. Sub-bottom echo sounders were developed capable to penetrate the seabed several tens of meters and display its vertical cross-section. Multibeam echo sounders became available in the 1970s. Their capability of simultaneous measurements covering a swath width beneath the ship track has provided the basis for accurate and efficient seabed mapping. At the end of the 1980s, the sidescan technique was integrated into multibeam echo sounders providing systems that measure both seabed topography and acoustic reflectivity. Multibeam systems have become essential for geological studies of seabed morphology and facies due to their capacity for seafloor coverage and accuracy (Lurton, 2002). Recent products still measure the travel time of the acoustic pulse through the water column. Measurement coverage, resolution and accuracy have improved much during the past decades due to beam forming, beam steering and focusing techniques as well as more accurate navigation to precisely determine a model of the seabed surface to meet scientific demands.

The Hydrosweep DS (Deep Sea) multibeam echo sounder installed onboard RV *Polarstern* in 1989 was developed by Krupp Atlas Elektronik (Bremen, Germany) between 1984 and 1986. In the years 1993 and 1994, the system was technically improved and multibeam sidescan and angular backscatter recording were installed. In 1997, the system was updated from DS-1 to DS-2. It is a deep sea system, operating at a frequency of 15.5 kHz and was used at a swath width of 90° during this study. This frequency is both low enough to cover the depth range up to the maximum ocean depths and high enough to receive a clear signal from the seabed rather than penetrating sediment layers to sub-bottom surfaces (Grant and Schreiber, 1990). Each ping provides 59 depth values perpendicular to the ship’s longitudinal axis to realize

efficient coverage of the seafloor (Gutberlet and Schenke, 1989). Detailed planning of parallel survey lines is necessary to generate a homogeneous data set with full seafloor coverage.

The sound velocity in water is the critical parameter to calculate the travelled distance of the acoustic pulse from the measured travel time. First results of the sound speed were obtained in Lake Geneva and published in 1827 (Colladon and Sturm, 1827, in Medwin and Clay, 1998). The sound velocity in saline water is higher compared to fresh water and the temperature is in general the most important parameter. The sound velocity is horizontally stratified in most parts of the world's oceans. Therefore, it is necessary to have information about the profile of the sound velocity along the ray path of the acoustic pulse to accurately convert travel time into depth.

For a rough estimation of the sound speed, a value of 1500 m/s in sea water is often used if information about the true velocity is not available. Another possibility is to use the echo sounding correction tables published by Carter and Matthews (1980). They are applicable in water depths greater than 200 m and assume a defined velocity in the echo sounder of 1500 m/s.

In deep sea bathymetry it is advisable to record conductivity, temperature and pressure (depth) (CTD) to determine the sound velocity directly from measurements. However, the multibeam system Hydrosweep DS-2 is able to determine the mean sound velocity based on depth profiles measured perpendicular to each other (calibration profiles). Therefore, it is possible to insonify the same spot of the seafloor from vertical and from oblique directions. Based on the depth differences of both measurements the true mean water sound velocity can be obtained (Grant and Schreiber, 1990). This method is advantageous during transit between sample stations, saving time in comparison to CTD measurements. However, data gaps occur due to the calibration measurements. For the surveys analyzed in this thesis, the water sound velocity profiles were determined using CTD measurements. A sound velocity sensor is installed at the hull of RV *Polarstern* to determine the true sound velocity at the transducer, which is essential to transmit correct beam angles.

The position of the depth measurements is determined based on GPS in connection with a ship's integrated inertial navigation system. The origin of the ship's coordinate system is centered at the transducer of the Hydrosweep DS-2 system.

Post-processing of bathymetric data consists of the correction of erroneous position data and cleaning of erroneous depth measurements. A variety of methods are available such as inverse distance weighting, spline functions, kriging and triangulated irregular networks to calculate a terrain model of the seafloor that is used for analysis, presentation and as the basis for contouring and charting.

For further general information about bathymetry see Cohen (1970), Cook (2000) and Lurton (2002).

3.3 Methods of acoustic backscatter analysis

Imaging the seabed using sonar systems is widely used in the marine environment. Sidescan sonar systems have been used intensively for information about the seabed and as a first indication of its geology (Blondel and Murton, 1997). Multibeam systems

are also used for seabed mapping beyond the measurement of seafloor topography (e.g. de Moustier, 1986).

In addition to the bathymetry data, Hydrosweep DS-2 provides multibeam echo amplitude data that can be implemented for seabed characterization (see section 4.4.6 and chapter 6). Two possibilities exist to record the echo intensity of emitted acoustic pulses of multibeam sonar systems. The multibeam sidescan represents the echo amplitude on a time reference. The echo amplitudes of all pre-formed beams are combined and densely sampled to derive the cross profile of amplitude values for each ping (up to 4096 amplitudes in the case of Hydrosweep DS-2) (Hagen et al., 1994b). This provides acoustic imagery that is comparable to regular sidescan systems that are towed close to the bottom and that transmit short pulses in a slant direction that sweep the bottom. The multibeam sidescan performance is reduced in comparison to towed sidescan systems because the acoustic pulse is longer, less grazing and affected by larger movements of the ship. However, hull mounted multibeam systems have accurate estimates of the geographic position.

Multibeam angular backscatter consists of one amplitude value for each beam of the swath. Therefore 59 backscatter values are available with the Hydrosweep DS-2 system for analyzing in this study. These values are directly linked to the corresponding beam with complete geographic reference.

3.3.1 Principles of multibeam backscatter theory

At that moment when the transmitted acoustic pulse impinges the seafloor it is scattered in all directions. Only a part of the incident wave is reflected in the specular direction. The part that will be scattered back towards the transducer is called backscatter (Figure 3-1). In contrast to plane wave reflection, backscattering means that the acoustic wave is reradiated from the obstacle acting like a new source (Lurton, 2002).

Multibeam sonar systems use backscattered echoes for measurements. Other returns of the transmitted pulse towards the sonar system that are not originating from the desired target (backscattering from fish, suspended particles, plankton) is called reverberation and not included in the term backscatter (Lurton, 2002).

The seabed is usually not a plane surface. However, it can be assembled from a locally plane surface with a micro scale roughness. The effect of the micro roughness on the sonar wave depends on the roughness characteristics, the angle of incidence and the acoustic frequency (Lurton, 2002). The roughness of the seabed is the reason why the incident wave is scattered in all directions. The ratio of scattered and specular components also depends on the surface roughness (ratio of relief amplitude and the sonar wave length) (Lurton, 2002) (Figure 3-1).

The backscatter strength of the seafloor (target strength) is defined as the ratio between the intensity of the acoustic pulse scattered back by the seafloor and the incident intensity. It represents the relative amount of energy sent back by the target. It depends on the physical nature of the seabed, its structure (roughness) and the characteristics of the acoustic pulse (incidence angle, frequency). Because of the large range of that ratio it is logarithmized to obtain the unit decibel (dB). The intensity of the echo received at the transducer depends on the transmitted source level, the transmission loss (absorption in the water column and geometrical spreading), and the

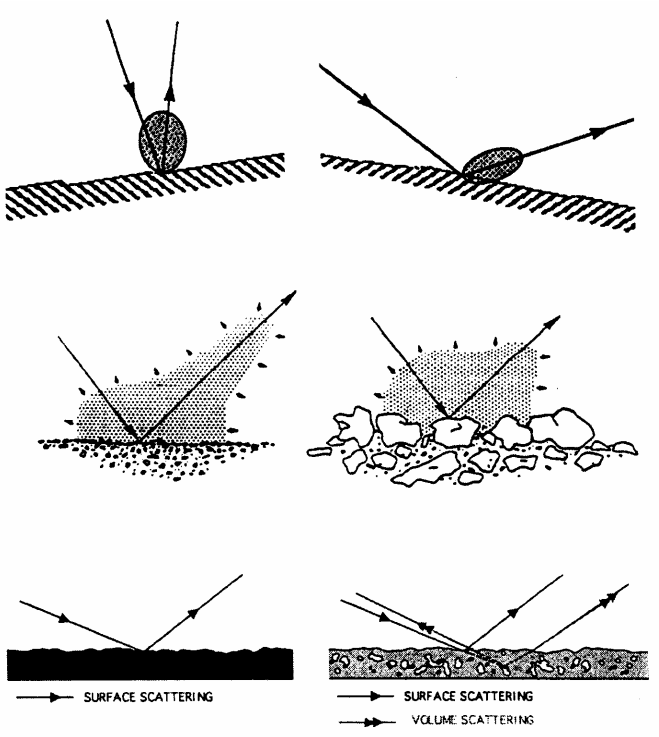

Figure 3-1. Backscattering from the seafloor is influenced by three factors (from top to bottom): local geometry of insonification, roughness of the seafloor at scales comparable to the sonar's wavelength, intrinsic properties of the seafloor (e.g. rocks vs. sediments) (from Blondel and Murton, 1997).

target strength. For small targets like fish, the target strength refers to the object. Because the entire seafloor cannot be insonified by the echo pulse at once, the backscatter strength is therefore referring to a unit scattering element (dB re $1m^2$) (Lurton, 2002) (compare section 3.3.3).

Acoustic frequencies that are used with sonar mapping systems lie in the range of tens to hundreds of kHz. Two main sources of backscattering act at these frequencies: interface and volume scattering (Lurton, 2002). The interface scattering is basically due to the surface relief. Volume scattering occurs due to heterogeneities in the sediment (e.g. buried stones, shells, organisms, gas bubbles) and affects the part of the acoustic signal that penetrates the seabed (Figure 3-1). It becomes dominant with increasing incidence angle and depends on the transmission and absorption in the sediment and on the volume backscattering strength of the sediment components. The lower the frequency the more acoustic energy penetrates the sediment (Urban, 2002).

Statistical geometrical models are appropriate to describe the interface backscattering (Lurton, 2002). They also account for the reflection coefficient of the interface. The interface roughness of the seabed can be described by the Rayleigh parameter which represents the ratio between the mean amplitude of the relief and the acoustic wavelength. It also considers the angle of incidence. However, it applies to coherent reflection instead of scattering and is not relevant when modelling echoes directly backscattered from the seabed (Lurton, 2002).

The seabed structures and characteristics that can be analyzed depend on the acoustic frequency used. Surface roughness at the seafloor (that is of interest at sonar frequencies) depends on geology and covers a scale range between millimeters and a

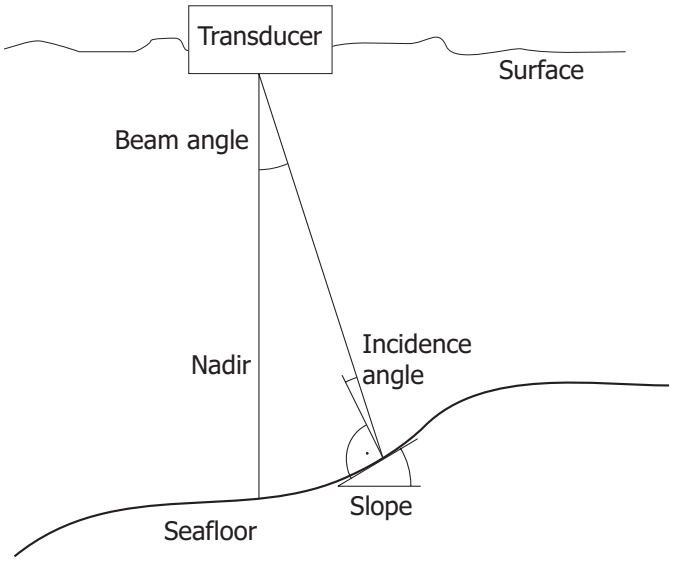

Figure 3-2. Sketch of basic elements acting in the multibeam – seafloor regime.

few meters (Lurton, 2002). A combination of different scales of micro-roughness can coexist. The seabed may show for example sand ripples having centimeter scale roughness overlaying large-scale sand dunes which differently affect the acoustic pulse.

Rocky and sedimentary seabed is in general referred to as rough and smooth surfaces, respectively. However, the backscatter data presented in chapter 7 are situated in sedimentary provinces (channels) but show an angular backscatter curve that indicates relatively rough seabed because a strong variation at near vertical incidence angles is not visible. A comparison with backscatter data of the same multibeam system from a seamount site exhibiting a rocky surface shows an even rougher angular backscatter function (Jacops, 2002).

3.3.2 Methods of measuring backscatter data

The Hydrosweep DS-2 system uses the echo of the seabed for both the depth determination and the backscatter measurement. The echo parameters required for the backscatter calculation are the two way travel time of the signal, the echo pulse length and the root-mean-square voltage of the echo. The received echo voltage response at the transducer is pre-amplified and corrected for acoustical losses with a time varying gain. The signal is than digitized and processed in the beam former unit to generate 59 pre-formed beams of the swath. The root-mean-square voltage is integrated within a -6 dB window around the peak amplitude and stored as output amplitude for each beam (Hagen et al., 1994a; MPL, 1991). The centroid of this envelop corresponds to the water depth. The time span of this window represents the echo duration. These data and all system relevant information (i.e. operation mode, source level, pulse length, time varying gain, etc.) are stored by the system and available for backscatter processing (see section 3.3.3).

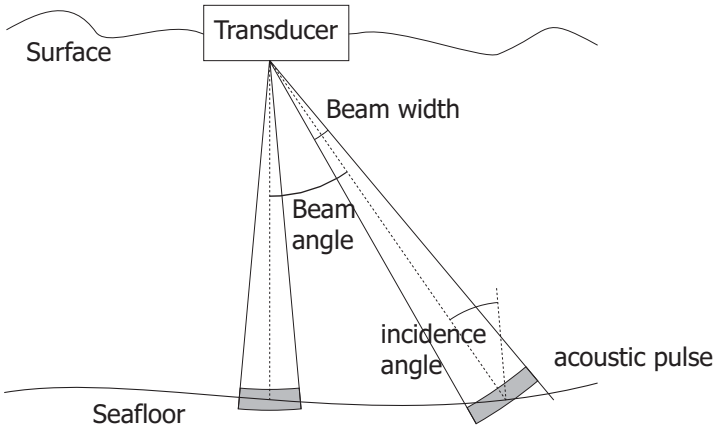

Figure 3-3. Geometry of the seafloor insonification by vertical beams, limited by the directivity and oblique beams, limited by the pulse length.

3.3.3 Processing of multibeam backscatter data

The software 'NRGCOR' is used to convert voltage amplitudes of the individual preformed beams recorded with Hydrosweep DS-2 into seafloor backscatter strength (MPL, 1991). This package was originally developed at the Marine Physical Laboratory, Scripps Institution of Oceanography, and has been customized for the Hydrosweep system.

The recorded signals of the individual beams are corrected for different terms in the sonar equation to yield the backscatter strength. First, the gain parameters applied during echo reception are recomputed and subtracted from the echo energy. Transmission level, propagation loss, signal duration and transducer directivity (beam pattern) at transmission and reception are also considered. Furthermore, two main corrections are performed by the software. The geometric correction determines the true angle of incidence on the seafloor which differs from the angle of arrival (beam angle at the transducer including refraction correction) that is recorded by the system (Figure 3-2). The use of the across track depth profile for seafloor slope determination was replaced in this study by a slope algorithm that is based on a terrain model taking into account the true slope of the seafloor. The physical corrections take into account the spherical spreading, absorption loss and the area insonified by each beam. These corrections are applied to the raw energy values to yield relative backscatter strengths as a function of incidence angle. The measurements can eventually be converted to absolute levels when a full acoustic calibration of Hydrosweep DS-2 has been performed (MPL, 1991).

The calibration of multibeam transducers is realized under laboratory conditions in a water tank. The true transducer directivity is determined using separate hydrophones in the tank that measure the distribution of the sound level of the transducer. These values can either be applied during the backscatter computation as calibrated beam coefficients or converted into correction values that are applied to already processed data.

The Hydrosweep directivity patterns of the transducers are theoretical values and lack standards of laboratory measurements. It is assumed that the directivity is symmetrical for the individual beams and identical for the transmitting and receiving

transducer (Anonymous, 1994). Calibration is hardly practicable at this frequency (15.5 kHz) because of the large array size of the transducers (3 m). Because there is no calibration of the individual beam measurements, it is difficult to provide the absolute angular backscatter function, however, normalized data can be obtained (Hagen et al., 1994a).

As the transmitted acoustic pulse sweeps the seafloor from the nadir towards outer beams, the size of the insonified area varies due to the directivity pattern. In the nadir area the footprint of the beams are insonified completely by the acoustic pulse while in the outer parts of the swath the pulse slice travels through the footprint (Figure 3-3). This situation is included during processing to yield backscattering strength. Therefore, the size of the effective insonification is considered. The change between complete insonification and travelling of the sound slice depends on pulse length and water depth, and occurs for example at an incidence angle of about 21° at 1000 m depth and 11 ms pulse length. For larger incidence angles the acoustic pulse does not completely insonify the footprint of the beam at one moment. The backscatter strength of the seabed (i.e. per unit surface, 1 m^2) can therefore be derived from the backscattering cross-section and the size of the seafloor portion effectively insonified by the acoustic pulse (Lurton, 2002). Detailed information about backscatter computation can be found in de Moustier and Alexandrou (1991), MPL (1991), Anonymous (1993) and Urban (2002).

3.3.4 Multibeam backscatter analysis

Detailed and accurate bathymetry is mandatory to calculate backscatter strength. Overlapping swaths of adjacent survey lines are a precondition to achieve accurate models of the seafloor. Therefore, the bathymetric data set is not completely available until the cruise has been completed. The calculation of the seafloor backscatter strength in this study was realized in post-processing. Furthermore, the recorded depth data are not sufficiently processed during real time data acquisition. The slope of the seafloor directly affects the computed angle of incidence of the transmitted beam. The available software only considered the across track slope of the seafloor which can be derived for each ping separately (even in real-time). However, at slopes and channel locations studied in this thesis, the along track slope is significant and cannot be neglected. Therefore, it is recommended to use data of a terrain model to determine the true slope of the seafloor at the footprint of the acoustic beams, as was done in this study.

The shape of the angular backscatter function and its spatial variation gives indication about the geological facies. The reason to relate backscatter of the seafloor to the type of seabed (mud, silt, sand, boulders, rock) originates from the observation that rocky seabed shows greater backscatter than muddy areas. However, the particle size of the sediment can only act as indirect indicator for scattering (Urick, 1983). The roughness of the seabed represents the main factor of the backscattering characteristic. Due to the relationship between surface roughness and seabed type, the roughness serves as proxy for the geological facies when using multibeam backscatter data.

Research is still ongoing regarding the connection between angular backscatter strength and seabed factors, i.e. incidence angle, local slope, micro roughness and

sediment properties (composition, density, relative importance of volume vs. surface scattering) (Figure 3-1) (e.g. Blondel and Murton, 1997; Simons, 2004). The Lambert law is the simplest model that describes the angular backscatter as linear function of the square cosine of the incidence angle. It only works in simple regimes (smooth surfaces and large scale undulations) and does not resemble the complex reality (Blondel and Murton, 1997). Other models are based on the interference of scattered elementary waves composing the echo acoustic field. The Helmholtz-Kirchhoff theory describes the seafloor using the root-mean-square roughness of the vertical dimension and the correlation radius in horizontal dimension (de Moustier, 1986). The composite roughness model combines the Kirchhoff and Rayleigh-Rice approximation to prevent shortcomings of the separate models (Jackson et al., 1986; Chakraborty et al., 2000). However, prior to the application of these models it is necessary to clearly distinguish facies that show different acoustic properties to determine its spatial validity. Furthermore, seabed information (sample data) is necessary to validate the models.

It should be noted that the Hydrosweep DS-2 swath covers a range at the seabed that corresponds to twice the water depth, one side of the swath covering the entire angular range (0° to 45° beam angle). Because of variations of the seabed type the angular backscatter data of individual beams may therefore correspond to different geological facies. The study described in chapter six is based on an areal selection of backscatter measurements instead of a swath-based selection taking into account the small size of the studied seabed features.

The model developed by Jackson et al. (1986) relates the angular backscatter data to a series of parameters describing the sediment (surface roughness, seabed/ seawater sound velocity and density ratio and ratio of volume scattering versus sediment attenuation coefficient). However, the seabed shows considerable heterogeneity in the upper meters which cannot be adequately described by the few input parameters of backscatter models (Hughes Clarke, 1994). Therefore, the approach suggested in Hughes Clarke (1994) was adopted in this study to characterize segments that have been selected based on the morphology and the backscatter strength. The key parameters are the slope of the mean angular backscatter curve, the predicted backscatter response at 20° incidence angle and the coefficient of variation (average ratio of the standard deviation to the mean).

REPRINTS OF SCIENTIFIC PUBLICATIONS

4 Multibeam bathymetry of the Håkon Mosby mud volcano*

Andreas Beyer, Rike Rathlau, Hans Werner Schenke

Alfred Wegener Institute for Polar and Marine Research (AWI), P. O. Box 12 0161, 27515 Bremerhaven, Germany

Keywords: bathymetry, terrain modelling, mud volcano

4.1 Abstract

The Håkon Mosby mud volcano is a natural laboratory to study geological, geochemical, and ecological processes related to deep-water mud volcanism. High resolution bathymetry of the Håkon Mosby mud volcano was recorded during RV *Polarstern* expedition ARK XIX/3 utilizing the multibeam system Hydrosweep DS-2. Dense spacing of the survey lines and slow ship speed (5 knots) provided necessary point density to generate a regular 10 m grid. Generalization was applied to preserve and represent morphological structures appropriately. Contour lines were derived showing detailed topography at the center of the Håkon Mosby mud volcano and generalized contours in the vicinity. We provide a brief introduction to the Håkon Mosby mud volcano area and describe in detail data recording and processing methods, as well as the morphology of the area. Accuracy assessment was made to evaluate the reliability of a 10 m resolution terrain model. Multibeam sidescan data were recorded along with depth measurements and show reflectivity variations from light gray values at the center of the Håkon Mosby mud volcano to dark gray values (less reflective) at the surrounding moat.

4.2 Introduction

The Håkon Mosby mud volcano is one of a number of deep sea structures that are linked to methane seepage along continental slopes (Milkov, 2000). They are characterized by fluid or mud ejection from deeper sources. The Håkon Mosby mud volcano was discovered as a sidescan feature during a 1989-1990 SeaMARC II sidescan survey (Vogt et al., 1991). Its discovery brought marine geoscientists and biologists together for the first time in the Nordic Basin (Vogt et al., 1999b). The Håkon Mosby mud volcano is associated with sediment slides and may have been formed as a result of rapid hydrate dissociation caused by the slide-induced pressure release (Vogt et al., 1997, 1999a). The volcano gradually became a major focus to study geological, geochemical and ecological processes related to deep-water mud volcanism and represents an ideal model system to study methane fluxes in polar seas (Klages et al., 2004). The mud volcano exhibits very high sub-bottom temperature

* Beyer, A., Rathlau, R., Schenke, H. W., 2005b. Multibeam bathymetry of the Håkon Mosby Mud Volcano. Marine Geophysial Researches 26, 61-75, doi 10.1007/s11001-005-1131-8.

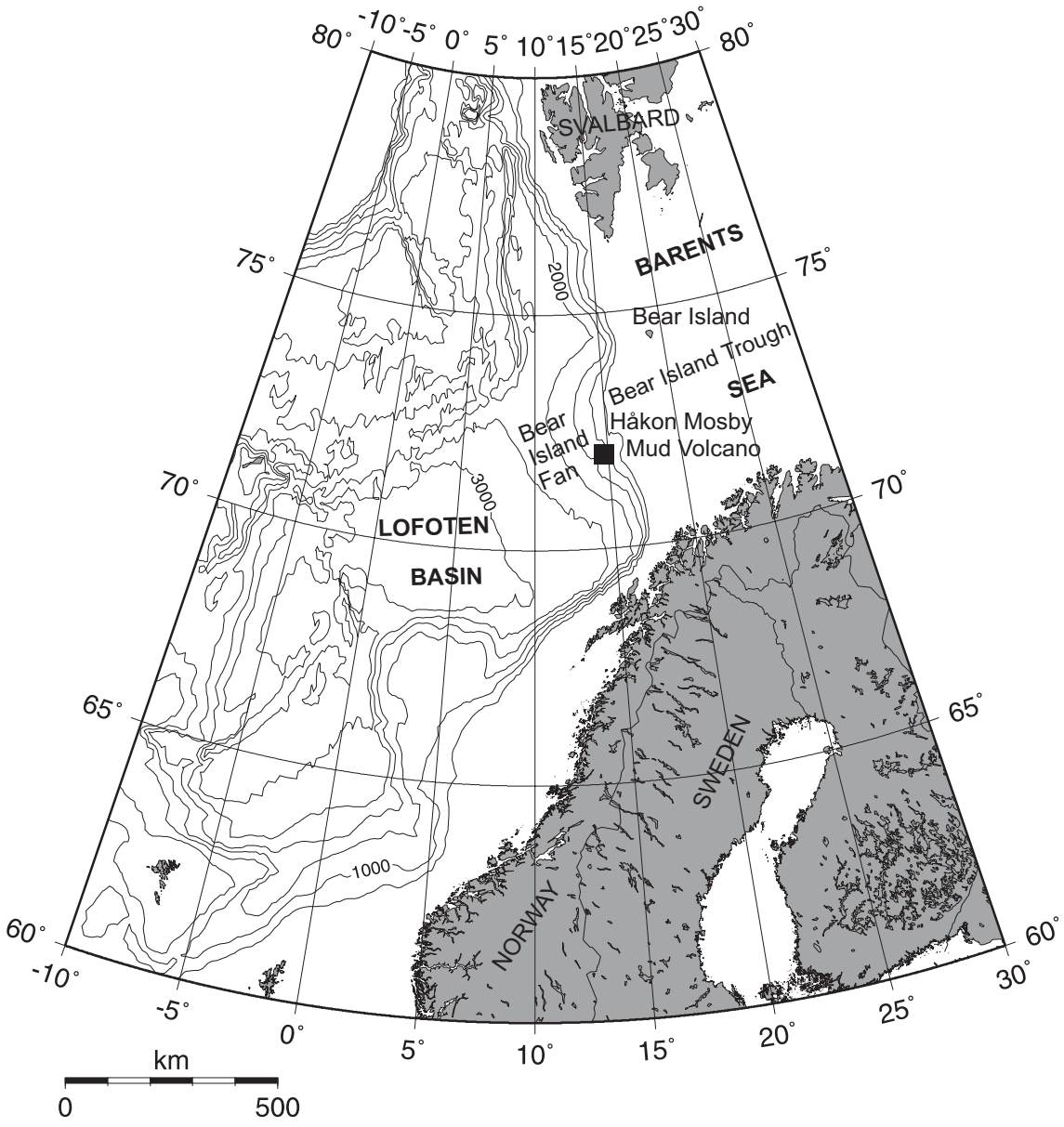

Figure 4-1. Overview of the area of investigation. The Håkon Mosby mud volcano is situated between northern Norway and Svalbard at the continental slope of the Barents Sea. Contour interval 500 m.

gradients (up to 5-10° K/m), positive bottom water temperature and dissolved methane anomalies. There is also a chemosynthesis-based ecosystem, methane hydrate in the uppermost few meters sub-bottom, and sidescan sonar evidence for mud flows reaching at least 4 km downslope from the mud volcano (Vogt et al., 1999a). It is the only mud volcano in a polar region that has been studied in great detail by photo and video camera observation (Klages et al., 2004). Multibeam bathymetry data are essential because the success of many current and future studies depends on the proper positioning of sampling and observation devices in space and depth coordinates.

Bathymetric data from the Håkon Mosby mud volcano were acquired in 2002 using the Hydrosweep DS-2 multibeam system onboard RV *Polarstern* (Sauter et al., 2003). The location of the Håkon Mosby mud volcano was mapped but data density was not

sufficient for high resolution contouring. The RV *Polarstern* expedition ARK XIX/3 (in 2003) was jointly organized between the Alfred Wegener Institute for Polar and Marine Research and the French Research Institute for Exploitation of the Sea (Ifremer). The unmanned deep-sea submersible *Victor 6000*, a remotely operated vehicle of the French Research Institute for Exploitation of the Sea, was deployed from RV *Polarstern* to study the Håkon Mosby mud volcano and related processes. Detailed investigations from various disciplines were carried out around the Håkon Mosby mud volcano, comprising biological, geophysical and geochemical data acquisition (Klages et al., 2004). Prior to these activities swath bathymetry was recorded to provide basic information of the seafloor in order to accurately locate sampling devices at different locations around the Håkon Mosby mud volcano. A 10 m digital terrain model was created from the high resolution multibeam bathymetry of the Håkon Mosby mud volcano. Data capturing and processing are described in detail. Accuracy assessment was made to evaluate the generated terrain model, which is used to depict the morphology. Due to the high data density of the RV *Polarstern* survey, a major improvement in the morphological interpretation was achieved compared to the bathymetric maps presented by Vogt et al. (1997) and Ginsburg et al. (1999).

4.3 Regional setting

The Håkon Mosby mud volcano is located on the Norwegian-Barents-Svalbard continental margin between Norway and Svalbard (Figure 4-1). The Barents Sea margin separates the Eocene-Early Oligocene oceanic crust of the Lofoten Basin from the continental crust in the Barents Sea (Hjelstuen et al., 1999). The Håkon Mosby mud volcano is located on oceanic crust within the Bear Island submarine fan, which reaches a thickness of approximately 3.1 km beneath the mud volcano (Hjelstuen et al., 1999). This fan is situated in front of the Bear Island Trough and covers the continental margin as well as parts of the northern Lofoten Basin (Hjelstuen et al., 1999). The Håkon Mosby mud volcano developed within a slide valley that incised the massive Bear Island fan (Ginsburg et al., 1999), and is assumed to be the result of a sediment slide (Vogt et al., 1999a). The water depth at the center of the Håkon Mosby mud volcano is approximately 1260 m. The Håkon Mosby mud volcano is a shallow concentric structure with high seafloor-sediment temperatures (for example 11°C at 0.5 m sub-bottom depth) and high thermal gradients (Crane et al., 1997; Eldholm et al., 1999; Ginsburg et al., 1999). It is also a gas hydrate-bearing structure with maximum hydrate content at about 200 m from the center. Gas hydrate composed predominantly of methane, was found by Vogt et al. (1997) in sediment cores in the upper 2 m of the sub-bottom of the Håkon Mosby mud volcano. However, there are no hydrates in the middle, most active area of the Håkon Mosby mud volcano (Ginsburg et al., 1999). The area around the center is covered by patchy bacterial mats with a benthic community characterized by pogonopheran species (tube worms, Pimenov et al., 1999). Multichannel seismic reflection surveys indicate free gas residing deeper than 3 km below the Håkon Mosby mud volcano (Hjelstuen et al., 1999).

The Håkon Mosby mud volcano is characterized by mud ejection and gas seepage. Shilov et al. (1999) analyzed gravity cores and discovered two periods of activity of the Håkon Mosby mud volcano: 10 to 30 ka ago and the recent activity. The Håkon Mosby

mud volcano is associated with very high heat flow >1000 mW/m^2 (Eldholm et al., 1999), an unusual occurrence over seafloor far from hot spots and plate boundaries. Thermal gradients surrounding the Håkon Mosby mud volcano show normal values around 60 mK/m, whereas gradients up to 800 mK/m have been measured at the western side of the Håkon Mosby mud volcano central structure (Vogt et al., 1997; Eldholm et al., 1999). Vogt et al. (1997) estimated 10000 mK/m in the thermal eye at the center of the mud volcano. These values have not been measured in situ and the sampling may have been biased, but they indicate the magnitude and character of the thermal gradient. The thermal maximum is thought to be at the center of the Håkon Mosby mud volcano with steep lateral gradients reaching background level values just beyond the circular moat of the Håkon Mosby mud volcano (Eldholm et al., 1999). The high thermal gradient is also limited to the extent of the Håkon Mosby mud volcano.

4.4 Data collection and processing

4.4.1 Bathymetric survey

One objective of the RV *Polarstern* expedition ARK XIX/3 was to improve the bathymetric data set of the Håkon Mosby mud volcano to analyze the relationship of the small-scale morphology to the distribution of benthic communities, gas hydrates and subsurface temperature gradients (Boetius et al., 2004). The multidisciplinary investigations on methane fluxes and related processes included sampling of sediments in areas dominated by gas hydrates, bacterial mats and tube worms. Heat flow measurements, bottom water sampling and the study of the biodiversity were also performed around the Håkon Mosby mud volcano. In order to provide updated depth data during the cruise, a small scale survey grid was performed prior to the deployment of sampling and observation devices including multibeam, sub-bottom and fishery echo sounders (Klages et al., 2004). The recorded bathymetry was also used to plan local micro-bathymetric surveys performed using *Victor 6000*.

Bathymetry of the Håkon Mosby mud volcano was obtained using the Hydrosweep DS-2 multibeam system. This operates at 15.5 kHz and provides 59 pre-formed beams covering a 90° swath width (Gutberlet and Schenke, 1989). Due to the fixed beam angle of 2.3°, the footprint size of the pre-formed beams varies between 50 m and 100 m for center and outer beams, respectively. The measurement accuracy depends on the water depth and is given by the manufacturer as 1% of the water depth.

The survey was performed at slow ship speed (5 knots) to provide sufficient point density in the along track direction. The along track point spacing was approximately 20 m with a ping rate of 7 to 8 seconds. A dense line spacing of approximately 200 m was selected to provide excellent coverage and point density. Seventeen survey lines were placed parallel in a north-south direction. The area surveyed has an extent of approximately 9 km by 6 km in the north-south and east-west direction, respectively. The weather conditions were calm with wind speed about 3 to 4 m/s.

4.4.2 Sound velocity profile

In order to achieve high quality bathymetric data, detailed sound speed information of the water column is needed. A SBE911plus device was used to measure conductivity, temperature and depth (CTD) of the water column in order to determine

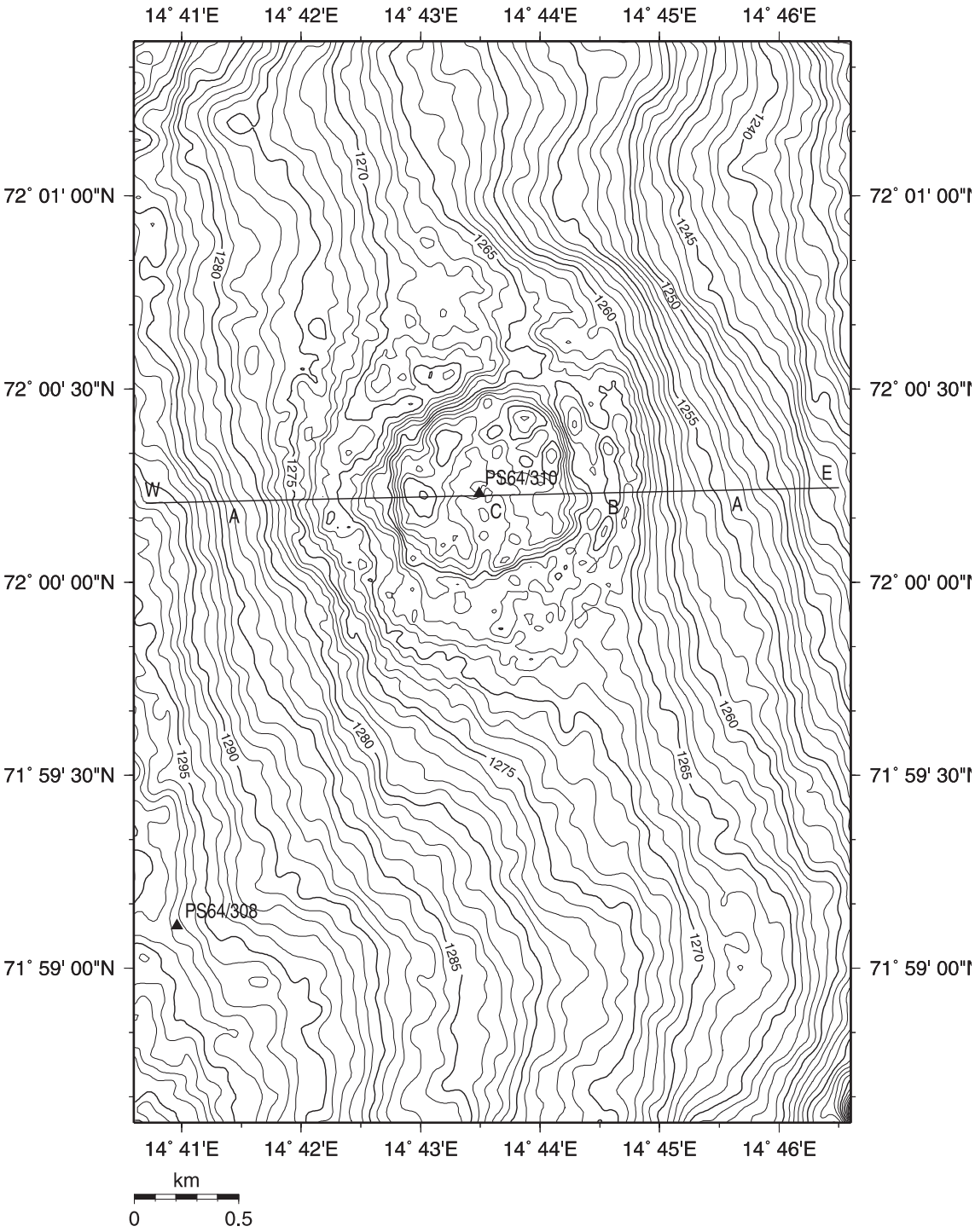

Figure 4-2. Terrain model and CTD stations of the study area. More topographic detail is visible towards the center of the Håkon Mosby mud volcano. The location of the profile in Figure 4-6 is shown. Contour interval 1 m.

from these values the water sound velocity profile. The initial accuracy of the conductivity, temperature and pressure was 0.0003 S/m, 0.001°C and 0.015% respectively (Sea-Bird) which is sufficient for the determination of the sound velocity profile in deep sea bathymetry. The sound velocity profile was determined using the formula of Chen and Millero (1977), which is used to convert the sound travel time into depth and to model the refraction of slant sonar ranges. Two CTD profiles were

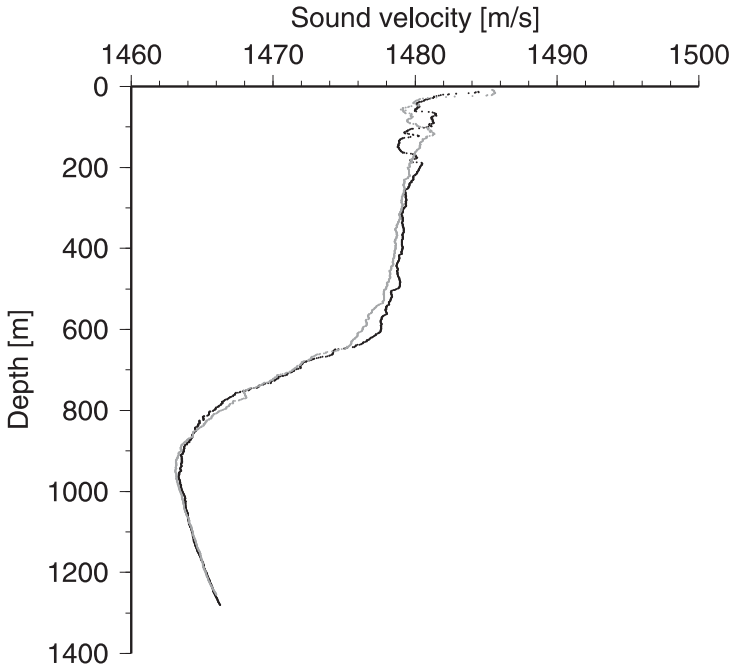

Figure 4-3. Water sound velocity profile of the stations PS64/308 (black) and PS64/310 (gray). Data of station PS64/308 were used for bathymetric processing. Differences are due to temperature and salinity variability within a time period of 15 h.

recorded prior (station PS64/308) and after (station PS64/310) the bathymetric survey within a time period of 15 hours (Klages et al., 2004). Station PS64/310 was situated at the center of the Håkon Mosby mud volcano structure 2.5 km north east of station PS64/308 (Figure 4-2). The sound velocity profiles of both stations are shown in Figure 4-3. Data from station PS64/308 were applied during the survey. Seventeen significant points on the profile were selected to represent the characteristics of the sound velocity profile of the water column in the study area. The sound velocity profile determined after completion of the survey (station PS64/310) shows differences of up to 2 m/s in a depth range between 50 m and 200 m. Between 300 m and 650 m the sound speed at station PS64/310 is on average 0.6 m/s lower. At around 700 m depth the data from both stations agree very well. The station PS64/310 CTD profile shows again lower sound speed values around 900 m depth. Generally, the sound speed data obtained from the two stations are in a good agreement below 950 m.

In order to investigate whether the temporal variability of the sound velocity in the upper 200 m of the water column is a result of natural fluctuations or an artifact of the CTD measurements, potential density was calculated with a reference pressure of 0 decibars (sea surface) using Ocean Data View (Millero et al., 1980; Schlitzer, 2003). The potential density of station PS64/308 (black) and PS64/310 (gray) is shown in Figure 4-4. The continuously increasing density towards greater depths indicates that the CTD device worked properly. In the upper 200 m of the water column and around 600 m depth, significant density differences are observed. However, there is a small density inversion visible at station PS64/310 near 780 m water depth. This is caused by erroneous CTD data since density inversions do not occur in the water column. A jump is visible in the sound velocity profile at this depth (Figure 4-3), which is also observed in both the salinity and temperature data. The salinity profiles of the stations indicate a

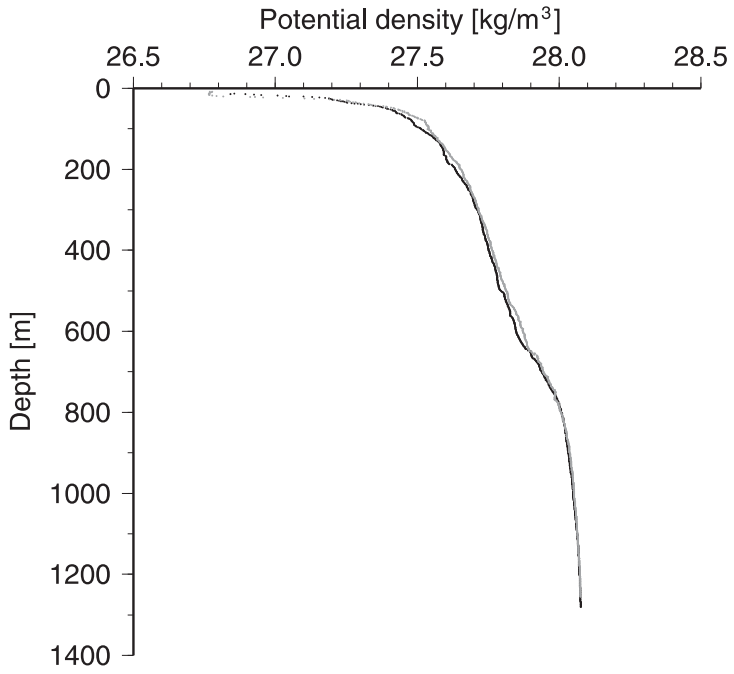

Figure 4-4. The potential density of the stations PS64/308 (black) and PS64/310 (gray) shows natural variation in the upper 200 m.

difference only in depths between 100 m and 200 m. The temperature profile shows higher variability and is the dominant source of the sound speed difference. Thus, natural variations of salinity and temperature are obvious over periods of 15 hours.

The depth and refraction of inclined sonar beams were calculated from echo travel time using the mean sound velocity of the water column. The survey area is quite flat and shows only small depth variations. Therefore, only changes of the mean sound velocity in depths greater than 1200 m affect the depth determination. The difference between the sound velocity profiles of the stations PS64/308 and PS64/310 is stable below 800 m and shows values around 0.2 m/s. The difference of the mean sound velocity is 0.18 m/s at depths below 1200 m. This corresponds to a depth difference of 20 cm at 1200 m. The difference results in a very small depth offset and does not affect the shape of the topography. Therefore, it was neglected in the subsequent processing.

4.4.3 Terrain modelling

Bathymetric data from the inner part of the survey which covers an area of 5.5 km by 3.5 km was used to generate a digital terrain model of the Håkon Mosby mud volcano. Due to overlapping of pre-formed beams of adjacent track lines, the depth data have an average density of 1.3 points/100 m^2. Small height variations of about 10 m in the survey area required some effort in data processing and modelling techniques in the course of data cleaning and terrain modelling. The presumed measurement accuracy of 1% of water depth indicates that surveying the terrain of the Håkon Mosby mud volcano could reach the limit of the multibeam system. However, the high data density required non-standard processing steps to be applied. Depth measurements of different quality, i.e. slant and near vertical beam angles are distributed evenly over the study area due to the dense spacing of the survey lines.

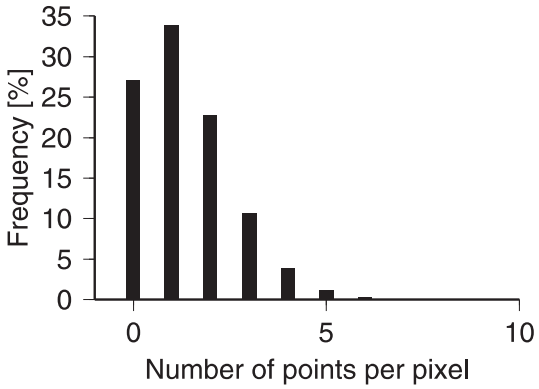

Figure 4-5. The histogram of the point density indicates the high point density of the study area.

In the standard processing, erroneous depth recordings (outliers) were rejected. An additional rejection criteria based on a two-fold statistical approach was also applied. Measurements were rejected when the depth differed by more than twice the standard deviation of the surrounding data. Subsequently, the standard deviation was re-calculated and depth data differing more than one standard deviation with respect to the surroundings were rejected in order to reduce measurement noise. Due to the particularly small height variations of the study area, it was difficult to distinguish between erroneous data and true depth information. In addition, the terrain model of the cleaned data was affected by track parallel artifacts. It is assumed that the main source of the artifacts is the rejection of the depth information of the outer beams. Therefore we decided to use the complete depth information of the data set and apply non-standard data processing.

The raw depth data were of good quality, since no clear outliers were detected. The depth data were only characterized by an increasing noise level towards outer beams. Therefore, all recorded data were used in the modelling process in order to retain the small scale depth information within the full data set. Due to the high point density we decided to use a 10 m grid size, although depth measurements did not coincide with all grid cells (Figure 4-5). The extension of the terrain model is limited to the region of multiple swath overlap. Depth values of the grid cells were calculated using inverse distance weighting, taking into account the relative position of the sounding within the multibeam swath, as well as the distance between sounding and grid cells. The gridding routine was developed earlier at the Alfred Wegener Institute for Polar and Marine Research and considers the accuracy characteristics of the Hydrosweep DS-2 swath. Depth measurements close to the grid cell and near center beam measurements were given a higher weight compared to outer beam depths and data from the limit of the search radius. The search radius is a dynamic variable and corresponds to the mean distance of the depth data within the swath, i.e. approximately 40 m in this area. These settings take into account the properties of the multibeam system. The resulting terrain model contains the entire depth information of the data. Due to the inclusion of all measured depth data, the terrain model and subsequently derived contour lines show a noisy appearance. In the next processing step a generalization was applied after the grid calculation in order to represent seafloor features appropriately. A slope dependent generalization technique was described in

Table 4-1. Areas and corresponding filters used during the generalization process.

Area	Filter technique
Central structure	3x3 binomial
Close surroundings	3x3 binomial, 5x5 binomial
Wider surroundings	3x3 binomial, 2 times 7x7 mean

Beyer et al. (2003b). Steep slopes and the crests of mounds are barely smoothed in contrast to flat areas that are more strongly smoothed. The surface slope of the Håkon Mosby mud volcano area is rather flat and therefore the slope dependent generalization technique was adapted to the characteristics of the study area. Little generalization was applied at the center of the Håkon Mosby mud volcano in contrast to stronger generalization in the surrounding area. Derived contour maps have been used for quality control during the generalization process and compared to the contours of the initial terrain model. Depth information contained in the generalized contour lines was evaluated visually to find the appropriate filter matrices. The filters used in different areas around the Håkon Mosby mud volcano are shown in Table 4-1. Low level 3x3 binomial filtering was applied to the entire terrain model to reduce measurement noise and preserve detailed structure. Outside the center of the Håkon Mosby mud volcano, additional generalization was realized utilizing a 5x5 binomial filter in the close surroundings and two times a 7x7 mean filter in the wider surroundings. The generalization of the surrounding area reflects the detail of a 50 m grid, which corresponds to the footprint of the sonar beams. The stronger generalization was chosen since significant small scale depth variations are not obvious in the surroundings of the Håkon Mosby mud volcano. Therefore, depth contours were adapted to the general morphology of the continental margin of that area.

Small depth offsets in the terrain model occurred at the transition between regions of different generalization. Therefore, a combination of the filters of adjacent regions was used to obtain a smooth transition and suppress artifacts in the contour maps and shaded views of the terrain model. The final generalized terrain model shows the bathymetry of the Håkon Mosby mud volcano and the surrounding area with increasing level of detail towards the center of the Håkon Mosby mud volcano (Figure 4-2).

4.4.4 Terrain model resolution

The pre-formed beams of the Hydrosweep DS-2 multibeam system have an apex angle of 2.3°. This corresponds to a center beam footprint of approximately 50 m at 1200 m water depth. However, two terrain models were determined using regular grid sizes of 10 m and 50 m based on the measured point density and the footprint size, respectively. For the detailed morphological interpretation based on the depth contours the 10 m grid is superior. The 50 m grid was determined for comparison based on the same input data and terrain modelling settings as the 10 m grid. Additional generalization was not applied because data density within the 50 m grid cells provided sufficient noise reduction. The 50 m grid was then resampled to 10 m resolution to ensure the identical geographic position of the grid cell values. This process produced the trend of the seafloor and that was then subtracted from the 10 m terrain model. The calculated differences represent both remaining noise and small scale morphology

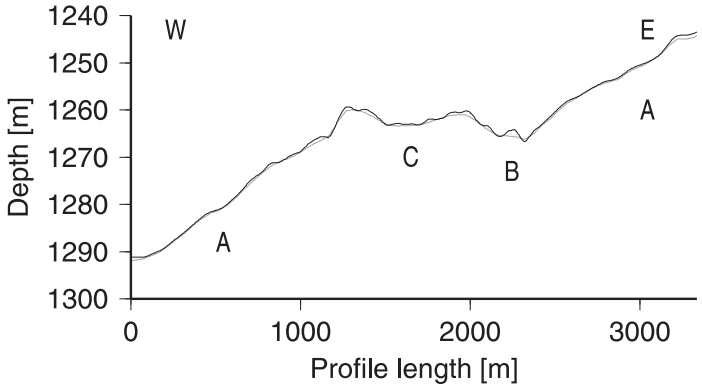

Figure 4-6. West-east depth profile across the Håkon Mosby mud volcano. Different morphological areas are visible, i.e. continental slope (A), circular embankment structure (B), central area (C).

covered by the 10 m terrain model. Visual investigations of 50 m ranging depth profiles based on the 10 m grid indicated depth variations of 0.5 m. It is assumed that these variations are dominated by morphological structures since weighting algorithms have been applied during the terrain modelling process to reduce noise. Depth differences between the 10 m terrain model and the 50 m terrain model are between -1.3 m and 2 m. Figure 4-6 shows a depth profile across the Håkon Mosby mud volcano based on the 10 m (black line) and 50 m (gray line) terrain model. The enhanced morphological detail is visible at the crater rim of the central area (C) and the circular embankment (B).

The statistical range of water depth variation was used to show the differences of the 10 m and 50 m grids quantitatively. It represents depth variations within the footprint of the sonar beams. Figure 4-7 shows the range of variation for the central structure (Figure 4-7a) and the surroundings of the Håkon Mosby mud volcano (Figure 4-7b). A median of variation of 0.15 m is visible for the strong generalized surrounding area, with only a few grid cells exceeding the 0.5 m difference. At the center of the Håkon Mosby mud volcano the variety of variation is up to 2 m with a median of about 0.6 m indicating surface variations within the 50 m footprint. Although it is a small value with respect to the measurement accuracy, morphological structures are represented in greater detail in the 10 m terrain model. This was not obvious because of the large footprint size of the pre-formed beams.

4.4.5 Accuracy assessment

The morphological structure of the continental margin in the vicinity of the Håkon Mosby mud volcano area is characterized by small depth variations. The general depth change is about 40 m trending in the southwest direction. The central structure of the Håkon Mosby mud volcano shows height differences of only ~10 m. Due to the accuracy limitation of the multibeam system (see section 4.4.1) a detailed assessment of the 10 m terrain model and its depth variations with respect to the depth measurements is necessary in order to evaluate the reliability of the terrain model. However, the results demonstrate that the resolution of the data is sufficient to map these small height variations.

The accuracy of the depth measurements was determined with respect to the 10 m terrain model. Weights, used during the terrain modelling process were not considered

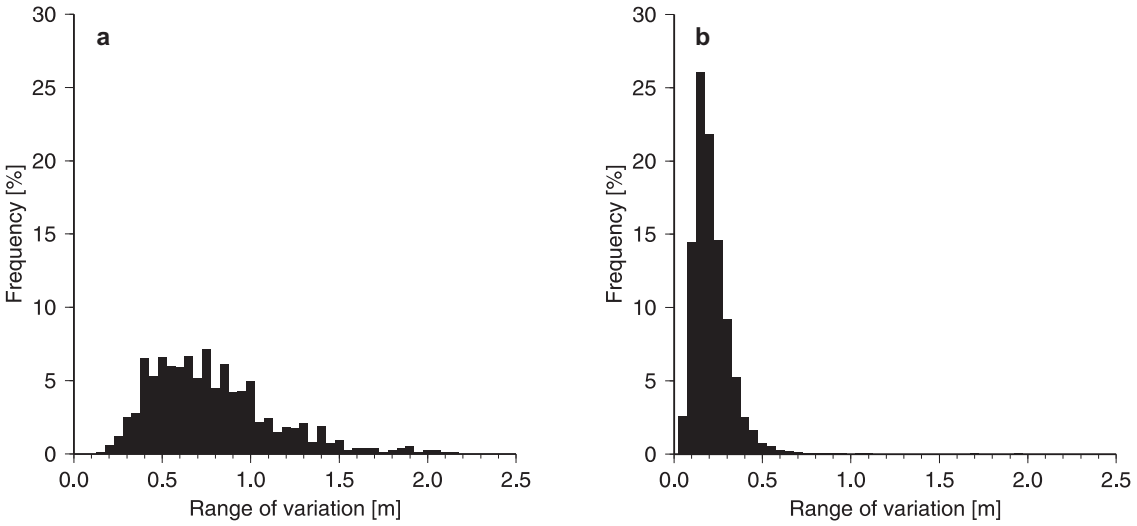

Figure 4-7. Range of variation within the 50 m footprint shows larger values at the center (a) of the Håkon Mosby mud volcano compared to the surroundings (b) due to different generalization methods.

because they are only used for terrain model calculations. The standard deviation of the multibeam measurements was determined with respect to the terrain model to be 5.6 m. This corresponds to an overall accuracy of 0.5% of water depth.

The accuracy of the terrain model was determined on a grid cell basis. Therefore, the residuals were combined with a 50 m grid, which provides enough data points to calculate statistics. It was found that the median is 5 m, i.e. 0.4% of water depth (Figure 4-8). Only four grid cells show lower accuracy, i.e. 1.1% and 1.2% of water depth.

The standard deviation determined for the individual pre-formed beams reflects the higher accuracy of the near vertical beams (lower than 0.3% of water depth) and reduced accuracy of the outer beams, i.e. 0.5% to 1% of water depth (Figure 4-9). Only the two outermost beams at the portside show lower accuracy. The inner 37 pre-formed beams, i.e. beam number 13-49, show accuracy values better than 0.4% of water depth. Degraded accuracy values of the outer beams are caused by the slant incidence angles of the sonar beams (higher noise level) and by the modelling process

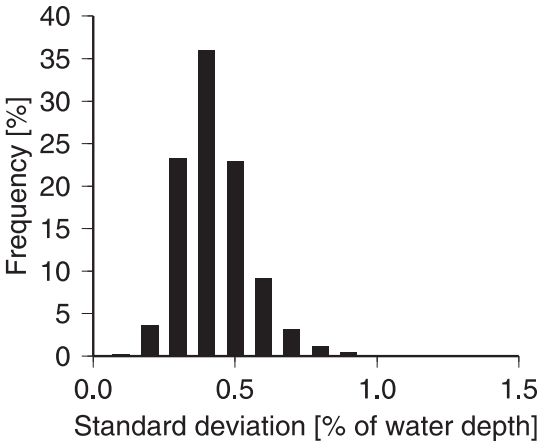

Figure 4-8. Histogram of the depth accuracy based on the grid cells. The median corresponds to 0.4% of water depth.

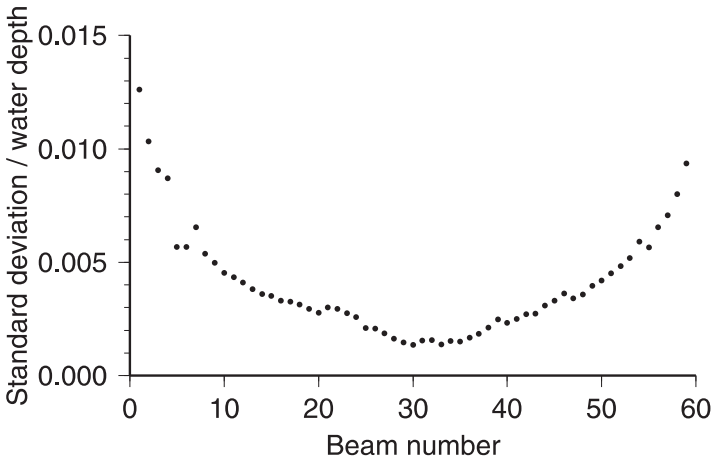

Figure 4-9. Beam wise accuracy values highlight the excellent accuracy values (<0.4% of water depth) for the beams 13–49.

which was designed to process all depth measurements to preserve small height variations. In addition, the outer beams had lower influence on the terrain model due to the weighting approach. Thus, outer beams affect the accuracy estimates due to their higher noise level.

In spite of the reduced accuracy of the outer beams they were included in the terrain modelling process to reduce track parallel artifacts. Figure 4-9 gives a realistic overview of the initial pre-formed beams accuracy since no editing was done prior to terrain modelling.

No significant difference is visible for the beam wise standard deviation values when using the terrain model without generalization as reference for calculating statistics. The maximum standard deviation difference is 0.01% of water depth at the center beams. This indicates that the process of clarifying morphology using terrain model filtering does not influence the noise level.

However, a circular structure of higher standard deviation values exists around the Håkon Mosby mud volcano. The location is correlated to the circular embankment (Figure 4-2 and Figure 4-6). Because the largest depth differences with respect to the terrain model are observed for the outer beams and the variation of the near center beam depth measurements is similar to those of other areas, it is assumed that the local micro topography and possibly seabed properties affect the depth determination of slant sonar beams. Thus, no significant artifacts are introduced into the terrain model in the area of higher standard deviation values.

4.4.6 Multibeam sidescan imaging

The Håkon Mosby mud volcano feature was first discovered on a 12 kHz sidescan image during a 1989-1990 SeaMARC II sidescan survey (Vogt et al., 1991). It shows stronger echo at the center of the volcano and a circular ring of lower reflectivity around the center.

Multibeam sidescan was recorded in parallel with depths during the RV *Polarstern* ARK XIX/3 bathymetric survey. The image quality and resolution is similar to the SeaMARC II data. Figure 4-10 shows the multibeam sidescan mosaic of the Håkon Mosby mud volcano central area extracted from the Hydrosweep DS-2 data (15 m

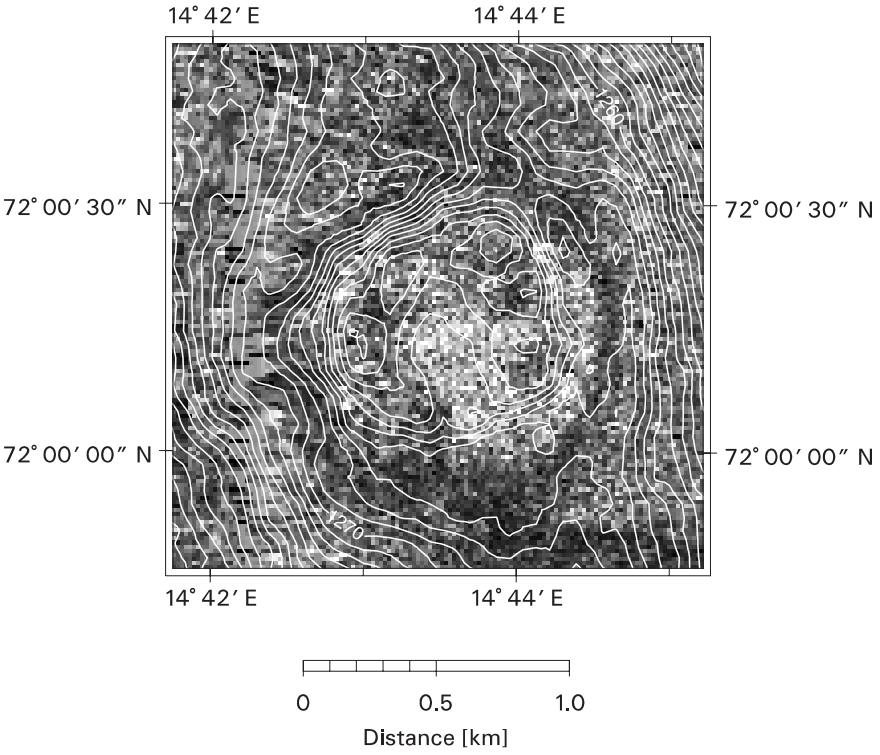

Figure 4-10. Multibeam sidescan of the Håkon Mosby mud volcano shows high amplitudes at the center (bright gray values) and lower amplitudes at the crater rim and the surrounding moat (dark gray values). Contour interval 1 m.

resolution) superimposed with contour lines (50 m terrain model). Stronger and weaker echo intensity is represented by bright and dark gray values, respectively. Four survey lines were selected to create the sidescan mosaic. For the selection of the lines an optimal ensonification direction of the central Håkon Mosby mud volcano was used as criterion. Two lines ensonify the Håkon Mosby mud volcano from an eastern direction and two lines from a western direction. Homogeneous image quality is achieved because data from the nadir part of the sidescan image have been avoided. Another criterion for line selection was their straightness, which results in homogeneous successive ping spacing and is the basis for good quality sidescan images. In order to correct for intensity decrease towards the outer beams, beam pattern have been taken into account during mosaicking. A comparison of sidescan data of the eastern and western ensonification direction in overlapping areas yielded similar gray value texture. This indicates that the direction of ensonification has only a minor influence on the gray values in this area. Thus, gray value variations in the combined mosaic are mainly caused by changing seafloor properties.

4.5 Results

The Håkon Mosby mud volcano is a shallow but remarkable morphological feature at the Norwegian-Barents-Svalbard continental margin. It has a circular structure and shows a distinctive rim in the northern part. In the area of the Håkon Mosby mud volcano, different morphological zones can be identified based on the generated terrain model (Figure 4-2 and Figure 4-11).

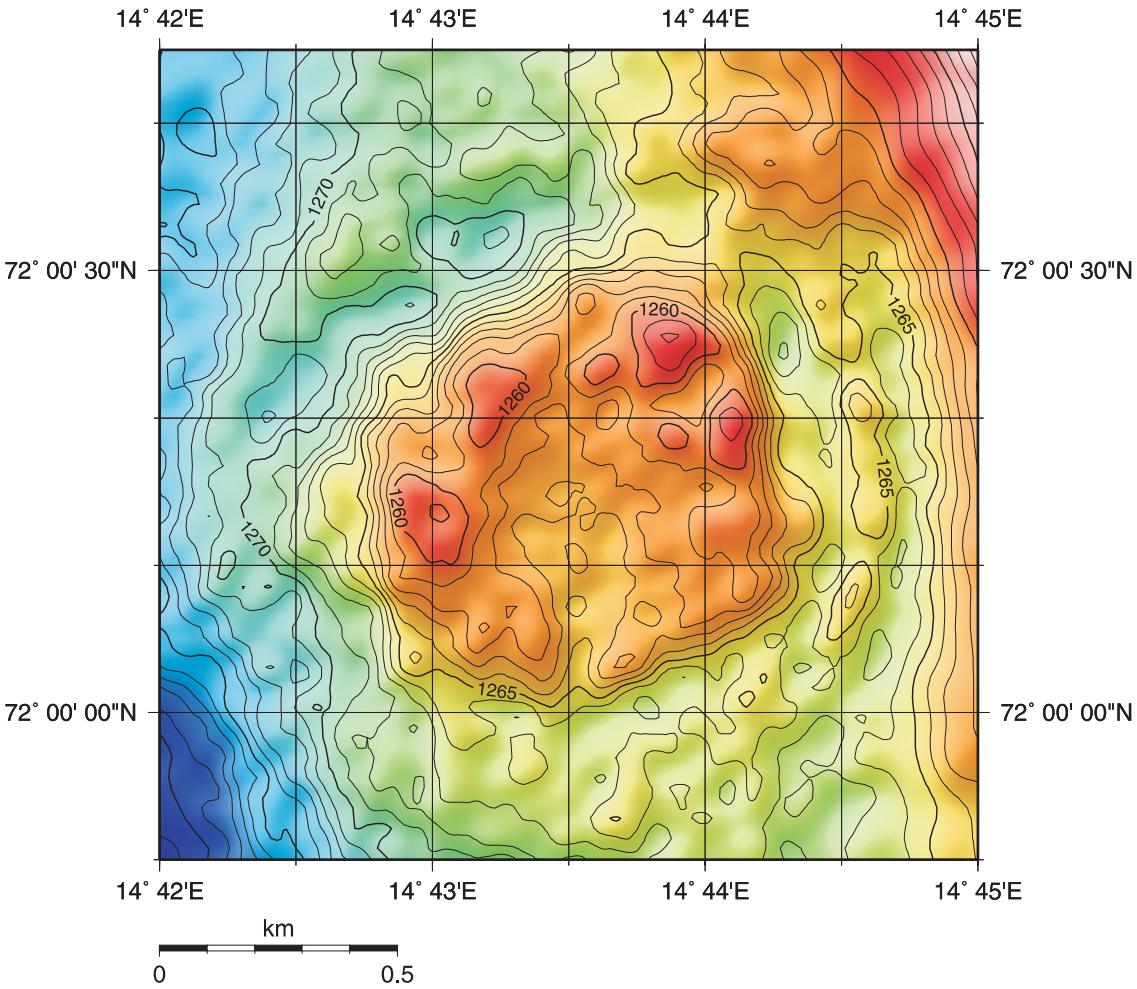

Figure 4-11. Detailed bathymetry of the center of the Håkon Mosby mud volcano. Contour interval 1 m.

The area of the Håkon Mosby mud volcano is situated on a gentle slope and is characterized by three zones. The central elevation of the volcano has a diameter of about 950 m and its rim shows a maximum relative height of 12 m. Around the central structure of the Håkon Mosby mud volcano a circular embankment 2 m heigh and with a breadth of about 100 m bordering the moat is seen (indicated as B in Figure 4-2). Its diameter is approximately 1350 m. The circular embankment is most pronounced in the northwest and east. The zone of the surrounding slope influenced by the Håkon Mosby mud volcano activity, indicated by a change in surface slope, has a diameter of about 2500 m. Figure 4-11 shows the center of the Håkon Mosby mud volcano in detail. Gray shading (illumination from northwest) enhances the identification of the circular moat and embankment structures.

A perspective view of the Håkon Mosby mud volcano area is shown in Figure 4-12. It is based on the 10 m terrain model with view directions from north and west for the upper and lower image, respectively (illumination from northwest). The rough appearance of the surface at the center of the Håkon Mosby mud volcano is due to the vertical exaggeration of 20.

The height of the volcano is greatest in the northern part of the rim and decreases towards the center and towards the south. Height differences between the northern volcano rim and the southern part are about 5 m. The central elevation forms a crater-

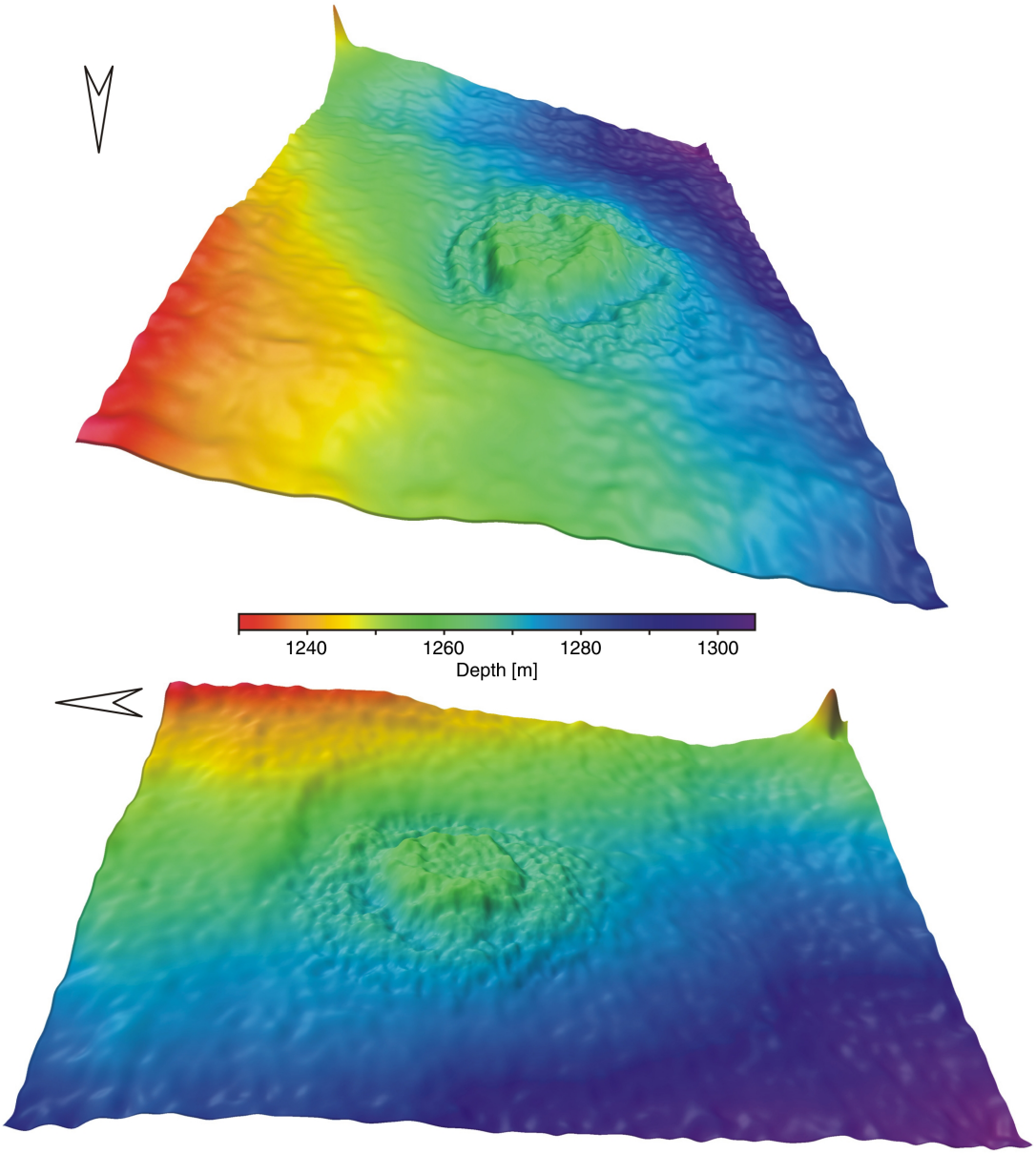

Figure 4-12. A 3-D perspective view of the Håkon Mosby mud volcano area. The view direction is from north and west for the upper and lower image, respectively. Vertical exaggeration 20.

like structure. The rim of the crater is most pronounced at the west, north and east sides. The southern edge of the Håkon Mosby mud volcano shows the smallest heights along with a less pronounced rim and indicates a narrow mud flow with a breadth of less than 100 m (Figure 4-11). However, there is no indication that the mud flows continue beyond the central volcano elevation, although sidescan images clearly indicate the extent of mud flows to the south and southwest (Vogt et al., 1999a). The center of the Håkon Mosby mud volcano is characterized by a flat area with a small slope (about 0.3°) towards the south. The height difference between the flat area and the crater rim does not exceed 5 m.

A west-east depth profile across the Håkon Mosby mud volcano is given in Figure 4-6. Different sections are visible which correspond to the continental slope (A), the circular embankment structure (B), and the central area (C). Greater detail is visible

for the profile based on the 10 m terrain model (black line) compared to the 50 m terrain model (gray line) (see section 4.4.4).

The mean surface slope of the continental margin within the study area is about 0.8°. The slope direction points approximately in a southwest direction and shows a distinct circular indentation in the surroundings of the Håkon Mosby mud volcano. The flanks of the Håkon Mosby mud volcano central elevation show a slightly steeper slope of up to 5° with an average of 3°. Down slope of the Håkon Mosby mud volcano structure the average slope is 1.3°.

A correlation of morphology and reflectivity variation can be identified from the sidescan image (Figure 4-10). The center of the Håkon Mosby mud volcano shows the brightest gray values extending to the south. Dark gray values are observed at the crater rim and at a circular ring around the central structure. This ring corresponds to the circular moat in the north, west and south. However, the moat shows bright gray values in its eastern part while low gray values of the ring extend to the circular embankment. The higher gray values at the east seem to originate from the center and extend via the southeastern edge of the central structure towards the north. The Håkon Mosby mud volcano shows a larger variability and higher reflectivity in the center part compared to the sidescan of the surrounding sediments.

4.6 Discussion

Though the location of the Håkon Mosby mud volcano was entirely mapped by two overlapping survey lines during expedition ARK XVIII/1, the data density was not sufficient to comprehend the detailed morphology. It was realized that the small height variations of the Håkon Mosby mud volcano could only be picked up by dense line spacing and large overlapping of multibeam swathes as performed in this study.

The depth variations of this small and shallow submarine feature are at the limit of the resolution of the ship-borne multibeam system. However, due to high point density and the specific data processing, it was possible to map the minor topographic structure of the Håkon Mosby mud volcano with appropriate resolution. The derived terrain model is a 10 m grid which allows mapping of the small scale topography. From this survey an accuracy of depth measurements between 0.2% and 1.0% of water depth was achieved for most measurements. Only the two outermost beams show less accuracy. Due to the multiple overlap of survey lines, typical multibeam artifacts were avoided.

The analyzed bathymetric data show the circular structure of the Håkon Mosby mud volcano. The moat between the crater rim and the circular embankment may be due to subsidence of surrounding sediments as result of mud extrusion (Milkov et al., 2004). The adjacent circular embankment may have developed by tilting of sediments during subsidence. ORETECH 30 kHz sidescan data (Vogt et al., 1999a) indicate that the close and western surroundings of the Håkon Mosby mud volcano are influenced by mud flows, whereas Milkov et al. (2004) state that sediments of the moat are similar to the sediments outside the Håkon Mosby mud volcano. Hydrosweep multibeam sidescan shows a significant gray scale difference for the center area and the surrounding moat indicating different acoustic sediment properties which may be related to the existence of gas or gas hydrate in the sediment.

The most active area of the Håkon Mosby mud volcano is located in the northern part of the flattish center where sediment and gas are extruded (Milkov et al., 2004). However, there is no consensus on the source of the Håkon Mosby mud volcano (Vogt et al., 1999b). Vogt et al. (1999a) suggested a sequence of events starting with an earthquake that triggered the slide related to the existence of the Håkon Mosby mud volcano, causing sidewall collapse and sub-bottom sediment destabilization. Deep-tow video and still photography revealed different seabed coverage at the center of the Håkon Mosby mud volcano with concentric zoning, corresponding to the morphology (Milkov et al., 1999). The inner center is characterized by seafloor dominated by white patches covering the seafloor (bacterial mats and/or gas hydrate), smooth seafloor and seafloor with micro relief. This separation of the flattish center cannot be discerned using the 10 m terrain model. The crater rim has hummocky morphology and is populated by tube worms (Pogonophora) (Milkov et al., 1999). For this area lower reflectivity is observed in the sidescan data (Figure 4-10). The concentric zonation is also visible in other parameters such as heat flow, geothermal gradient and pore water composition (Milkov et al., 2004).

Hydrosweep DS-2 multibeam sidescan shows a spatial resolution similar to SeaMarc II sidescan data. Structures such as the strong reflectivity zone at the center area of the Håkon Mosby mud volcano and low reflectivity at the crater rim can be distinguished. These zones of different reflectivity are also visible in the ORETECH sidescan data collected 1996 on board RV *Logachev* (Vogt et al., 1999b). Higher resolution was achieved by the ORETECH system since it was towed 40 m above the seafloor and operates on a higher frequency (30 kHz). The ORETECH sidescan shows detailed morphology at the crater rim and homogeneous strong reflectivity at the central part of the Håkon Mosby mud volcano. Reflectivity differences between Hydrosweep DS-2 and ORETECH sidescan exist in the southern part of the Håkon Mosby mud volcano where ORETECH sidescan shows high reflectivity and Hydrosweep DS-2 sidescan indicates low reflectivity, similar to the surrounding moat. The morphological structures that are visible in the ORETECH sidescan data were achieved using an ensonification geometry of slant incidence angles. Therefore the combination of reflections and shadows dominate the sidescan image. In contrast, the Hydrosweep DS-2 sidescan mainly represents reflectivity variations caused by varying seafloor properties.

4.7 Summary

The topography and morphology of the Håkon Mosby mud volcano was acquired utilizing Hydrosweep DS-2 multibeam system onboard RV *Polarstern* during the ARK XIX/3 expedition. As a pre-condition, dense line spacing and low ship speed were used during the survey, in contrast to typical bathymetric surveys, in order to record dense and detailed depth data in this area.

Sound velocity profiles of the water column were recorded utilizing a CTD device. CTD profiles before and after the survey showed significant differences in depths between 50 m and 200 m, indicating natural fluctuations. Because the study area is characterized by small depth differences, the effect of variation of the mean sound velocity on depth was negligible.

For the terrain modelling all depth measurements were used including the outer preformed beams in the overlapping areas to preserve even small height variations. Appropriate weighting, depending on the location of the sonar beam within the swath and the distance between depth measurement and grid cell, was used to calculate the 10 m terrain model. Generalization was applied to represent the seafloor topography appropriately. Small height variations were mapped precisely and represent small scale structures at the center of the Håkon Mosby mud volcano. The surrounding area was generalized representing the resolution of a 50 m terrain model.

The Håkon Mosby mud volcano has small lateral extension. The height variation at the center of the Håkon Mosby mud volcano is at the limit of the accuracy and resolution of the utilized multibeam system. The accuracy achieved from this survey is estimated between 0.2% and 1% of water depth.

Accuracy analyses of the depth measurements demonstrated, that morphological structures are well represented in the terrain model. Therefore, the final 10 m terrain model is considered as a reliable terrain model of the Håkon Mosby mud volcano area. Thus, the small scale morphology of the Håkon Mosby mud volcano is represented very well, mainly as a result of high data density and measurement accuracy.

Based on the morphology, three segments of the Håkon Mosby mud volcano can be identified: a) crater-like center of about 1 km diameter showing 10 m height variation, b) circular embankment of about 100 m breadth, 2 m height and 1350 m diameter, c) surrounding area influenced by the mud volcanism, characterized by a different surface slope compared to the larger continental margin, 2.5 km diameter. The multibeam sidescan image reveals stronger echoes at the center of the Håkon Mosby mud volcano and lower echo intensity at the surrounding moat, indicating varying sediment properties.

The described 10 m terrain model provides a homogeneous data set of the Håkon Mosby mud volcano and the surrounding area. It represents a major improvement for morphological interpretation and analyses of processes related to deep-water mud volcanism compared to existing bathymetric maps presented for example in Vogt et al. (1997), Ginsburg et al. (1999) and Milkov et al. (2004). Detailed bathymetry of the study area is now available for future studies that require accurate depth coordinates for a proper positioning of scientific equipment at the Håkon Mosby mud volcano.

4.8 Acknowledgements

The RV *Polarstern* expedition ARK XIX/3 was jointly organized by the Alfred Wegener Institute for Polar and Marine Research and the French Research Institute for Exploitation of the Sea. We are grateful to the captain and the crew of RV *Polarstern* for their cooperative efforts during this cruise. We would like to thank H. Rohr for operating the CTD device.

5 High resolution bathymetry of the eastern slope of the Porcupine Seabight*

Andreas Beyer, Hans Werner Schenke, Martin Klenke, Fred Niederjasper

Alfred Wegener Institute for Polar and Marine Research (AWI), Columbusstraße, 27568 Bremerhaven, Germany

Keywords: bathymetry, multibeam, carbonate mounds, Porcupine Seabight, Gollum Channel System

5.1 Abstract

The topography of the eastern margin of the Porcupine Seabight was surveyed in June 2000 utilizing swath bathymetry. The survey was carried out during RV *Polarstern* cruise ANT XVII/4 as part of the GEOMOUND project. The main objective was to map and investigate the seafloor topography of this region. The investigated area contains a variability of morphological features such as deep sea channels and giant mounds. The survey was planned and realized on the basis of existing data so as to guarantee the complete coverage of the margin. In order to achieve a resolution of the final digital terrain model (DTM) that meets the project demands, data processing was adjusted accordingly. The grid spacing of the DTM was set to 50 m and an accuracy better than 1% of the water depth was achieved for 96% of the soundings.

5.2 Introduction

A high precision multibeam survey, covering the eastern slope of the Porcupine Seabight, was performed with the German RV *Polarstern* during the cruise ANT XVII/4 within the framework of the GEOMOUND project (GEOlogy of carbonate MOUNDs). The survey was carried out between 11 and 16 June 2000. The GEOMOUND project focuses on the geological evolution of giant, deep-water carbonate mounds in the Porcupine Basin and the Rockall Trough off western Ireland. A number of large carbonate mounds have been earlier identified in the Porcupine Basin by seismic profiles (Hovland et al., 1994). In order to understand their structure and genesis as well as the processes which exist in conjunction with these mounds, the bathymetry of the region has to be known in detail. For this reason, the survey was performed in combination with sub-bottom profiling.

The goals of the survey were primarily to create a large scale bathymetric chart of the mound and the canyon areas along the slope, to create a mosaicked sonar image from the multibeam sidescan data, and finally to investigate the scientific benefit of calibrated backscatter data derived from multibeam measurements. Calibrated backscatter data can be used to derive information on the seafloor surface, for

* Beyer, A., Schenke, H.W., Klenke, M. and Niederjasper, F., 2003b, High resolution bathymetry of the eastern slope of the Porcupine Seabight, Marine Geology 198, 27–54, doi:10.1016/S0025-3227(03)00093-8.

example, on grain size. Changes in the seafloor roughness can be linked to bathymetric features which will be the topic of a separate publication. This contribution focuses on the swath bathymetry and its results.

5.3 Methods and data

The area of investigation is part of the European continental margin west of Ireland. Prior to track planning, the existing bathymetric data in this region were evaluated. The survey lines were planned mainly on basis of the depth contours extracted from the GEBCO Digital Atlas 1997 (GDA 97) (GEBCO, 1997). Due to considerable morphological variabilities within the area of investigation and in order to minimize depth changes along the survey lines, the tracks were planned parallel to the slope. The spacing between adjacent lines was chosen to realize 10% overlap between adjacent swathes, and, consequently, coverage of the entire area. In order to keep the ship on the tracks, differential GPS was used for navigation. During the survey, several corrections to the preplanned track lines were required because of the coarse depth data available from the GDA 97.

The survey was completed in 4.5 days. It covered an area of approximately 2500 square kilometers with 14 track lines of approximately 130 km length. The weather conditions were moderate with a wind velocity of about 10 m/s mostly coming from southwestern direction, foggy air and rather strong groundswell during the first part of the survey. The average ship's speed was about 10 knots.

During the survey of the first line, sediment samples from the seafloor were collected using a multicorer. Two profiles of conductivity, temperature, and depth (CTD) were measured in order to calibrate the sound velocity data needed for the correction of slant sonar pre-formed beams (PFBs). These profiles are located on the southern edge and in the middle part of the survey area.

5.3.1 Equipment

The equipment consisted of the hydrographic multibeam survey echosounder Hydrosweep DS-2, the parametric narrow-beam deep sea sub-bottom profiler Parasound, and the CTD instrument SEACAT profiler SBE 19plus.

The multibeam system Hydrosweep DS-2 records depth measurements, multibeam sidescan and echo amplitudes. It operates with a sonar frequency of 15.5 kHz (Gutberlet and Schenke, 1989). Depths from 10 to 11,000 m can be measured. In total, 59 PFBs, covering each 2.3°, form the sonar swath with an apex angle of 90°. Thus, the center lines of adjacent PFBs are about 1.53° apart. Due to the fixed PFB angle, the footprint size changes with depth and is approximately 4% of the water depth near the center beam and 7% at the outer beams. Hydrosweep DS-2 is capable of switching between survey mode and calibration mode. In the calibration mode depths are measured along the ship's longitudinal axis instead of athwartship in the standard survey mode (Figure 5-1). This method enables determining the mean sound velocity of the water column which can be used to correct the slanting PFBs for refraction. However, information about the water column was derived by CTD measurements. The expected accuracy of Hydrosweep DS-2 depends on water depth and is given by the manufacturer as 1% of the water depth.

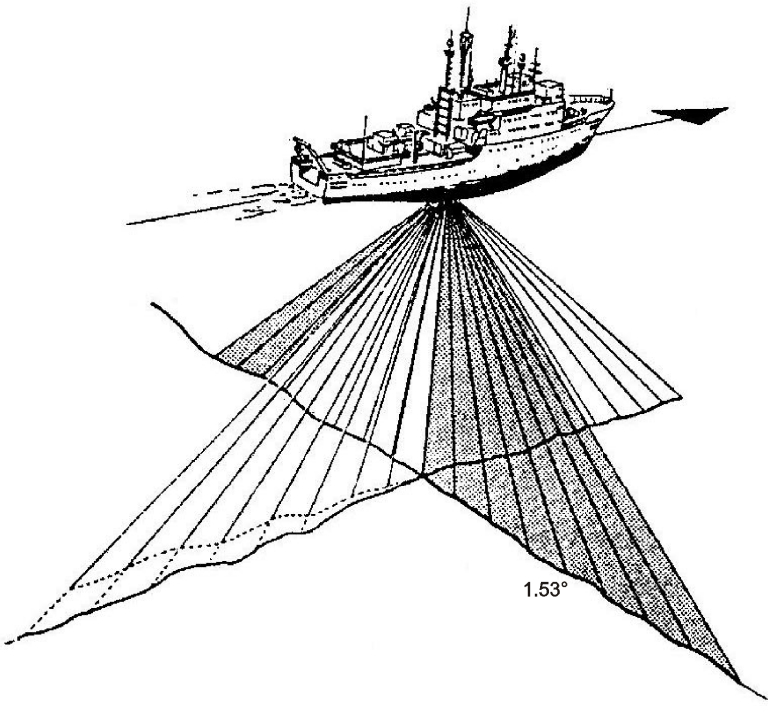

Figure 5-1. A functional sketch of Hydrosweep DS-2 (Grant and Schreiber, 1990). The fan along the ship's length axis is only used in the crossfan calibration mode. For calibration, slant PFBs of the calibration fan are compared with center PFBs of the athwartship fan. The PFBs are approximately 1.53° apart.

Sub-bottom profiling was performed along all lines using the Parasound to collect information about the stratigraphic structure of the seafloor sediments. The system uses the parametric effect in which two high frequency source signals interfere and generate a lower frequency pulse that retains a narrow beam width (Grant and Schreiber, 1990). During this survey, one frequency was fixed at 18 kHz and another one was set to generate a 4 kHz pulse. This low frequency transmission pulse ensures a greater penetration into the sediment. The apex angle is approximately 4° (Kuhn and Weber, 1993). The narrow apex angle provides high resolution data but also results in a reduced reverberation on steep slopes. Depending on the type of sediments and water depth, it is possible to penetrate sedimentary layers to a depth of up to 100 m with a vertical resolution of up to 30 cm.

The CTD SBE 19plus was used to obtain physical information in the water column. It is a self-powered mini-CTD that measures conductivity, temperature and pressure down to 7000 m depth. It records data (4 Hz data acquisition rate) in FLASH RAM memory. The accuracy of salinity, temperature and depth is 4 ppm, 0.005°C, and 1.4 m, respectively (Sea-Bird, 2001). This accuracy is suffcient for the sound velocity profile (SVP) determination in deep sea bathymetry.

During the entire cruise real-time differential GPS (RT D-GPS) was used for navigation, which provides an accuracy of 3-5 m for positioning. Thus, it was easily possible to follow the determined survey lines and to ensure the overlap of neighboring swathes.

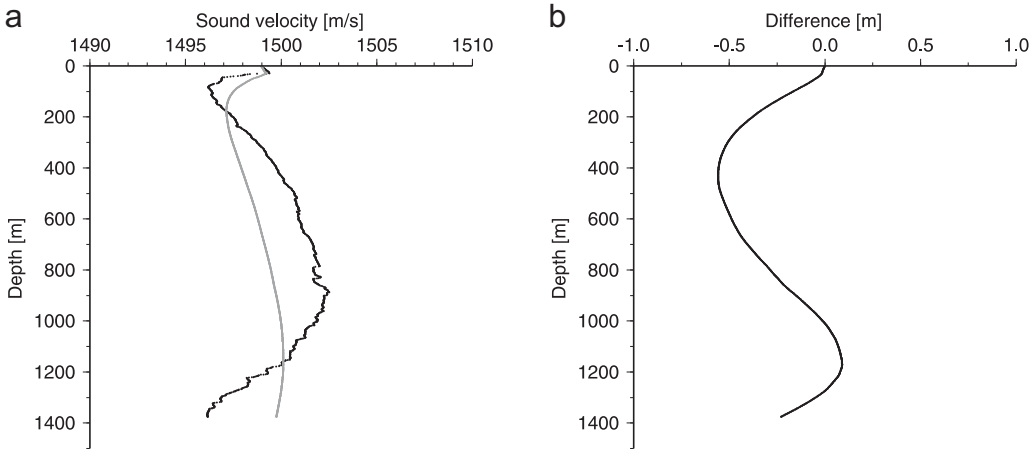

Figure 5-2. **a** The sound velocity profile obtained from the CTD profile (black). The gray line shows the mean sound velocity of the water column (integrated over the depth range). **b** Difference between depths calculated using the sound velocity profile and depths normalized to 1500 m/s sound velocity. Negative differences mean that the normalized depths show larger depths.

5.3.2 Sound velocity profile

The multibeam sonar system Hydrosweep DS-2 measures the sound travel time of acoustic pulses from the ship to the sea bottom and back. Generally, the corresponding depths are calculated using the mean sound velocity in the water column. The SVP utilized for this process is determined from CTD measurements using the formula of Chen and Millero (1977). Sound velocity changes in the water column are applied to model the refraction of slant sonar ranges. The SVP can significantly vary between different locations in the oceans. The spatial variation can only be taken into account when CTD profiles are measured in regular intervals in the survey area.

Since SVPs, which are utilized to calculate the local mean sound velocity, are not available in most cases, depth determination is generally performed applying the standard sound velocity value of 1500 m/s over the entire survey area. These values are called ‘soundings’.

The DTM presented in this paper was derived from soundings. The refraction correction for the slant sonar beams was calculated from the SVP based on the local CTD measurements. The ‘true’ depths can be calculated by using actual SVPs or values from standard sound velocity tables like those of Carter and Matthews (1980).

This procedure of creating a homogeneous bathymetric chart enables the scientific user to apply a locally observed SVP for the determination of ‘true’ water depths. Generally, experience shows that especially deep sea sonar measurements from different vessels are more consistent when the depths have been determined with a sound velocity of 1500 m/s.

The comparison of the two measured CTD profiles indicates a difference of 1 m/s mean sound velocity and no difference in refraction. This is not relevant for the DTM due to the application of 1500 m/s sound velocity. Thus, the deeper ranging CTD profile was used.

However, the DTM of the investigated area is hardly affected by the difference between the mean sound velocity and 1500 m/s. Figure 5-2a shows the measured SVP (in black) and the corresponding mean sound velocities integrated over the depth

range (in gray). The graph in Figure 5-2b documents the depth difference determined from the observed sound velocities and the standard 1500 m/s. The largest depth difference is 0.6 m and occurs near 430 m depth. The graph demonstrates that the depth difference between the soundings and depths obtained utilizing SVP in this region is less than 0.1% of the water depth. With regard to the accuracy of the multibeam data this difference is negligible in the investigated area.

5.3.3 Data processing

The modelling process of the final DTM requires proper multibeam and navigation data input. Hence, prior to the modelling, the ship's position and all soundings were thoroughly analyzed and checked in order to remove systematic effects and data outliers. In particular, a few survey lines which cross steep slopes were fudged by the 'omega effect' (de Moustier and Kleinrock, 1986). This occurs when the echo of the beam pattern's side lobe reaches the transducer prior to that of the main lobe. The measurements are distorted towards smaller depth which causes the contour lines to take the shape of a capital omega.

The data cleaning process was done utilizing automated and manual error detection techniques with Hydrographic Data Cleaning Software. First of all, the data were examined by checking each multibeam swath visually. During this step, obviously wrong measurements were rejected. Afterwards an automatic quality control was performed based on the standard deviation of the data. In order to identify incorrect soundings, the standard deviation of a subset of soundings was computed by creating a simple mean surface. For each sounding a classification value was determined depending on the standard deviation of the mean surface and its deviation from the mean surface. The classification level was set to the value two, which predominantly rejects erroneous soundings within areas of overlapping swathes. This algorithm was applied twice successively. Because the soundings are homogeneously distributed and neighboring swathes overlap, the use of classification values for data examination is an effective technique (CARIS, 1998).

The cleaned multibeam data form the basis for modelling the seafloor topography. Due to the high data density and evenly distributed data points, for this particular data set a raster digital terrain model (DTM) had advantages over a triangulated irregular network. The final DTM served as a base for generating the depth contours of the accompanying bathymetric chart.

The individual PFBs of the multibeam system have a fixed apex angle, meaning that the spacing of data points at the seafloor increases with water depth and off track distance. Water depths range from 350 to 2300 m within the investigated area. Hence, the PFB spacing on the seafloor varies between 10 and 60 m around the center beam. The maximum value of approximately 110 m only exists in the outer PFBs at a depth of 2300 m. Due to the uniform ship's speed during the survey (10 knots), the point spacing along track is approximately 40 m. Since the survey lines overlap and the major part of the area is shallower than 1700 m, the area is covered by a point density which provides at least one sounding within a radius of 25 m. As the entire area had to be modeled in one single DTM, the chosen grid spacing was 50 m. This size ensures full coverage and retains the full information content of the soundings both in deep and shallow waters. Thus, the mound structures and channels are well represented.

Several tests have been performed in order to generate an optimal DTM from the multibeam data. In this respect the major task was to take the characteristics of the multibeam data into account, i.e. the measurements of the outer PFBs are less accurate than those of the center PFBs. Therefore, a DTM routine, developed earlier at the AWI, was utilized and different settings were investigated (e.g. weighting and search radius).

The number of neighboring soundings inside a given search radius, which is used to determine a grid point depth, is significant for surface modelling. In the case of the search radius being too small, remaining noise cannot be reduced sufficiently, whereas a large search radius could smooth real surface characteristics. In addition to the data point selection, the soundings were weighted depending on the distance between grid point and sounding position. This weight algorithm also considers the typical characteristics of the multibeam system, i.e. the relative position of the soundings within the swath is weighted accordingly. Due to the depth dependent point density, the search radius is a dynamic variable and was set to twice the mean horizontal distance between the footprints of two neighboring PFBs. This prevents gaps in the DTM even when data points were rejected during the data cleaning process. In addition to the weight algorithm, a grid point depth is only computed if data points are uniformly distributed around the grid point. To ensure this, the soundings need to be spread over 3 of 4 quadrants around the grid point. This procedure provides a good representation of the data.

The final DTM has been further processed using Arc/Info which provides full advantage of a Geographic Information System. Contour lines are accepted as the standard visual representation of a continuum like the seafloor. They were derived from the DTM. Despite the effort of data cleaning, the contour lines seem to be affected rather strongly by a noise in the DTM. In order to reduce this effect, a slope dependent generalization algorithm was developed. This approach takes into account that the signal-to-noise ratio degrades in plane regions, i.e. the contour lines are more affected by noise. The generalization algorithm was designed to affect the original DTM rather than the contour lines. The final contour lines were derived from a generalized DTM. For the realization of the algorithm, the DTM was subdivided into five slope classes. In order to prevent mound tops and depressions from being filtered, the surface slope of the surroundings was also considered during classification. The grid points of each class were filtered with respect to their neighborhood using filter matrices. The slope class limits and their respective filters are listed in Table 5-1. The class containing the steepest slope was not filtered because the signal-to-noise ratio is relatively high and thus noise is not apparent in the contours near mounds and channel flanks. The class

Table 5-1. Surface slope classes and corresponding filter matrices used in the generalization process of the DTM.

Class number	Surface slope	Filter technique
1	> 15°	none filtering
2	< 15°	3 x 3 binomial
3	< 6°	5 x 5 binomial
4	< 3°	5 x 5 mean
5	< 1.7°	7 x 7 mean

containing the smallest slope was filtered rather strongly because the contour lines were obviously affected by noise (e.g. a flat area west of the mound region in the north and at the bottom of the channels). The slope class limits were adapted to this DTM of the investigated area and they are not applicable offhand for other DTMs.

Using this filtering algorithm, most of the noise of the contour lines was removed. However, distinguishing between noise and a weak signal is very difficult, and few small systematic effects may still affect the contour lines. This is visible in the area around 50°50'N which shows even slopes. The resulting contours still seem to be affected by the ship's survey lines. On single contour lines these effects cannot be observed because they are only recognizable in combination. Thus, it is nearly impossible to detect systematic errors in the original data and to remove them utilizing an automated technique. Overall, this generalization technique produced an optimal result and we consider the morphologic structures are well represented by the bathymetric contours.

In order to evaluate the final DTM, a sectoral DTM with 10 m grid size was processed in the northern, shallower part of the working area. Within the deeper waters (>1000 m), the point density from the multibeam survey is not sufficient for a grid spacing smaller than 50 m. Besides a reduced generalization of the 10 m DTM, a significant information gain is not evident. However, additional surface properties could be obtained by investigating the seafloor slope. Even small depth changes which are not observable in the contour lines become visible that way and could provide clues for investigating physical processes at the seafloor such as erosion. However, attention must be paid to the accuracy of the swath bathymetry, regarding to the signal-to-noise ratio.

5.3.4 Sub-bottom profile

The sub-bottom profiler Parasound recorded data throughout the survey. In this investigation, Parasound was primarily used to identify probable locations of carbonate mounds. Besides mounds on the seabed surface, buried reefs embedded in drift sediments exist on the eastern slope of the Porcupine Basin (Henriet et al., 1998; 2000). Only a few mounds were directly crossed by the survey lines because the exact mound positions were not known prior to the survey. First visualizations of the data indicate a poor penetration into the steep mound areas, but a good penetration (20-50 m) was observed into the sediments of the Porcupine Seabight.

Due to the narrow apex angle of Parasound, the penetration into the seafloor and sediment layers can be reduced due to slant surfaces. The acoustic energy is partly reflected at the surface. In particular, on slopes steeper than 4° a reduced reverberation is observed. Naturally, mounds have a relatively large surface slope which reduces penetration. Due to their structure, the penetration into carbonate mounds is also reduced. Thus, it is difficult to recognize a carbonate mound by means of parametric echosounding only. Only measurements directly on top of a mound can distinguish these effects.

Figure 5-3 shows a sub-bottom profile that indicates a carbonate mound. Accidentally this mound was crossed directly on top. Poor penetration exists on the rather flat top of the mound, and only the surface of the mound seems to reflect the acoustic pulse. This is characteristic evidence that the mound is a carbonate mound

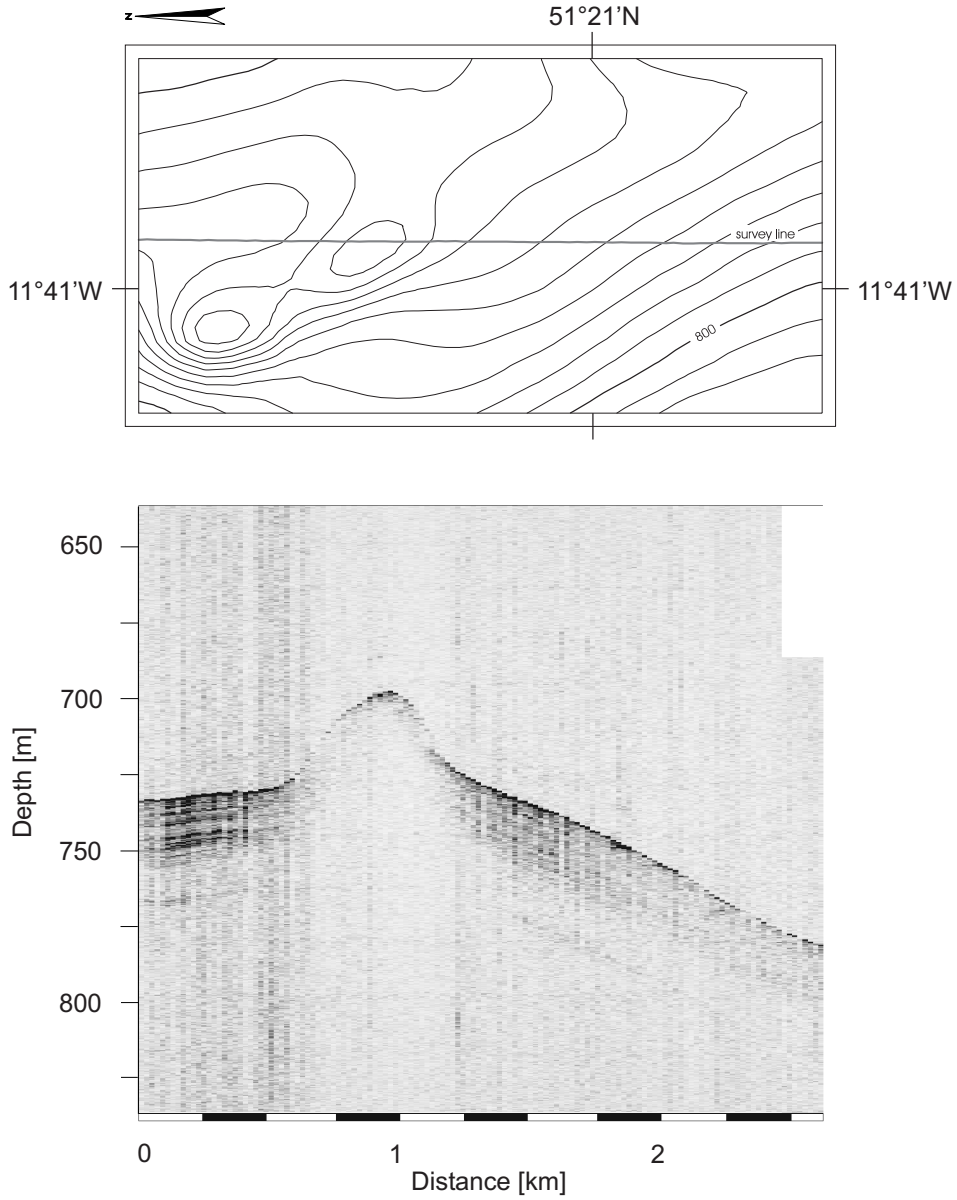

Figure 5-3. Sub-bottom profile of a mound and the respective bathymetry (10 m contour interval). Low Parasound penetration on the flat top of the structure indicates a carbonate mound.

(low penetration due to structure). In addition, the intensity of the echo is lower compared to the surrounding sediments meaning that part of the energy has been absorbed or reflected elsewhere. The reduced reverberation due to the slope of the mound is visible on its flanks. The reverberation is also reduced near the sediments on the right part of Figure 5-3. The surface slope (about 5.5°) is similar to the slope of the mound flanks. But, in contrast, the sediment layers are still visible even though they are weak.

The sub-bottom profile in Figure 5-4 shows the same mound characteristic as the one displayed in Figure 5-3. North and south of this feature the sediment is evenly layered. On the mound itself penetration is reduced. However, a mound occurrence is not obvious in the bathymetry. Only a weakly pronounced ridge exists at this location. On the other hand, the mound structure seems to continue below the surface as a

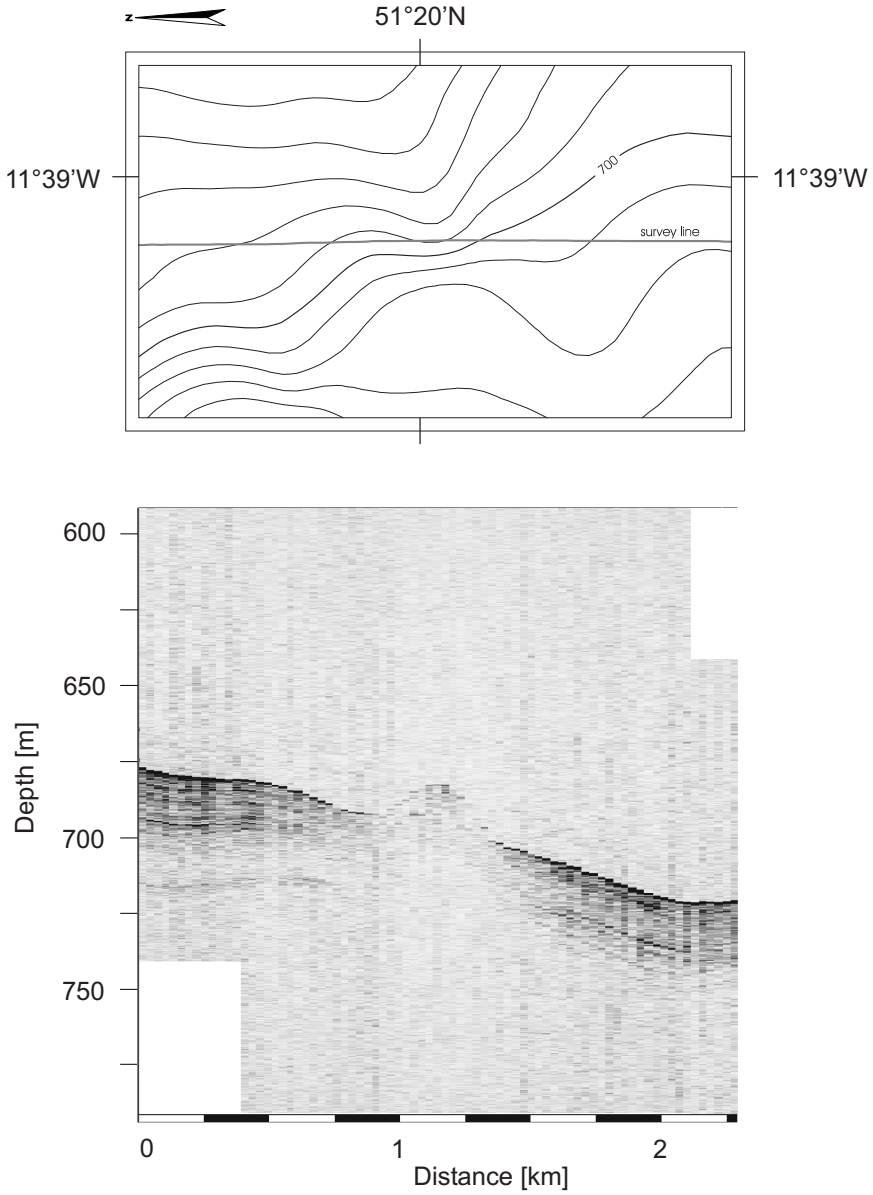

Figure 5-4. Sub-bottom profile of a feature similar to Figure 5-3 (10 m contour interval). This feature looks like a carbonate mound although the bathymetry does not indicate a mound feature. The structure seems to continue below the surface and is probably partly buried by sediments.

structure similar to the mound in Figure 5-3, i.e. a buried carbonate mound. The surroundings of the mound may be covered by sediments. Such buried mounds were described earlier in the Porcupine Basin (Henriet et al., 1998). However, this interpretation needs further investigation because the surface slope reaches up to 9° and reduces penetration.

Only few mounds are as clearly identifiable by direct observation in the bathymetry and the sub-bottom profiling as shown in Figure 5-3. In the bathymetry, mound morphology can be reliably detected. But without further investigation, for example by seismic profiling and coring, it is hardly possible to identify a carbonate mound. Because mounds are highly correlated with surface slope, it is difficult to identify carbonate mounds exclusively based on the Parasound data. They can be recognized only next to low surface slope areas. The examples in Figures 5-3 and 5-4 provide

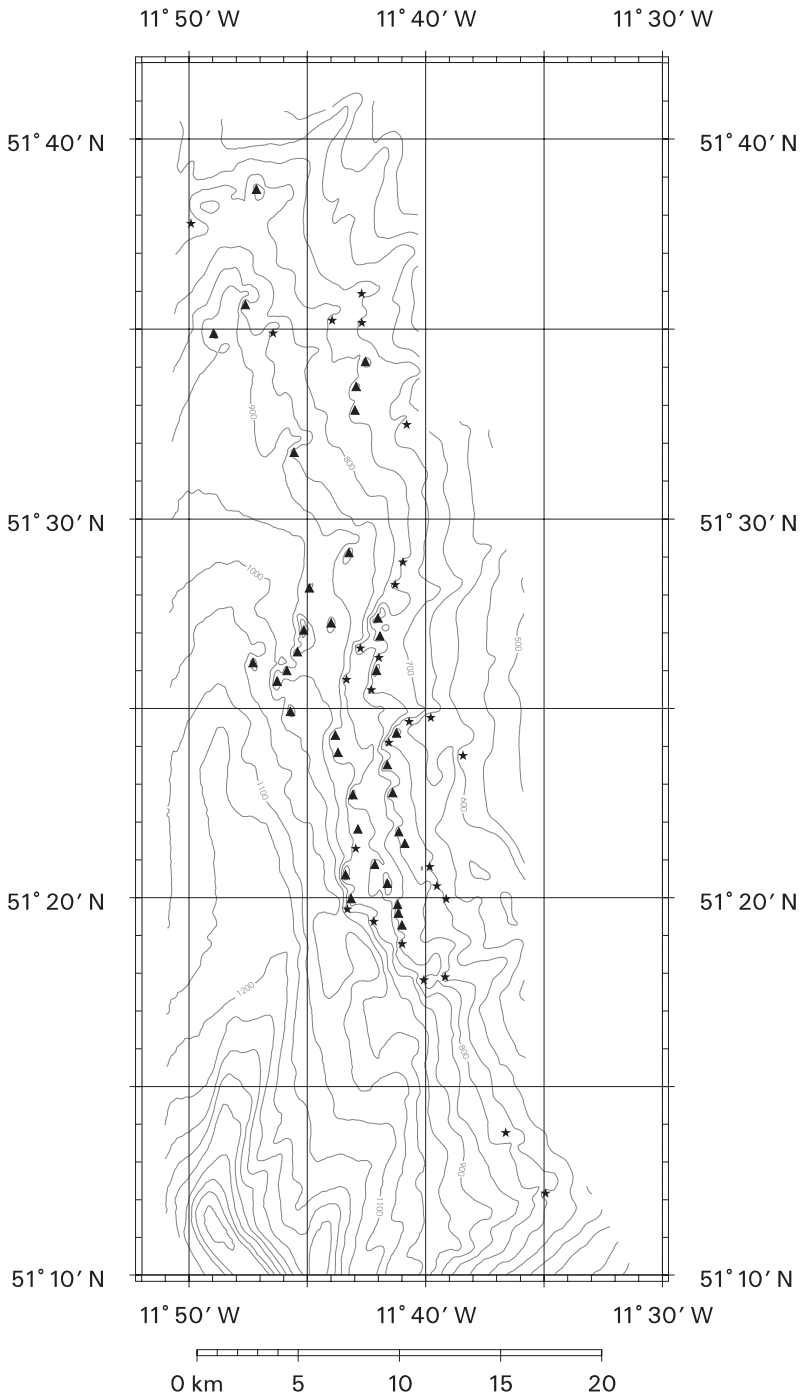

Figure 5-5. Bathymetric chart showing mound locations (50 m contour interval). Triangles indicate mounds that are clearly visible in the bathymetry. Features identified as buried carbonate mounds by means of the sub-bottom profiles and bathymetry are indicated by asterisks.

indications where carbonate mounds could exist. Features that look like carbonate mounds in the sub-bottom profile may be hardly pronounced in the bathymetry. Other mounds are clearly visible in the bathymetry but the penetration of the sub-bottom profile is reduced. Based on these examples, possible mound locations were detected and are displayed in Figure 5-5. The locations were identified based on typical mound morphology and a ridge-like structure showing a steeper slope at one side. For this analysis, contour lines with 5 m equidistances were utilized. In addition, the occurrence

of depressions near the mounds and the direction of their slopes were taken into consideration. Mounds clearly identified from bathymetric contours are labeled with a triangle, and possible carbonate mounds based on morphological interpretation in combination with sub-bottom information are labeled with an asterisk.

5.4 Results

5.4.1 Morphology of the continental margin

The Porcupine Seabight west of Ireland extends from approximately 49° to 52°N lat and from 14° to 11°W long. In this section, a general bathymetric description of the eastern margin of the Porcupine Seabight will be given. The northern and southern boundaries are 50°25'N and 51°40'N, respectively (see Figure 5-6). During the multibeam survey only the major parts of the slope were systematically surveyed. Due to time constraints, the margin could not be completely covered from bottom to top.

The morphology of the investigated area can be separated into a mound region in the northern part and a channel region in the south. Within the area north of 50°15'N giant mound occurrences emboss the morphology along the slope. The southern region is dominated by several submarine channels. In particular the channels south of 50°45'N are very pronounced.

The GEOMOUND project focuses on carbonate mounds. The mound cluster analyzed in this study is called the Belgica province. Our data show that in particular the mound structures north of 51°30'N are not as significant as the southern mounds. In addition, there may be buried mounds which cannot be seen in the swath bathymetry.

A number of about 30 mound structures have been discovered in the northern part. The morphology of the mounds, their distribution and orientation are clearly revealed by the multibeam data (see Figure 5-6). In addition, there exist morphological structures that could be carbonate mounds but they are not clear mounds in the bathymetry. Their locations were determined by means of sub-bottom profiling in combination with morphology analysis. Based on this analysis 62 mound structures could be identified.

The mounds exist in a depth range of approximately 1000-700 m, their distribution following the direction of the continental margin. Moreover, they seem to be arranged following the depth contours because most of the mounds rise from the 1000 m and 800 m contours.

The shape of most mounds resembles an ellipse extending along the continental slope. Their axes range approximately from 0.5 to 1 km and from 1 to 1.5 km, respectively. Heights of about 50 m are typical but they can reach 100 m. Other mounds form small ridges. In addition, a number of mounds do not represent single mounds but form terrace-like structures. Interesting features include small depressions situated at the foot of a number of mounds. Their depths vary between a few meters and 50 m. From swath bathymetry, no evidence is given to help analyzing the relationship between mounds and depressions.

Pretty clear mound features are the Thérèse Mounds around 51°26'N, 11°46'W. The northernmost mound of this cluster is more than 100 m high. The mounds east of 11°44'W are aligned more along a north-south axis. However, incidences of mound occurrences seem to be depth dependent which can be concluded by the mound

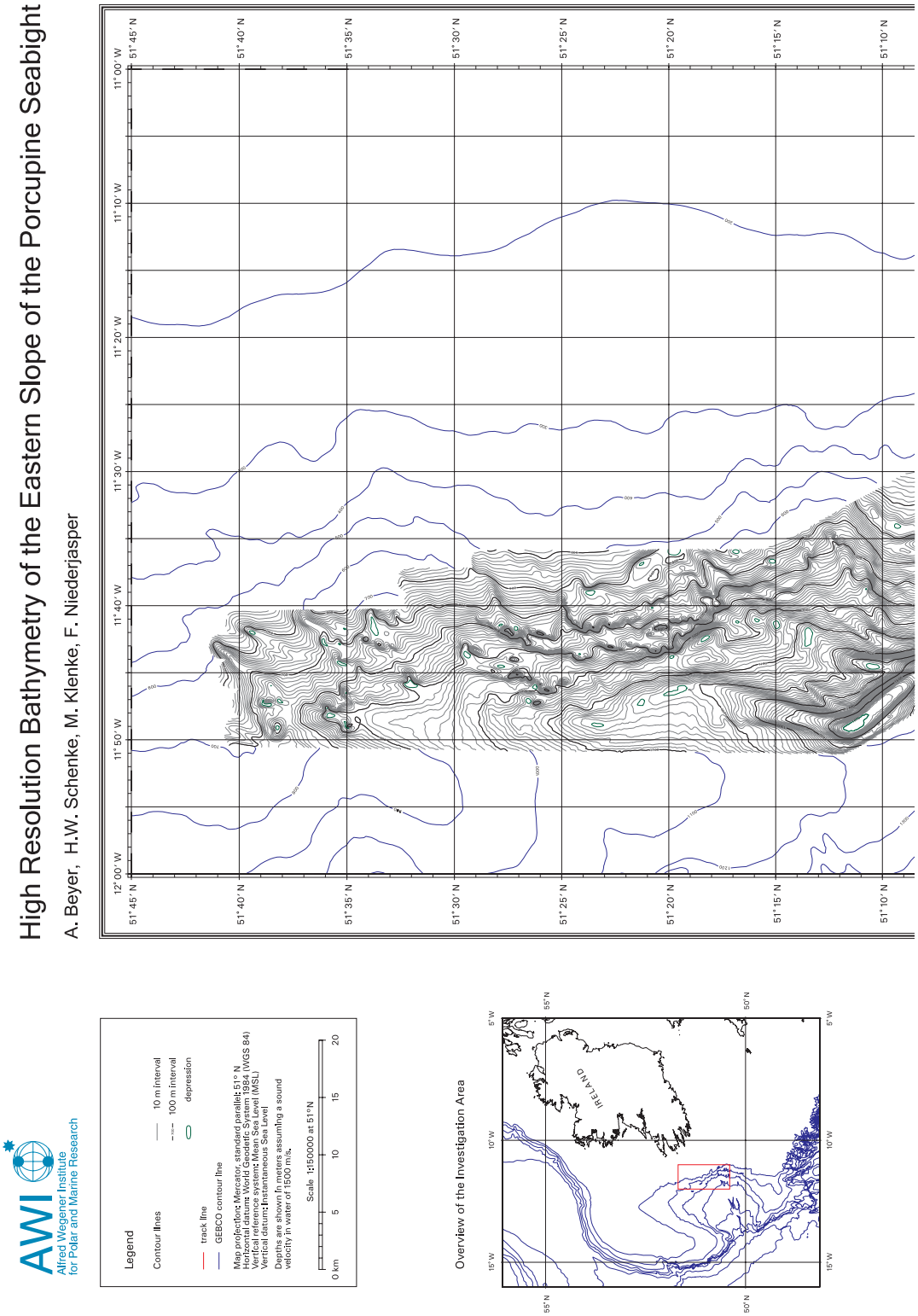

Figure 5-6. Bathymetric chart (The bathymetric chart in original size can be found in Beyer et al., 2003b).

alignment along the contour lines.

The mounds are located along the slope but their orientations seem to vary. The overall orientation appears to be the north-south direction. But in detailed view, differences are obvious. The orientation of the western mounds is northward, whereas that of the eastern mounds is northeast. In particular the mound located at 51°27'N,

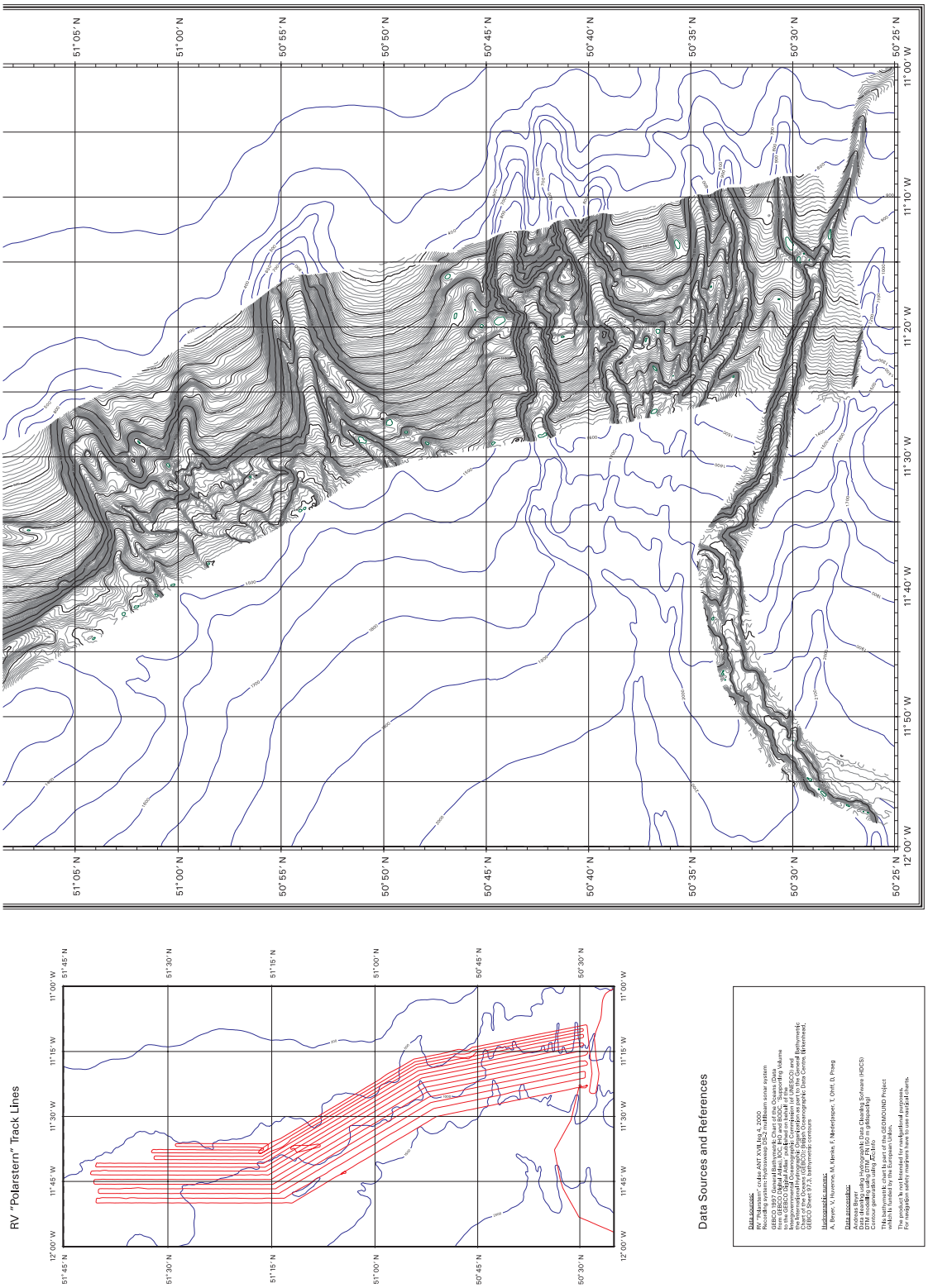

11°42'W seems to combine both orientations. The southern part of this mound shows a northeast orientation while its northern portion tends to a northern one.

The steepest slopes at the mounds are to be found on their west and northwest sides. They reach up to 30° surface slope, whereas the typical slope of the mound

flanks is about 20°. For comparison, the average slope of the margin in the mound area is about 5°.

Utilizing other visualization methods such as shaded relief or surface slope images, small scale features on the seafloor that are not identifiable in the contour lines become visible. The slopes near some mounds seem to be covered by ripples or sediment waves perpendicular to the surface gradient. An example of these ripples is displayed in a surface slope image (Figure 5-7a). The gray shading shows the surface slope, not the slope direction. Therefore, a few contour lines (25 m interval) have been added to the image in order to visualize the topography and to support interpretation. The surface slope in the area of these ripples varies between 2° and 5°, and the flanks of the mound west of the ripples reach up to 30° surface slope. Figure 5-7b shows an example of a ripple profile. The wavelength of the ripples is about 100 m and they are 1-2 m high. Form and orientation of these ripples could serve as input for local current analysis. However, they are only visible in the DTM with 10 m grid spacing and their clearness depends on a good signal-to-noise ratio. Areas indicating ripples show a measurement accuracy of 1-4 m. Thus, the size of these ripples is smaller than the measurement accuracy. But they are horizontally aligned and their occurrence is not systematically affected. A high point density due to an overlap of adjacent survey lines of up to 50% in the mound area ensures the reliability of the DTM at this location. Evidence for sediment waves on the lower mound slopes was independently identified by means of side scan sonar imagery by Wheeler et al. (2000).

The middle part of the investigated area is variably structured. It is characterized by two canyons which cut the generally smooth sloped margin ending in a rather changeable deeper area. The canyon flanks are up to 20° steep and the southern canyon has a width of 2 km at the bottom. The northern channel shows a variable structure and a mean width of 4 km. In this region the continental margin indicates a clear southwest slope gradient. The structure of the deeper part seems to be formed by a number of sediment slides. Sharp edges indicate the main scarp of the slides and show an extent of some kilometers.

The southern part of the investigated area is dominated by submarine channels which are very pronounced and form part of the Gollum Channel System (Kenyon et al., 1978; Tudhope and Scoffin, 1995). The northernmost of these five channels is the widest and deepest. It reaches an incision of about 400 m, whereas the other channels have a typical depth of approximately 200 m. Its width reaches up to 1.5 km at the bottom whereas the other channels show a width of 1 km. The channels proceed in a rather linear manner without pronounced meandering. The channel slopes are up to 25° steep. They are not straight but undulating. Especially the slopes of the southernmost channel undulate very regularly. This undulation has a wavelength of about 800 m. In many channel sections, the contour lines at the bottom of the channels show similarity with the contours of flowing rivers. The bottom of the outward bending of particularly the smoothly curving southern channel is about 30 m deeper. This characteristic may indicate particle flow in the channels. Sediment transport in the channels is also proposed by Tudhope and Scoffin (1995).

The southernmost channel of the area reaches its maximum relative depth of approximately 250 m within the steepest slope of the margin. In areas deeper than 1800 m the channel depth decreases to approximately 100 m; in the shallower area its

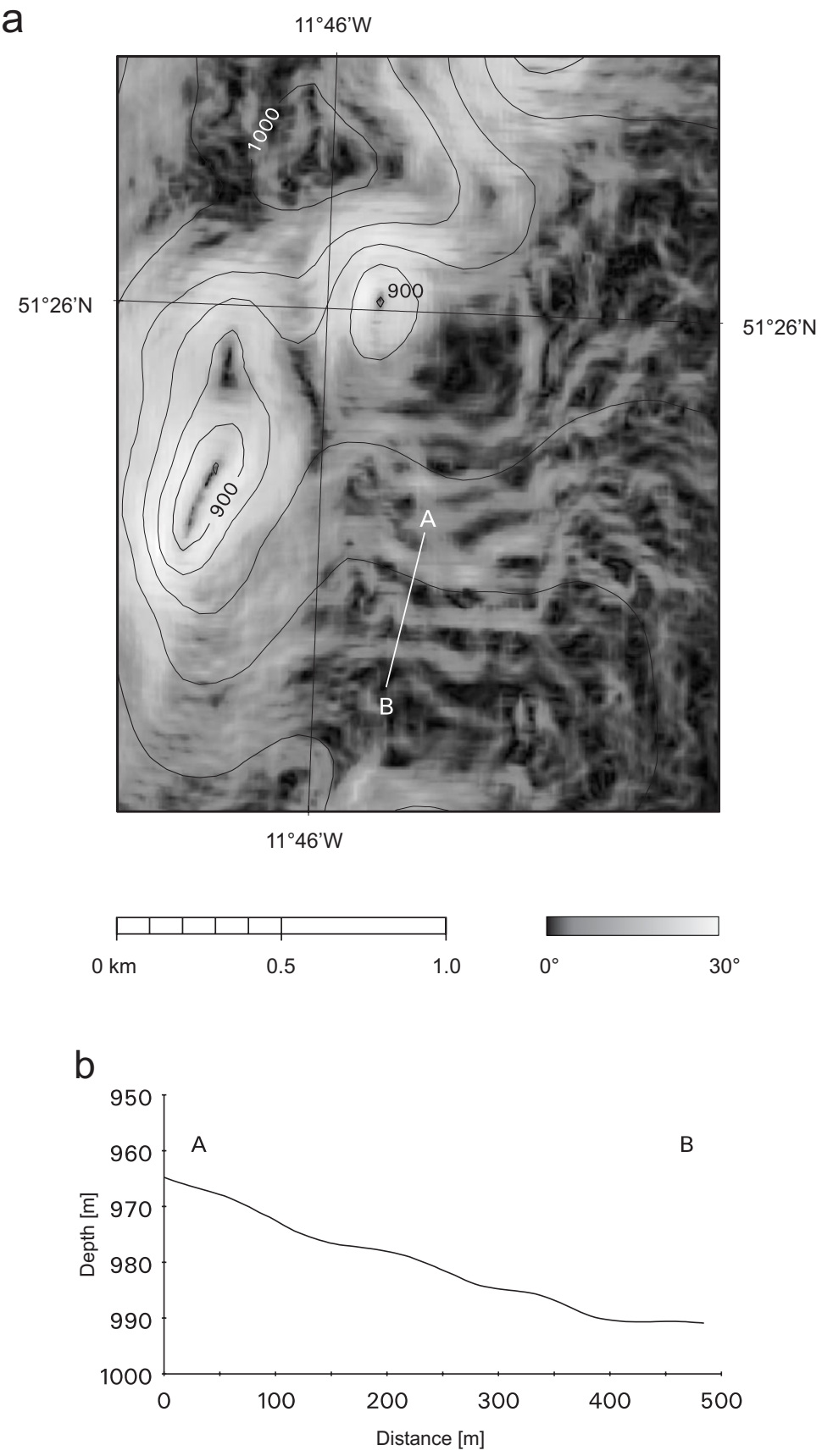

Figure 5-7. **a** Surface slope of the Thérèse mound area (25 m contour interval). Ripples can be recognized by the regular change of the surface slope. The ripples are aligned perpendicular to the gradient. Their heights are between 1 and 2 m. **b** Surface profile indicated in (a) by the line from A to B.

depth is also smaller. This morphological setting points to an increased current speed at the margin. It indicates a reduced sedimentation or even erosion compared to the upper and lower parts of the channel. Especially the smooth morphology of the channel bottom in the deeper part of the channel might be due to increased sedimentation.

5.4.2 Accuracy assessment

In order to assess the accuracy of the generated DTM, a statistical analysis was performed. As stated above, Hydrosweep DS-2 is specified for a depth accuracy of 1% of the water depth. Hence, for this investigation in the Porcupine Seabight the overall accuracy should vary approximately between 3 and 24 m.

In order to estimate the accuracy of the swath bathymetry in particular, the standard deviation of the soundings with respect to the DTM was computed. This overall accuracy includes measurement accuracy and DTM modelling deficiencies. However, it is hardly possible to distinguish between both effects. The standard deviation (RMS) was computed for each grid cell using the soundings coinciding with the corresponding grid cell. The mean standard deviation of the entire DTM was 3.9 m. However, this number includes both the measurements in shallow regions, where a higher precision exists, and deeper regions with probably degraded accuracy.

The RMS data clearly indicate a correlation with the survey lines. This means that the large RMS values are mainly located in the overlap area of neighboring swathes. In addition, within deeper regions this effect increases. Generally speaking, center beams have a better accuracy than outer beams. Thus, overlapping of outer beams supports a rising standard deviation. Slightly increased errors are found at steep channel edges and mounds. These features seem to be difficult to model using an automatic DTM technique. On the other hand, steep slopes amplify other error sources (e.g. heave, pitch, roll, heading) which now may stronger affect the measurements and the DTM modelling. In Figure 5-8 two RMS histograms of the DTM are shown. The presented values are summed values, i.e. the bar representing value 1 contains all values between 0.5 to 1.49 m. Both graphs display the frequency of corresponding RMS values but with different references. Figure 5-8a represents the absolute values of the RMS in meters. The RMS expectation is about 2 m.

In order to obtain an accuracy estimate comparable with the manufacturer's accuracy statement and to account for the depth dependence of the measurement precision, the RMS was recalculated considering the corresponding depth. The derived RMS values are displayed in Figure 5-8b. The expected RMS value is 0.2% of the water depth. 96.3% of all measurements show an accuracy better than 1% of the water depth. Within the presented swath bathymetry, most soundings outperform the accuracy given by the manufacturer. But it also means that almost 4% of the soundings do not satisfy the accuracy expectations.

5.5 Discussion

The area of the Belgica mound province has a dimension of approximately 40x30 km for the north-south and east-west directions, respectively. A lack of mound occurrences exists around 51°30'N separating the Belgica province into a northern and a southern mound cluster. Two scenarios are possible to explain this situation. Either

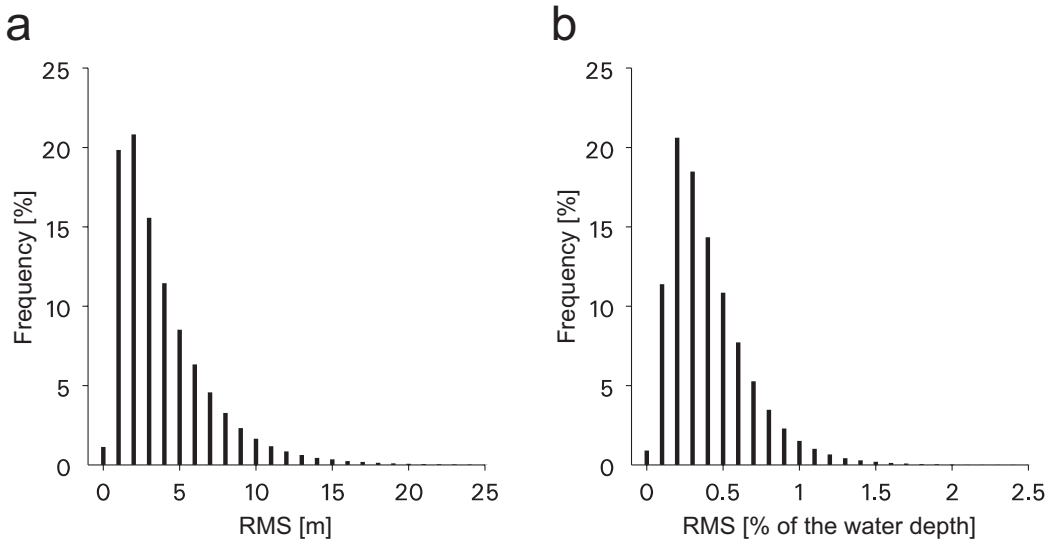

Figure 5-8. **a** Histogram of the depth RMS values in meters. The expected RMS value of the soundings is 2 m. A few measurements exceed the RMS value of 15 m. **b** Histogram of the RMS value in percent of the water depth. The expected RMS value of the soundings is 0.2% of the water depth. Approximately 96% of the depth measurements have a better RMS value than the accuracy expected by the manufacturer, i.e. 1% of the water depth.

the conditions for settling and growth of the corals were unfavorable (for example, missing hard ground or insufficient nutrient flow) or mounds exist in that area but they are buried by sediments. These sediments could have been deposited by currents flowing downslope. Small channel-like structures showing a south-west orientation support this interpretation.

The mounds north of 51°30'N have smaller heights compared to the other mounds. Since the mound basement is not visible in the bathymetry, the total height of the mounds cannot be analyzed. Therefore, the height differences of the mound clusters north and south of 51°30'N need not stand for the total height differences. Huvenne et al. (2003) propose that the mounds within the Belgica province started growing at one moment in the Early Pliocene. Thus, the height differences of the mound clusters should not be explained by age differences. Either the smaller northern mounds were subject to a higher sedimentation rate which has led to a smaller bathymetric height, or a lower nutrient supply limited the growth of the corals in that region.

In comparison to the Magellan mound province described by Huvenne et al. (2003), the mounds of the Belgica province located between 51°20'N and 51°30'N show a lower density of approximately one mound per 5 km^2 compared to one mound per km^2. The mounds north of 51°30'N even show a significantly lower density of approximately one mound per 11 km^2. In addition, the number of mounds in this area is reduced. Note that more than 300 mounds have been detected in the Magellan province in contrast to 62 in this study of the Belgica province. A comparison of the size of the mounds is hardly possible due to different data acquisition methods (seismic profiling in contrast to swath bathymetry). However, the heights of the mounds in both provinces are almost equal but the Belgica mounds show a width which is roughly four times that of the Magellan mounds. This difference of mound size could be due to more favorable conditions for coral settlement and growth in the Belgica province. Stronger currents

could have maintained a sufficient nutrient flow and prevented the corals from being buried with sediments. The corals could cover large continuous areas that afterwards formed the basement of larger mounds.

There may exist other, smaller, mounds on the seabed surface which cannot be identified based on the derived terrain model and the sub-bottom profiles due to the size of these mounds. Such smaller mounds were discovered near 11°46'W, 51°31'N by Kozachenko et al. (2002) utilizing sidescan sonar. They may represent the early stages of carbonate mounds. These mound structures show heights of a few meters and a horizontal dimension of some tens of meters.

5.6 Conclusion

The multibeam data were thoroughly cleaned and processed. Overall the multibeam data are of high quality. The standard deviation is mostly better than 1% of the water depth and underlines this statement. The high accuracy level could be obtained by continuously overlapping of adjacent survey lines and a high accuracy navigation using differential GPS.

The final DTM has been adjusted to completely cover the investigated area. If future investigations require a more detailed view on the data, the DTM can be recalculated and regeneralized based on the original data. The grid size can be adjusted to the local point density and to the aim of the investigation. A grid size of 10 m is achievable in areas shallower than 1000 m.

The acoustic measurements were refraction-corrected using the CTD data. Afterwards, the multibeam observations were normalized to a sound velocity of 1500 m/s in order to obtain consistency with other data sets from RV *Polarstern*. However, the difference between the DTM and the depths calculated from the CTD profile is smaller than the measurement accuracy.

The eastern margin of the Porcupine Seabight has been mapped and the different morphological characteristics such as mounds and channels have been described. A distribution of mounds and structures which indicate partly buried carbonate mounds was obtained based on the seafloor morphology and the sub-bottom profiles.

The bathymetric chart (Figure 5-6) presents the eastern slope of the Porcupine Seabight between 50°25'N and 51°45'N. It shows the contour lines (10 m interval) of the described multibeam survey. The adjacent area is represented by contour lines (100 m interval) from the GEBCO Digital Atlas 1997. It gives a detailed view of the Belgica mound province and the mound distribution between 51°15'N and 51°30'N. In the south, part of the Gollum Channel System has been mapped. The large scale meandering of the channels and the small scale undulation of the channel flanks are visible in detail. The enhanced morphological information of the multibeam survey is a significant enhancement compared to the bathymetry of the GEBCO Digital Atlas.

5.7 Acknowledgements

We are grateful to the crew of RV *Polarstern* for support during cruise ANT XVII/4 and to R. Usbeck for operating the CTD device. Financial support of these investigations was granted by the European Commission (Contract No. EVK3-CT-1999-00016).

6 Seafloor classification of the mound and channel provinces of the Porcupine Seabight: an application of the multibeam angular backscatter data*

Andreas Beyer[1], Bishwajit Chakraborty[2], Hans Werner Schenke[1]

[1] Alfred Wegener Institute for Polar and Marine Research (AWI), Columbusstraße, 27568 Bremerhaven, Germany
[2] National Institute of Oceanography, Dona Paula, Goa 403 004, India

Keywords: multibeam sonar, angular backscatter, carbonate mounds, seafloor channels, Porcupine Seabight

6.1 Abstract

In this study multibeam angular backscatter data acquired in the eastern slope of the Porcupine Seabight are analyzed. Processing of the angular backscatter data using the 'NRGCOR' software was made for 29 locations comprising different geological provinces like: carbonate mounds, buried mounds, seafloor channels, and inter-channel areas. A detailed methodology is developed to produce a map of angle-invariant (normalized) backscatter data by correcting the local angular backscatter values. The present paper involves detailed processing steps and related technical aspects of the normalization approach. The presented angle-invariant backscatter map possesses 12 dB dynamic range in terms of gray scale. A clear distinction is seen between the mound dominated northern area (Belgica province) and the Gollum Channel seafloor at the southern end of the site. Qualitative analyses of the calculated mean backscatter values i.e., gray scale levels, utilizing angle-invariant backscatter data generally indicate backscatter values are highest (lighter gray scale) in the mound areas followed by buried mounds. The backscatter values are lowest in the inter-channel areas (lowest gray scale level). Moderate backscatter values (medium gray level) are observed from the Gollum and Kings channel data, and significant variability within the channel seafloor provinces. The segmentation of the channel seafloor provinces is made based on the computed gray scale levels for further analyses based on the angular backscatter strength. Three major parameters are utilized to classify four different seafloor provinces of the Porcupine Seabight by employing a semi-empirical method to analyze multibeam angular backscatter data. The predicted backscatter response which has been computed at 20° is the highest for the mound areas. The coefficient of variation (CV) of the mean backscatter response is also the highest for the mound areas. Interestingly, the slope values of the buried mound areas are found to be the highest. However, the channel seafloor of moderate backscatter

* Beyer, A., Chakraborty, B., Schenke, H. W., 2005a. Seafloor classification of the mound and channel provinces of the Porcupine Seabight: an application of the multibeam angular backscatter data. International Journal of Earth Sciences (Geologische Rundschau), doi 10.1007/s00531-005-0022-1.

response presents the lowest slope and CV values. A critical examination of the inter-channel areas indicates less variability within the estimated three parameters.

Financial support of this study was granted by the European Commission Fifth Framework Project GEOMOUND (contract no. EVK3-CT-1999-00016).

6.2 Introduction

Large scale oceanographic explorations are presently continuing around the Porcupine Seabight area, which is located towards the south-west of Ireland. This area is an embayment of the North Atlantic continental margins. Its importance due to the dominant hydrocarbon resources is well documented (Croker and Shannon, 1987), and ongoing experiments are important due to the involvement of higher order variability (in terms of physical and geological settings) around this area (De Mol et al., 2002). This area shows northward flowing slope currents following the North Atlantic continental slope contours. Geologically, it is a sedimentary environment controlled by drift deposits, and highly complex channel and levee systems. The Porcupine Seabight area possesses dominant carbonate mounds (Hovland et al., 1994; Henriet et al., 1998) and channel systems related structures, and understanding of the seafloor morphological aspects was initiated by applying long and short-range sidescan sonar data, extensive sediment sampling, and single channel seismic profiles (Tudhope and Scoffin, 1995 and Kenyon et al., 1998 and references therein; Huvenne et al., 2002).

Recent initiatives of the European Union's GEOMOUND programme provided detailed high-resolution multibeam bathymetric survey results from the Porcupine Seabight area during the RV *Polarstern* expedition ANT XVII/4 (Beyer et al., 2003b). Analyses of bathymetric data reveal interesting features at the eastern slope of the Porcupine Seabight starting from numerous mounds and associated buried mounds which are part of the Belgica mound province at the northern end of the area followed by the east-west trending Kings Channel and Gollum Channel systems (bathymetric map in Beyer et al., 2003b).

Apart from acquiring seafloor topographic data, seabed characterization can also be implemented using angular backscatter data. The multibeam backscatter data were acquired simultaneously with the bathymetric data (Hydrosweep DS-2). Qualitative sidescan sonar based backscatter data analyses and quantitative texture analyses of the surrounding areas close to the presently studied locations are available (Kenyon and Akhmetzhanov, 1998; Huvenne et al., 2002; Wheeler et al., 1998), but no quantitative multibeam angular backscatter analyses have so far been made from the Porcupine Seabight.

In order to study various seafloor systems, a semi-empirical approach for the angular backscatter data of the GLORIA sidescan sonar was implemented by Hughes Clarke (1994). Such a classification technique for the seafloor sections involves the shape, variance, and magnitude of the angular response of the measured multibeam angular backscatter strength and is applied in this study. However, a careful selection of seafloor segments is necessary to provide the entire angle range of backscatter data within the segments. If the seafloor properties vary within a very small area, the full angular coverage may not be available for analyses due to the swath coverage. Furthermore, the scattering of the backscatter values needs to be reduced using

binning to calculate representative angular backscatter parameters.

In this paper, section 6.3 deals with the processing of the angular multibeam Hydrosweep DS-2 backscatter data. It also involves the normalization technique of the angular backscatter strength, which provides a segmented seafloor based on the sediment lithology of the varying mounds and channel seafloor from the Porcupine Seabight. A mention about the survey sites is included in section 6.4 along with a presentation of the angle-invariant backscatter results from the mounds and the channel seafloor. A semi-empirical method is applied to the multibeam dataset to employ seafloor classification in section 6.5.

6.3 Multibeam backscatter data processing

The multibeam echo-sounding system Hydrosweep DS-2 operates at 15.5 kHz (Gutberlet and Schenke, 1989). It uses a beam-forming technique to generate 59 pre-formed beams (PFBs) covering beam angles from -45° to +45°. The received signals are pre-amplified and corrected for real-time transmission loss with a time varied gain. These 59 beams are sampled and converted into echo root mean square voltages using a window of -6 dB around the central peak amplitude. In order to compute seafloor acoustic backscatter strength, an off-line data processing algorithm known as ‘NRGCOR’ is employed (Anonymous, 1994). Necessary system settings are stored and available for backscatter processing (for example source level, pulse length). The computed gain-corrected electrical signal values are converted into acoustic echo levels by employing receiving voltage response. The next step of the ‘NRGCOR’ algorithm is a geometric correction using the beam-wise bathymetric data for the computation of the seafloor slope (along track and across track slope) and true angles of incidence on the seafloor. The third important step is a computation of the seafloor area insonified by each beam. The computed backscatter strength is used for the present study with binning at 1° incidence angle interval.

The angular backscatter strength is a function of seafloor characteristics. Sediment type (combination of for example grain size, porosity, density) and surface structure affect the backscattering. Furthermore, backscattering occures not only at the seabed surface but also in the sediment body. The penetration into the seabed depends on sediment type and frequency. However, there is no data from the Porcupine Seabight available to the authors but we expect not more than 1-2 m penetration for the sonar frequency used (Vogt et al., 1999a). Angular backscatter shape variations are dominant due to the closeness of the beams to the normal incidence direction. For smooth seafloor sediments, this function varies steeply compared to a rough seafloor surface. However, to generate a backscatter map similar to the bathymetry for seafloor interpretation, such systematic effect needs to be removed (de Moustier and Matsumoto, 1993). The angle-invariant backscatter data provide sufficient basis for first-order seafloor classification based on the sediment lithology (Hughes Clarke, 1993). In order to remove the angular dependency from the presently studied area of the Porcupine Seabight, a scheme is proposed in this paper.

The original processed backscatter output file of the ‘NRGCOR’ comprises the backscatter strength values (with respect to the incidence angles and beam numbers) and position data. At the very beginning, stored backscatter strength values with

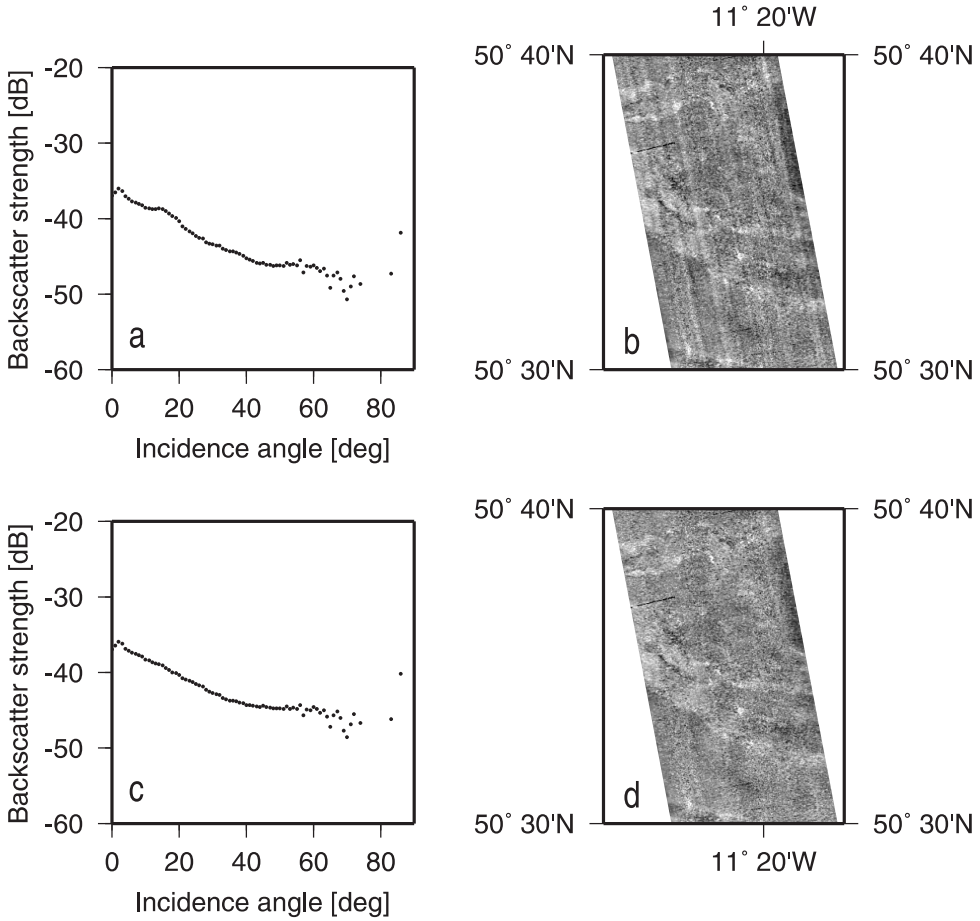

Figure 6-1. Changing of the angle-invariant backscatter map by applying the mean angular backscatter function and beam pattern determined during the processing. **a** shows the mean angular backscatter function of the area. This function has been removed from the data shown in (b). Beam pattern effects visible in (b) (track line parallel artefacts) are removed from the data in (c) and (d) which show significant improvement between the incidence angles 10-20°. **b** and **d** show a combination of five parallel track lines of the same area.

respect to the 1° binned incidence angles are averaged utilizing the entire 'NRGCOR'-processed dataset (Figure 6-1a). Then, this averaged angular backscatter function is utilized to normalize each set of the angular backscatter strength with respect to a reference incidence angle. Since fluctuations of the backscatter data are dominant close to the normal incidence direction we have chosen the 10° angle as a reference angle. The results of such a process allow the removal of the angular effect in the sense that the mean angular fall of the backscatter strength is removed from the data (Figure 6-1b).

However, fluctuations parallel to the ship tracks and local variations are still seen in the normalized data. The effects of seafloor type on the backscatter are expected to be normalized in the angular backscatter strength values. Therefore, the systematic effect which is consistently appearing in the normalized data (parallel lines around the track lines) is realized to be related to the beam pattern effect (Figure 6-1b). This systematic effect due to the beam patterns (function of beam number) is recovered from the normalized angle-invariant backscatter data on ping by ping basis as an average backscatter value with respect to the beam number. An improvement of the 10-20°

angular part of the mean angular backscatter strength of Figure 6-1a is seen in Figure 6-1c where the averaging of the angular backscatter data is carried out after incorporating corrections due to the beam pattern effect. The effects due to the beam patterns are found to be removed considerably at the end of the initial process (Figure 6-1d). In a similar manner, further iterations prove to be effective in normalizing the entire Porcupine Seabight area data set. We have employed, in total, three iterations to remove the beam pattern effect along with the normalizations, which have considerably improved the present set of data. However, more iterations can be made for the improvement of the image quality, but an increase in the height of the angular backscatter function towards the higher incidence angles is realized when iterations are increased. This is due to the correlation of the incidence angle and beam number within the areas chosen for averaging.

Such a technique provides gray scales compatible with the seafloor sediment lithology of the area which can form a useful basis of homogeneous seafloor segments. Interestingly, the achieved homogeneously segmented data can be utilized for seafloor characterization. Once iterations are completed, a grid has been calculated out of the point distribution of the backscatter data. The grid size of 50 m and data points within a radius of 75 m around each grid point were used to calculate the grid cell value. These settings correspond to the largest footprint size of the beams and averaging is performed. On the whole, the multibeam backscatter processed data, free from mean angular backscatter shape parameters from the Porcupine Seabight area, is presented in Figures 6-2a, b. A gray scale dynamic range of 12 dB (-42 dB to -30 dB) is observed within the angle-invariant backscatter image, which comprises mound and channel systems. The gray level contrast variations among different feature types are distinctly clear for the Porcupine Seabight backscatter data.

6.4 Porcupine Seabight – study area description and angle-invariant backscatter data

The Porcupine Seabight extends approximately from 49°N to 52°N in latitudes and from 14°W to 11°W in longitudes. For the present study, we have processed multibeam data acquired between 50°25’N and 51°40’N at the eastern margin of the Porcupine Seabight (Beyer et al., 2003b). In order to maintain consistency in the backscatter processing, the area chosen for this backscatter study is lying within the Deep Sea mode of the multibeam system (i.e. 800 m to higher depths) since the operational aspects e.g. transmission beams and reception beams, coverage, and pulse lengths are changing in different modes.

The morphology of the investigation area can broadly be separated into a mound region in the northern part and a channel region in the south. A clear difference in gray scale level can be noticed while comparing between the northernmost-end mound system and southern-end channel system (Figure 6-2) of the study area. Towards the north of 50°15’N latitude, the bathymetric trace of the giant mounds is reported in (Beyer et al., 2003b). Though, we have presented angle-invariant multibeam backscatter data operated in the deep-sea mode, overlying bathymetry is presented for the entire area covered during the RV *Polarstern* expedition. Towards the northern part of the survey area, few blank parallel lines are seen which represent a data gap of the

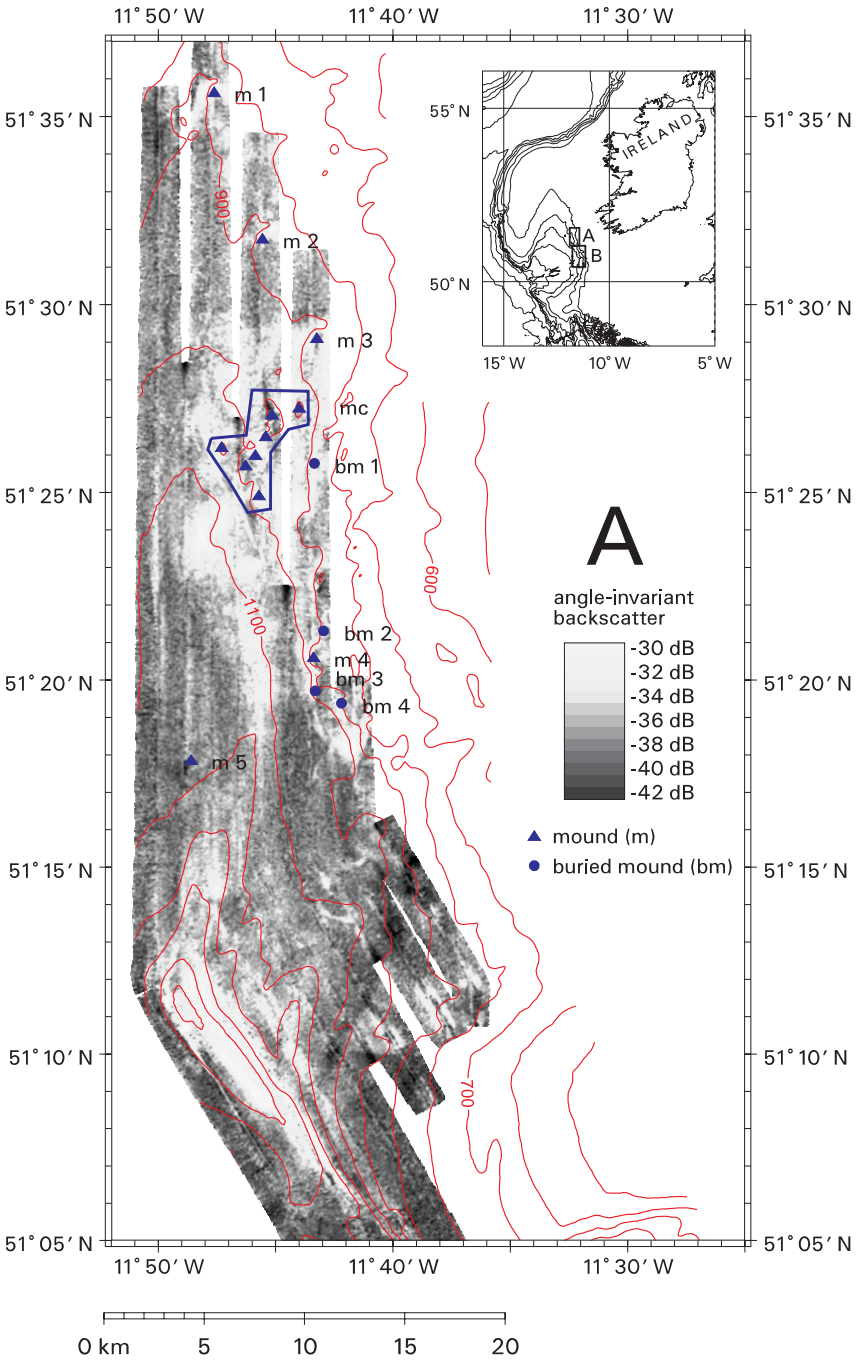

Figure 6-2. Backscatter map of the angle-invariant backscatter data recorded in the Deep Sea mode of the Hydrosweep DS-2 multibeam system. Hundred meter bathymetric contour lines are also accommodating this figure. **A** The locations of the mounds and buried mounds are drawn using triangles and circles respectively. **B** gives the boundaries of the areas used for backscatter analyses.

Deep Sea mode due to the survey utilizing the medium depth mode which is not considered here (Figure 6-2a). Relative backscatter values (since the multibeam Hydrosweep DS-2 system is not calibrated) varying from the highest backscatter -30 dB (light gray scale) to the lowest i.e. -42 dB (dark gray scale) are observed within the area. Mounds of the Belgica province are present in this northern part. Details of the Belgica mound province are also given in Wheeler et al. (submitted). A complex gray scale i.e. combination of gray scales varying from light to medium is observed

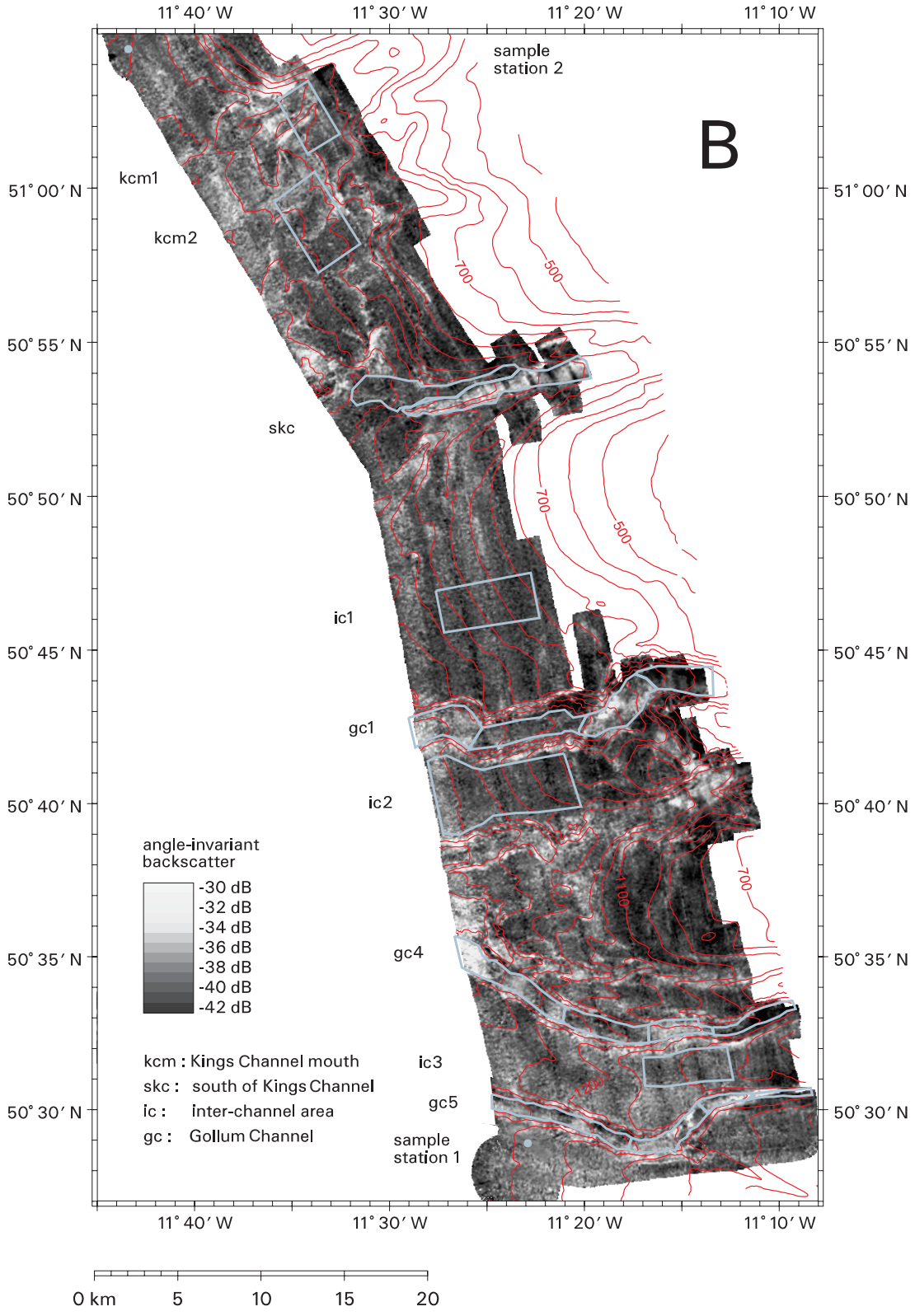

within the clustered mound area of seven mounds (areas coded mc, having an average value of -34 dB within the area marked in Figure 6-2a). In addition, four isolated mounds having moderately higher backscatter are shown. Table 6-1 provides the dimensional aspects of these mounds along with the mean backscatter values acquired from the angle-invariant data. The backscatter level in the mound area is varying from

the highest value (-32.20 dB) for the northernmost mound (m1) to the lowest (-33.97 dB) for the mound (m2). Associated medium gray levels though negligibly close to the mound structures may be identified as a shadow zone, and are insignificant in the multibeam backscatter data. No correlation is obtained with the dimensional aspects of the mounds and backscatter values from this area. The seafloor in the wider surroundings of the mound cluster shows high backscatter but no further mound occurrences were found there. Thus, the lighter gray scale is not solely due to the existence of mounds but because surrounding seabed is also affected. Darker gray scale around -37 dB is seen for the associated background sediment areas. Patchy high-backscatter regions having light gray scales (-30 dB) are also observed in this mound-dominated channel area. The channels within the seafloor slope closer to mound areas are due to the current scouring which leaves coarser material in the seafloor while sweeping away the fine materials. Parallel examinations of Figure 6-2a and the bathymetry map of Beyer et al. (2003b) around the mound structures indicate

Table 6-1. Statistical parameters of the areas under study including number of measurements, covered area and mean angle-invariant backscatter value (BS). The areas are coded as m (mounds), mc (mound cluster), bm (buried mound), kcm (Kings channel mouth), skc (south of Kings channel), ic (inter-channel area) and gc (Gollum Channel, channel number - channel section). The sections of the Gollum channels are numbered from west to east. The remarks section gives extension and height of the individual mounds located in Figure 6-2. Ht represents the height of the downslope/upslope side of the mounds respectively.

Area code	Number of measurements	Area covered [km^2]	Mean angle-invariant BS [dB]	Remarks
m1	1531	1.44	-32.20	500 m E-W, 850 m N-S, Ht 100/15 m
m2	1451	1.34	-33.97	500 m E-W N-S, Ht 90/20 m
m3	3103	3.59	-32.74	800 m E-W, 2000 m N-S, Ht 90/50 m
m4	3185	2.75	-33.88	700 m E-W, 1400 m N-S, Ht 160/70 m
m5	1952	1.74	-37.18	1400 m E-W, 1100 m N-S, Ht 70/20 m
mc	15429	14.67	-34.36	
bm1	967	0.98	-32.80	
bm2	856	1.01	-34.17	
bm3	813	0.88	-35.30	
bm4	1022	1.22	-34.49	
kcm1	9047	8.13	-37.80	
kcm2	15329	15.46	-38.66	
skc up	11534	11.03	-36.66	
skc low	8268	10.09	-39.47	
ic1	14773	15.54	-39.64	
ic2	22339	29.26	-39.27	
ic3	13001	10.11	-38.40	
gc1-1	3812	7.45	-37.03	
gc1-2	6338	7.82	-38.88	
gc1-3	9120	7.61	-37.31	
gc1-4	5756	6.11	-41.16	
gc4-1	4874	8.68	-36.61	
gc4-2	5271	5.78	-38.28	
gc4-3	4092	3.37	-36.07	
gc4-4	5004	3.46	-41.70	
gc5-1	9510	7.03	-37.33	
gc5-2	5735	4.65	-37.22	
gc5-3	2365	1.77	-35.35	
gc5-4	1901	1.28	-40.34	

directions of coarse grained material flow along the depth contours. Reports about the existence of seafloor ripples or sediment waves in the mound-dominated ridge areas were made which are found to be perpendicular to the surface gradient (De Mol et al., 1999; Wheeler et al., 2000). Sediment waves having a wavelength up to 100 m and a height varying from 1 m to 2 m, are only visible in Digital Terrain Model analyses (Figure 5-7a). ORETECH sidescan sonar (operating frequency 30 kHz; lines ORAT 4 and 9) from the Intergovernmental Oceanographic Commission (IOC) initiatives (Kenyon et al., 1998) indicates the presence of two suspected barrier reef mounds at the core sampling locations TTR7-AT-19G (51°17.43'N and 11°48.59'W) and 20G (51°17.82'N and 11°40.78'W) (Swennen et al., 1998). At TTR7-AT-19G top (0–5 cm) sediments of foraminiferal sand with silt are obtained. Sediment sample descriptions of the TTR7-AT-20G core are found to be similar to TTR7-AT-19G. We could locate the barrier reef mound (m5) at the sediment sampling location of TTR7-AT-19G with low bathymetric height. Backscatter strength at the sediment sampling location TTR7-AT-19G is lower (-37.76 dB) and corresponds to the backscatter of background sediments. The TTR7-AT-20G location is situated on the lower 'terrace' slope, and is not considered for our study. Four buried mound structures of variable sizes occur in the study area having mixed backscatter levels varying from -32.80 dB to -35.30 dB for (bm1) to (bm4) (Figure 6-2a). The backscatter levels of the buried mounds are comparable with the backscatter level obtained from the mounds. Bathymetry-wise, a pronounced depression is observed south of the mound province having very high backscatter. The presence of strong backscatter (-30 dB) at the slope in the topographically depressed area indicates the presence of active seafloor currents which may be guiding coarse material towards the depression. Two parallel low backscatter bands showing northeast to southwest orientation extend between 51°10'N and 51°20'N and have a width of about 1 km. Though no close link with the bathymetry is seen, the change in backscatter level indicates changes in sediment properties which may be related to down-slope currents and sediment transport.

The middle part of the investigation area is characterized by two canyons which cut the generally smooth-sloped margin, ending in a rather changeable deeper area (Figure 6-2b). Twenty degree steep canyon flanks are observed and the southern canyon has a width of 2 km at the canyon bottom. Similarly, the northern channel (Kings Channel) shows a variable structure and a mean width of 4 km. We have chosen our study data at the mouth of this channel (kcm1). The second site was chosen slightly away from the channel mouth towards the area indicated as sediment slump (kcm2). Variability in sediment lithology is observed within the two chosen areas. In general, this area has a mixed backscatter level. However, a higher backscatter level (-37.80 dB) is seen for the (kcm1) area compared to the area (kcm2) i.e. -38.66 dB. The presented gray scale levels (Figure 6-2b) of the backscatter data can establish the difference between the areas. In this region, the existence of current-generated symmetric seafloor ripple patterns (wavelengths varying from 0.1 m to 0.3 m and height of 2.0–5.0 cm) affect the seafloor backscatter, associated with dropstones, reported by Tudhope and Scoffin (1995). However, towards the southern end of the Kings Channel, areas devoid of current-generated ripples were seen to support bio-turbidity effects (Tudhope and Scoffin, 1995). Dominant fine sand with associated fine materials is reported here. Grain size distribution indicates that the area has 'silty sand' similar to

the mound site (Tudhope and Scoffin, 1995; De Mol et al., 2002). Distinctly different backscatter level variations are seen from the channel sections' (skc) top end (-36.66 dB) with respect to the associated lower seafloor channel end (-39.47 dB) towards the southern end of the Kings Channel area. Though exact sediment distribution is unavailable from this area, we consider the seafloor to be 'silty sand' like in the Kings Channel mouth area (kcm). However the 3 dB fall towards the western side of (skc) suggests significant changes of the seafloor microroughness in this channel.

The Gollum Channel System is one of the very few lengthy leveed channel systems known from the NW European margin. It is a E-W striking tributary system with sinuosity and narrow steep sided channels. The continental seafloor towards the eastern side of this channel system varies between the depth of 400 m and 800 m, whereas for the western side it is observed to be varying up to 1700 m in the study area. The northernmost channel (gc1) of the five channel systems is the widest and deepest (Figure 6-2b). It reaches an incision of about 400 m, whereas the other channels have a depth of 200 m. The width of this extreme channel reaches up to 1.5 km at the bottom compared to the other channels having a width of 1 km (Beyer et al., 2003b). Within these channels, various types of channel structures are observed. The northernmost channel shows straight characteristics, whereas the two southernmost channels show a distinct extent of meandering while proceeding to the southeast side (gc4 and gc5).

Tudhope and Scoffin (1995) had reported the detailed morphological aspects of the Gollum Channel System. According to their observations and understandings (based on the references of Lampitt, 1985), the channel floors having 0.0-0.3 m of thick blanketing deposit of flocculant fine grained organic detritus – the origin of phytoplankton, and its varying concentration in the channel floor are due to the funnelling into the topographic depression. The sediment beneath the phyto-detritus layer appeared to be monotonous white ooze. All the sediment samples (five stations) from various locations with varying water depth (400-2800 m) are indicative of 'silty clay' sediments (10% fine sand, 15-20% silt and 70% clay). For the present study, backscatter data from three complete channel systems are considered out of the five channels surveyed i.e. the northernmost channel (gc1) and channel numbers (gc4) and (gc5) towards the southern end. Backscatter data of the channels (gc2) and (gc3) were not analyzed because the high variability of the gray scale prevents to create seafloor segments that cover the entire incidence angle range of the backscatter data. Interestingly, indications of slope failure is seen in the backscatter plot within the intermediate area of the channel systems (gc2 and gc3), not considered for the present study. Indication of such slope failure was clearly absent in the bathymetric plot. In an examination of the angle-invariant backscatter data (Figure 6-2b) for the northernmost steep channel (gc1), four segments are observed in terms of backscatter level variation indicative of sediment lithology. Towards the western-end section of this channel (gc1), section one shows moderately lighter gray scale (-37.03 dB) followed by the medium gray scale (-38.88 dB) in the channel section two. Then again relatively higher backscatter (-37.31 dB) is observed in section three. The dark gray i.e., lowest backscatter is observed for the flank section of this channel section four (-41.16 dB), having dominant ridge structures. Moderately lighter gray scale in certain parts of the

Gollum Channel System can be correlated with the presence of the white ooze having stiff gelatinous texture as observed by Tudhope and Scoffin (1995), and is dominant at the sections of the channel where it is constricted. In section two of this channel, medium gray level cannot confirm the presence or absence of a phyto-detritus layer. Similar ideas may be drawn about the gray scales for the other two channels (gc4 and gc5). For channel (gc4), the backscatter levels are varying from: -36.61, -38.28, -36.07 and -41.70 dB for the sections from 1 to 4 respectively. Similar variations are observed within the channel (gc5) also. However, the gray scale variations (sediment lithology) within the channel sections suggest that the chosen segments are fairly homogenous.

6.5 Seafloor classification using angular backscatter response – a semi-empirical approach

The local variations in the shape of the angular backscatter strength can be determined by estimating 'mean angular backscatter response' with lines corresponding to standard deviations from the mean (Hughes Clarke, 1994). Regression fits to such angular backscatter curves from different seafloor areas can be utilized to compare their shape-related parameters. The 'slope' of the mean angular backscatter response curve (slope of the linear regression) along with the estimation of a predicted backscatter response at a known angle and the average ratio of the standard deviation to the mean i.e. 'coefficient of variation' (CV) are important classification parameters. These estimated three parameters are utilized as classification parameters for the present study. The area angular backscatter response curves are computed by averaging the measured backscatter strength values within particular angle bins on a linear scale (equation 4 in Hughes Clarke, 1994). Similarly, standard deviations from the average values are also computed using equation 5 in Hughes Clarke (1994). Figure 6-3 provides the mean angular variations in backscatter strength with respect to the incidence angle for specific areas (total six area types): cluster of mounds (mc), buried mound (bm2), channel mouth of the Kings Channel system (kcm1), area between the channel 1 and channel 2 (ic2) within the Gollum Channel area. Also, similar variations are presented for two adjacent sections (sections 1 and 2) of the Gollum Channel (gc1) System seafloor having different textures (Figure 6-2b). Distinctly different shapes of the backscatter response patterns are observed for these areas. In order to keep the homogeneity aspects, data of the close surroundings were selected around the mound and buried mound area. Due to the limited data amount from the buried mound area, fluctuations are seen in the mean angular response and standard deviation curves. The estimated standard deviation values from these areas indicate a small range of variations within 3.5 dB, also indicating generally homogenous seafloor. Predicted mean angular response for the 20° incidence angle (estimated by using regression fit) is found to be the highest (-34.76 dB) for the mound area (m1), and the lowest (-43.19 dB) for the Gollum Channel area (gc4). Similarly, the absolute values of the slope for the buried mound areas (bm3) are found to be the highest (0.367) and the lowest for Gollum Channel (gc4) section 1 seafloor (0.172) respectively. The coefficient of variation (CV) is comparatively higher (0.422) for the clustered mound (mc) area and the lowest (0.312) for the buried mound area (bm2). The estimated values are provided within Figure 6-3

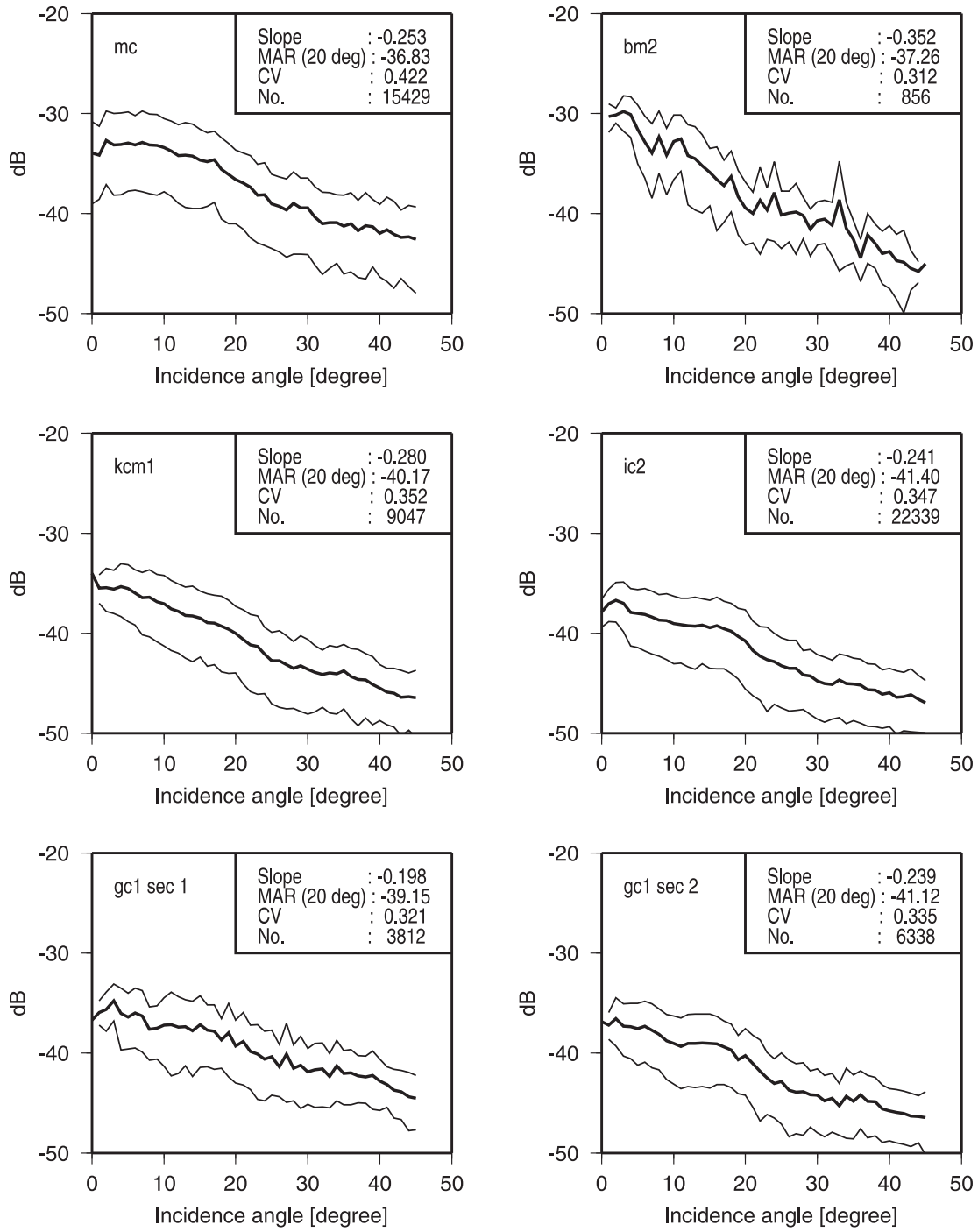

Figure 6-3. Mean angular backscatter response (thick lines) and associated standard deviation (thin lines) of six seafloor segments: mound cluster (mc), buried mound (bm2), Kings channel mouth (kcm1), inter-channel area (ic2) and two sections of the northernmost Gollum Channel (gc1 sec 1, gc1 sec 2). The calculated parameters slope, mean angular response at 20° incidence angle (linear regression fit), coefficient of variation (CV) and number of measurements are given inside the figure box.

for different Porcupine Seabight area seafloor types, which gives enough ground to differentiate among seafloor facies. However, inclusion of more data from different facies may provide a useful trend of the parameters for a specific type of seafloor in the study area.

Table 6-2 presents estimated parameters for different acoustic facies from the

Table 6-2. Parameters of the different facies in the study area: backscatter strength (BS) at 20° incidence angle (linear regression fit), slope (linear regression fit), coefficient of variation (CV). The remarks section gives specific aspects of the facies.

Area	BS (20°) [dB]	Slope [dB /deg.]	CV	Remarks
Mound	-34.76 to -39.40	-0.219 to -0.291	0.333 to 0.422	Highest BS and highest CV of all
Buried mound	-35.68 to -38.30	-0.185 to -0.362	0.312 to 0.367	Highest slope of all
Inter-channel	-40.38 to -41.79	-0.229 to -0.254	0.336 to 0.349	--
Channel	-37.12 to -43.19	-0.172 to -0.258	0.312 to 0.392	Lowest slope and lowest CV of all

Porcupine Seabight. Most of the parameters are found to be dominant for the mound, buried mound and channel facies. Comparatively, limited activities may be underlined from the inter-channel area data.

In Figure 6-4, three inter-parameter relationship plots for mound, buried mound, Kings Channel mouth seafloor, Gollum Channel seafloor and inter-channel areas are provided. Figure 6-4a provides a scatter plot of the slope of the angular backscatter curve versus a predicted backscatter value at 20° (regression fit) for all locations. Overall, a low correlation (correlation coefficient ~0.2) among slope and predicted backscatter at 20° is seen amongst the data from seafloor areas of the Porcupine Seabight. As already explained, the predicted 20° degree angular backscatter is estimated by means of regression fit to the mean angular backscatter response curves following the methods given by Hughes Clarke (1994). This value is somewhat different from the average angular backscatter strength. We have estimated a correlation coefficient of 0.98 between the average backscatter strength and predicted backscatter values at 20° based on the data of all seafloor segments which indicates that the estimated 20° predicted backscatter response can be an alternative to the mean angular backscattering strength at least for our data. Within a limited change of slope values, variations in the 20° backscatter response is dominant for the Gollum Channel seafloor which is indicative of a strong change of channel seafloor backscatter. Similarly, dominant variations of backscatter response are seen for generally higher slopes of the buried mounds. However, for carbonate mounds (higher backscatter and moderate slope) and inter-channel seafloor areas (ic1-ic3) (low backscatter and moderate slope), data clusters were found to be localized within very closed areas. For the cluster of seven mounds, the slope and 20° predicted backscatter values are in accordance with the other isolated mound data. No significant parametric variations are observed between the Kings Channel mouth areas (kcm1 and kcm2), whereas the other two data points from the channel system south of the Kings Channel (skc) indicate higher variations. The significant changes of the backscatter values within limited slope values for the Gollum Channel seafloor may indicate a presence or absence of a seafloor material contributing to the change. Occasional presence of white ooze within the channel seafloor is well correlated with the backscatter (Lampitt, 1985).

Figure 6-4b provides a plot of the CV values with respect to the predicted

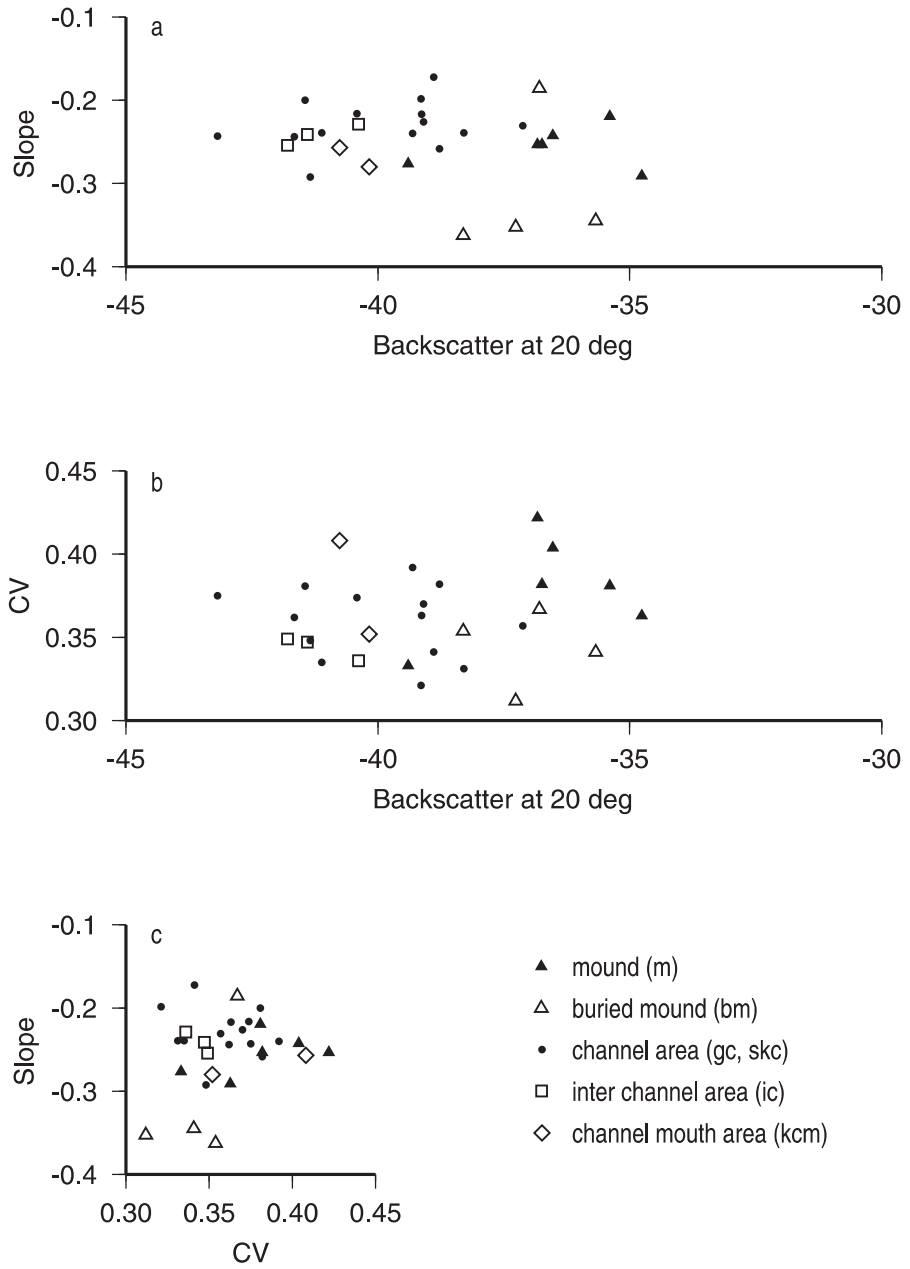

Figure 6-4. Statistical characteristics of the analyzed seafloor segments. **a** Shows the slope of the linear regression fit of the backscatter data versus the backscatter strength (linear regression fit) at 20° incidence angle. **b** Shows the coefficient of variation (CV) versus backscatter strength at 20° incidence angle (linear regression fit) and the slope of the linear regression fit of the backscatter data versus the CV is shown in **c**.

backscatter values at 20° incidence angle. The CV values are found to be decreasing with respect to the increase in the 20° backscatter response for mound area data, showing a fairly good correlation of ~-0.8. Station TTR7-AT-19G (m5) is not considered because the backscatter data correspond to background sediment data. For the buried mound areas, no such relation is seen i.e. CV is independent to the backscatter response. For Gollum Channel area seafloor, higher variations of the backscatter response are found to be unrelated with the CV. Though very limited sites are available from the interchannel areas, a very negligible fall in CV is seen with the backscatter response. On the whole, we presume that a moderate correlation among the CV and

20° predicted backscatter is observed for the total dataset.

Figure 6-4c presents a plot of the CV versus slopes. No correlation is observed between these two parameters when the entire dataset is considered. For the mound and buried mound areas, a moderate and good correlation is seen respectively (~0.5 to ~0.65). Within the channel seafloor, poor correlation (~-0.2) is observed between the CV and slope parameters. Overall, the slope of the backscatter curves does not show a significant change for various seafloor regimes within the Porcupine Seabight.

6.6 Conclusion

In this work, analyses of the multibeam angular backscatter data acquired in the eastern slope of the Porcupine Seabight area are carried out. Processing of the angular backscatter data using the 'NRGCOR' software is made for 29 locations to classify different geological provinces like: carbonate mounds, buried mounds, seafloor channels, and inter-channel areas. A detailed methodology is developed to produce angle-invariant (normalized) backscatter maps to clarify different seafloor sediment lithological aspects. Such a presentation has advantages above the raw angular backscatter data since the impact of the incidence angle is removed. The presented angle-invariant backscatter map possesses 12 dB dynamic range in terms of gray scale and reflects the lithology of various seafloor features. A clear distinction is seen between the mound-dominated northern side (Belgica province) and the Gollum Channel seafloor from the southern end of the site. A qualitative analysis of the calculated mean backscatter values i.e. gray scale levels, utilizing angle-invariant backscatter data generally indicates that backscatter values are highest (lighter gray scale) from the mound areas followed by buried mounds. The backscatter distribution also shows that mound structures not only impact their immediate vicinity, but also the wider surroundings illustrate mound-typical backscatter values (gray scale). However, mound-related backscatter patterns only exist within the depth range of the mounds. Patchy backscatter variations at 'off-mound' locations might correlate with inhomogeneous occurrences of corals in mound areas (Huvenne et al., 2002). Reported contour currents are also supported by the backscatter data. High backscatter around the mounds was also stated in Huvenne et al. (2002) based on 30 kHz ORETECH sidescan data. However, by means of multibeam backscatter data analyses, the main part of the margin was covered. The backscatter values are the lowest from the inter-channel areas (lowest gray scale level). Though moderate backscatter values (medium gray level) are observed from Gollum and Kings channel data, data show significant variability within the channel seafloor provinces. The segmentation of the channel seafloor provinces is made based on the computed gray scale levels for the present analyses as well as further studies based on the angular backscatter strength.

The application of the semi-empirical approach employed to the angular backscatter data provides three major parameters to classify the four major seafloor provinces of the Porcupine Seabight seafloor. Implementation involves the shape, variance and magnitude of the angular response applied to the measured multibeam angular backscatter strength data and provides effective classification and comparisons. The predicted backscatter response at 20° dB is the highest for the mound areas. The CV

of the mean backscatter response is also the highest for the mound areas. This indicates higher seafloor roughness compared to the surrounding sediments. However, reduced volume roughness is also expected in the mound-associated areas. Interestingly, the slope values are found to be the highest for the buried mound area. However, the channel seafloor of moderate backscatter response presents lowest slope and CV values. Interestingly, a critical examination of the inter-channel areas indicates less variability within the estimated three parameters.

The present study is a semi-quantitative effort. In order to understand the complex seafloor conditions, we are working on this subject employing quantitative methods to estimate seafloor roughness parameters. However, the presently produced imagery provides good information for marine science because it shows the degree of variability in terms of acoustic sediment properties. The technique developed is essentially applicable for geological interpretation, because changing sediment properties can be related to areas of different seafloor facies. The extent and variety of the seafloor facies gives an indication for the geological interpretation of the upper part of the seafloor sediments and its spatial validity.

SYNTHESIS

7 Synthesis

This chapter summarizes the main results of the previous chapters followed by outstanding problems and future perspective. The studies presented in chapters 4, 5 and 6 are one facet of multidisciplinary research undertaken to understand seabed structures and related processes at passive continental margins such as the Håkon Mosby mud volcano situated at the Norwegian-Barents-Svalbard continental margin, and the carbonate mounds in the Belgica province together with adjacent channels in the Porcupine Seabight. This research is an important facet because it gives an overview of the structures at the study sites and indicates sedimentary processes that guided their development. It gives further insight into the characteristics and variability of continental margins. The following sections refer to the aims listed in section 1.1.

The objectives of this thesis were two-fold: on the one hand bathymetric and angular backscatter data of different seabed structures were analyzed that are related to hydrocarbon seepage and that are of significant ecological importance. On the other hand multibeam angular backscatter data are used to quantify interpretations of shape invariant angular backscatter maps and to distinguish different seafloor facies.

7.1 Detailed bathymetry of the study areas and geological mapping

7.1.1 Håkon Mosby mud volcano

The Håkon Mosby mud volcano is an active seep and characterized by migrating hydrocarbon, pore water and mud expulsion. The small spatial extent and the weak topography of the Håkon Mosby mud volcano were obtained by densely spaced survey lines resulting in a multiple overlap of adjacent swathes (see section 4.5). The Håkon Mosby mud volcano is characterized by three morphological elements, i.e. flat crater like center (950 m diameter, 12 m height), circular embankment (1350 m diameter, 100 m breadth, 2 m height) and surrounding area influenced by the mud volcanism noticeable by a reduced surface slope compared to the general margin (2500 m diameter). The mud volcano shows greatest height in the northern part of the crater rim that decreases towards the center and towards the south. The slope of the continental margin is about 0.8° pointing in south-western direction. Down slope of the mud volcano the slope is about 1.3° and reaches up to 5° (average 3°) at the crater rim. The flat center of the Håkon Mosby mud volcano tends towards the south with a slope of about 0.3°.

7.1.2 Eastern slope of the Porcupine Seabight

Different morphological segments of the eastern slope of the Porcupine Seabight were analyzed separating the carbonate mounds and channel areas from the surroundings. The northern part of the eastern slope of the Porcupine Seabight is characterized by the Belgica mound province. Furthermore, a subdivision of the mound province into a northern (smaller mounds, less dense) and southern part based on the morphology of the mounds was observed. The number of mounds, their size, shape and occurrence with respect to the morphology of the continental margin were

quantified in this study and provide input for further investigations (e.g. Van Rooij et al., 2003; Huvenne et al., 2005; Wheeler et al., 2005). Altogether 35 surface mounds and 27 buried mounds have been distinguished (see section 5.4.1). The mounds have an ellipsoidal shape. They occur in a depth range of 1000 m to 700 m and are aligned along the margin. Other mounds form ridge-like or terrace-like structures. The occurrence of the mounds indicates depth dependence because most of them seem to rise from the 1000 m and 800 m depth contour. The range of their axes is approximately 0.5 km to 1.0 km and 1.0 km to 1.5 km, respectively. The height of the mounds is about 50 m but can reach 100 m. Moats have been recorded at the foot of some mounds with a depth up to 50 m. The typical orientation of the mounds is north-south. However, the eastern (shallower) mounds indicate a northeast orientation. Slopes of about 20° are typical but can reach 30° at the steeper west and north-west sides of the mounds. The continental margin shows a slope of about 5° in that area. Sediment waves have been found at the slopes of some mounds. They show a wave length of about 100 m and have heights around 2 m. Stratigraphy data based on sub-bottom profiles of the upper sediment layers was used together with bathymetry for interpretation of morphological structures to classify mound structures. Buried mounds and partly buried mounds have been identified in addition to surface mounds. De Mol et al. (2002 and 2005) analyzed seismic profiles of the Belgica mound province and classified some of the mounds as surface mounds which are assigned to buried mounds in this study. They also identified additional buried mounds that are not visible in the bathymetry data of this study.

The Belgica mounds (single, conical mounds or elongated clusters) exhibit different characteristics in contrast to the Hovland mounds (large mounds, conical shape) and Magellan mounds (small mounds mostly buried, various shapes; De Mol et al., 2002). An area of submarine canyons is situated south of the mound province. Two canyons with steep flanks of about 20° and 2 km to 4 km width cut the smooth sloped margin. Sharp edges in the deeper parts of the area indicate main scarps of sediment slides.

The southern part of the study area is dominated by the Gollum Channel System. The channels show deep incisions of about 200 m (400 m maximum) and proceed linearly without pronounced meandering. They have widths between 1 km and 1.5 km. The channel slopes are up to 25° steep. A regular undulation exists at the flanks of the southern channel with a wave length of about 800 m.

7.1.3 Discussion of bathymetric mapping

The multibeam bathymetry data of this study provide a snapshot of the Håkon Mosby mud volcano and the Belgica mound province and form the basis for spatial and temporal variability studies based on the morphology. They are also an essential basis for the success of multidisciplinary studies that require accurate position of sampling and observation devices.

The accuracy and resolution of the obtained terrain model of the Håkon Mosby mud volcano provide best depth information based on hull mounted multibeam systems. The subdivision of the Håkon Mosby mud volcano into morphological segments enables scientists to select sampling sites of spatially confined processes and different structural and ecological provinces. Further, the multibeam bathymetry of this study served as planning tool to conduct a remotely operated micro bathymetry survey

focusing on surface variability of the mud volcano. Towed sidescan and micro bathymetry data published by Milkov et al. (2004) and Edy et al. (2004b) revealed that the center of the Håkon Mosby mud volcano can additionally be divided into a crater and a hummocky periphery (crater rim).

The bathymetric data from the Belgica mound province supplement recorded seismic and sidescan data of other studies in the Porcupine Seabight (e.g. Huvenne et al., 2003; Kenyon et al., 1998; 1999). Mounds recognized on seismic profiles by Crocker and O'Loughlin (1998) in the area of the Gollum Channel System are not evidenced by the multibeam bathymetry of this study. The mound occurrence is limited to the north of the study area clearly separating the mound and channel area.

Coral reefs exist in conjunction with carbonate mounds and accommodate rich ecosystems. Impacts on coral reefs in the Porcupine Seabight and Porcupine Bank by trawling activity were documented for example by Grehan et al. (2004). Accurate locations and delineation of these habitats in the Belgica mound province based on this study provide the basis to establish conservation areas to preserve ecosystems and reproduction areas of fish as basis to fishery industry. The delineation of the mound provinces west of Ireland provides the basis to establish protected areas around the carbonate mounds and their associated cold water coral ecosystems. This is already realized for example in Norwegian waters to prevent destruction of the coral reefs by human impact (Fosså et al., 2005).

7.2 Use of multibeam data to determine sediment characteristics and seabed structure

7.2.1 Håkon Mosby mud volcano

Different sedimentological facies were identified at the Håkon Mosby mud volcano based on multibeam data. The bathymetry data of this study shows an outflow channel in the south of the central area indicating soft sediments with fluid characteristics at the center. The crater rim indicates more variable morphology compared to the center which points to more compacted sediments. The circular moat might result from subsiding sediments due to mud discharge or sediment compaction.

Multibeam sidescan data show higher backscatter at the center of the mud volcano in contrast to the low backscatter of the surrounding moat indicating different sediment properties. The high backscatter at the center might be related to the existence of free gas and gas hydrates in the sediment but could also be caused by the irregular seafloor and the erupting mud breccia (Huguen et al., 2004) or could be a combination of both. The low backscatter of the moat seems to be related to a combination of a flat sediment surface and soft sediments with low interface and volume heterogeneities (homogeneous structure) which provide penetration and hardly scattering targets.

Detailed information on the surface of the Håkon Mosby mud volcano was also acquired using video techniques (Jerosch et al., 2004b; Edy et al., 2004a). The bathymetry and backscatter data of this study agree well to the micro bathymetry findings of Edy et al. (2004b) in terms of surface structure. The distribution of bacterial mats and benthic communities and their relation to gas occurrence is described for example in Jerosch et al. (submitted) and cannot be revealed from the multibeam data.

7.2.2 Eastern slope of the Porcupine Seabight

The multibeam bathymetry provides the first three-dimensional picture of the seabed form and the distribution of the Belgica mound province. The mounds are built up of corals and occur in a small bathymetric window with a distinct alignment along the slope. The limits of the mound province and the variability in size relate to the mound growth and indicate areas of optimal nutrient supply and favorable growing conditions for the corals due to enhanced currents and low sedimentation. The results provide important constraints on models of mound formation and growth in relation to lateral (along slope) and vertical (down slope) sediment transport processes on the continental margin (Wheeler et al., 2005). The initiation of mound growth seems to be restricted to the delineated areas of the present mound provinces (De Mol et al., 2002) and the occurrence of mounds may act as indicator for (strong) bottom currents (Van Rooij et al., 2003). Sidescan and video observation identified small Moira mounds that are not recorded in the bathymetry of this study. Moira mounds possibly represent early stages of the carbonate mound development whose growth depends on the hydrodynamics and sand transport (Wheeler et al., 2005).

Different sediment characteristics are obvious for the mound and channel areas. In the mound area coarser material is expected compared to the smooth channel floors and the area of sediment slides. The sediment characteristics of the well delineated mound province are also expected to be different compared to the area outside the mound province because of the changing current regime and the impact of the mounds themselves on currents and sedimentation. Seismic profiles and sidescan data of other studies clarify the relation of the mounds to the surrounding drift sediments and current features like sediment waves and moats (De Mol et al., 2002; Van Rooij et al., 2003).

The southernmost channel of the study area shows the deepest relative depth at the steepest part of the margin. Therefore, increased current speed is expected at the margin indicating reduced sedimentation or erosion compared to other parts of the channel. The smooth morphology in the deeper part of the channel indicates increased sedimentation.

7.2.3 Results based on multibeam analysis of seabed structures

Sediment transport creating different seabed types can be recognized based on bathymetry and backscatter data. However, the intrinsic source of the transport is not contained in the multibeam data. The source of transport and the type of sediment can be identified for example from the oceanographic conditions (e.g. current speed and direction). Interpretation of sediment types can be realized based on a few sediment samples at locations determined based on multibeam data analysis. A distinct description of sediment types delineated by multibeam bathymetry and backscatter data should be supplemented with sediment samples.

The combination of bathymetry and angle-invariant or sidescan backscatter data forms a useful tool to recognize sediment transport structures. Channels, scarps of sediment slides, current scours and moats can be recognized. Backscatter lineations were observed at various locations in the study areas and are not depictable based on bathymetry only. In the Belgica mound province, parallel lineations of low backscatter are observed indicating down slope sediment transport. Striations mainly west of the Håkon Mosby mud volcano also indicate sediment transport.

Due to the resolution and footprint size of the deployed multibeam system, the data density is not sufficient to analyze variations at individual mounds in the Belgica province. The spatial coverage with the full range of incidence angles is necessary to study the patchy occurrence of corals at the mounds. The recent coverage supports full bathymetric coverage but is not appropriate to detect features like the Moira mounds and coral patches at the mounds. Dense survey lines are preferred as realized at the Håkon Mosby mud volcano. However, data from different mounds and mound provinces can be compared and distinguished from other seafloor facies.

Beyer (2002) tried to determine the coral coverage of mounds based on backscatter data. Different types of angle-invariant backscatter characteristics have been found at the mounds but due to the multibeam operation in Medium Depth mode and the small scale distribution of corals around mounds it was finally not approved to discriminate coral thickets from debris fields and background sediments.

Multidisciplinary analyses of the data acquired in this and other studies agreed that only the drilling of one exemplar mound including its base could clarify the origin of the carbonate mounds in the Belgica province and their relation to hydrocarbon seepage. Mapping techniques provided not sufficient information about the internal structure of the carbonate mounds and the initiation of the mound growth. Drilling of a carbonate mound was performed during IODP 307 and yielded cores of more than 100 m length at three sites (mound and background sites) that also contain the mound base (Expedition Scientists, 2005). Analyses of the data provide detailed information about the age of this mound and its internal structure. The link between the cold water corals, carbonate mounds and gas discharge is not yet finally answered and still topic of scientific investigations (Hovland, 2005; Expeditions Scientists, 2005).

7.3 Use of multibeam bathymetry and angular backscatter data to determine spatial and temporal variations of surface seabed matter

7.3.1 Håkon Mosby mud volcano

The small spatial extent of the Håkon Mosby mud volcano with respect to the swath width of the multibeam system and the multiple overlap of the survey lines provide outstanding pre-conditions to seabed based segmentation. The study site at the Håkon Mosby mud volcano proved that spatial selection of backscatter segments has advantages above the analysis of swath wise backscatter analysis. Dense angular seabed coverage of this study provides data to determine backscatter variability within the swath.

Angular backscatter data indicate the spatial variability of the echo intensity of the Håkon Mosby mud volcano. The center of the mud volcano and the surrounding moat can be separated based on the angle-invariant backscatter data which agrees with the multibeam sidescan data (see section 7.2.1). Higher backscatter at the center might be caused by the existence of free gas and gas hydrates in the sediment. Irregular seabed surface might also contribute to higher echo strength. Flat and homogenous sediments at the surrounding moat might result in the observed low backscatter strength.

However, the backscatter shows incomplete agreement with morphology indicating sedimentary processes that are not represented in the bathymetry. The eastern part of

the circular moat indicates significant higher backscatter strength than the low backscatter western side. Sediment transport around the mud volcano is indicated by lineated backscatter variation. It provides hints of down slope sediment transport by gravity or seabed currents.

7.3.2 Eastern slope of the Porcupine Seabight

Bathymetry data were used to identify current activity proven by distinctly deeper depths at the outward bending of the channels in the Gollum Channel System. The southern channel indicates a 30 m deeper channel floor at the outward bending. This characteristic becomes visible in particular in the cross profile of the channels and indicates particle flow in the channels. Sediment variability at the channel floor becomes evident in combination with the angle-invariant backscatter data indicating transport processes. Sediment transport is also proposed by Tudhope and Scoffin (1995).

The angular backscatter analysis of this study shows different characteristics for channel, mound and inter-channel areas. The morphological separation is also proven by the angular backscatter data which delineates different seabed facies. The backscatter variation provides a major indication for changing sediment characteristics. It turned out that the recognized variations of the angular backscatter data can be used to distinguish seabed facies. Segments of the channel seafloor indicate small scale variations, but analyses of sediment samples and video observations did not always show significant sediment changes (Beyer et al., 2004d; Winkler 2005). This might be due to the different scales of the underlying data. Sediment samples represent a seafloor area of about 6 cm diameter, video observations 1 m up to a few meters, and the backscatter data is based on the Hydrosweep DS-2 footprint of about 50 m diameter. Some backscatter variation at the channel seafloor might result from varying sediment surface micro topography.

7.3.3 Applicability of this method

Seafloor provinces were distinguished in this study based on multibeam bathymetry and backscatter data. The extent of the separated segments agrees in many cases in terms of morphology and backscatter characteristics. Additional information is available in cases when backscatter data indicate spatially different characteristics compared to morphology. Small scale sediment variation were detected that separate morphological homogeneous segments or that combine different morphological facies. Variable backscatter characteristics resulted in sub-segments of the channels in the Porcupine Seabight. At the Håkon Mosby mud volcano, the crater and circular moat are connected by an area of high backscatter strength. Backscatter variations that differ from the morphological boundaries provide additional information about seabed characteristics and transport processes. Such analysis is only applicable when bathymetry and backscatter data of similar resolution and quality is available. The areas of overlapping morphological and backscatter segments indicate locations that require additional detailed investigations. The scale of separated segments based on backscatter and morphology variation depends on the quantity of measurements and ranges from sizes smaller than the multibeam swath to areas that extent across the entire survey area.

Temporal variations at the seabed are expected to be ascertainable at a regional scale when the study sites are revisited. Variations in depth and backscatter strength need to be at least of the size of the determined accuracy of the depth measurements and the coefficient of variation, respectively, in order to be detectable. Transport processes that resulted in accumulation of sediment could not be verified with the multibeam data of this study. Areas of sediment slides were detected and provide the basis for modelling the seabed surface prior to the slide event.

7.4 Use of multibeam backscatter data to map geological provinces

7.4.1 Håkon Mosby mud volcano

The multibeam backscatter data revealed different sedimentological facies at the Håkon Mosby mud volcano. Geological provinces can be distinguished based on multibeam sidescan and angular backscatter data that indicate variable echo intensity around the mud volcano. The main characteristics of the separated provinces are the existence of free gas and gas hydrate at the center of the mud volcano and smooth, homogeneous sediments at the surrounding moat.

Multibeam sidescan variations at the Håkon Mosby mud volcano are also supported by multibeam angular backscatter data (Beyer et al., 2004a; 2004b). The center of the mud volcano shows the highest backscatter and the lowest slope. At the circular moat the backscatter is lowest and the slope of the angular backscatter curve is steepest. However, the angle-invariant backscatter shows incomplete agreement with the morphology indicating sedimentary processes that are not represented in the bathymetry. The eastern part of the circular moat indicates significantly higher backscatter strength which is connected to the central part of the Håkon Mosby mud volcano than the low backscatter western side. Sediment transport around the mud volcano is indicated by lineated backscatter variation. It provides hints of down slope sediment transport by gravity or seabed currents.

7.4.2 Eastern slope of the Porcupine Seabight

Bathymetry data were used in combination with angular backscatter values to identify different seabed facies. A number of 29 locations were assigned to mounds, buried mounds, channel, inter-channel and channel mouth areas. Based on the quantitative analysis of the multibeam angular backscatter data, three parameters were used to distinguish seabed facies comprising the slope of the angular backscatter curve, the mean angular response at 20° incidence angle and the coefficient of variation. Mounds show highest backscatter values and highest coefficients of variation. At buried mounds, the highest slope of the backscatter curve is observed. In contrast, slope and coefficient of variation is lowest for the channel facies. Less variability within the parameters was observed for the inter-channel areas indicating homogeneous sediments across the segments. The generated angle-invariant backscatter map shows a 12 dB dynamic range.

A relation between backscatter and grain size in the study area was observed by Beyer et al. (2004c) indicating coarser material for the mound province and fine material for the inter-channel areas. However, the grain size is but one parameter

affecting the seabed roughness. The backscatter data is also affected by interface and volume roughness of the seabed. Variation of the angle-invariant backscatter indicates changes in the sediment properties in the canyon area and the channels of the Gollum Channel System. In particular, the alternating gray scale of the northern most channel of this channel system indicates different provinces. The backscatter strength variation between adjacent channel segments (succession of high and low angle-invariant backscatter) cannot be explained by grain size. The grain size showed finer sediments towards the lower part of the channel (Winkler, 2005). The interface roughness seems to dominate the backscattering and shows different spatial variability compared to the sediment grain size. The segmentation of the channel floor, therefore, relates to changes of seabed roughness which is difficult to verify with seabed samples. It is assumed that the variation of seabed roughness also originates from bottom currents which sort the sediment.

The backscatter gray scale map of this study has lower resolution (50 m) compared to the sidescan images (0.4 m and 6 m) analyzed by Huvenne et al. (2002 and 2005). They also identified small mounds and pockmarks that have smaller size than the data of this study. Therefore, variations within a single mound structure cannot be identified based on this data. In contrast to the sonar image analysis of towed sidescan systems, this study focuses on parameters of the angular backscatter curve and delineates seabed facies on a larger (regional) scale.

7.4.3 Applicability and advantages of multibeam backscatter data

Ship-borne multibeam surveys are a remote sensing tool and capable to cover large areas in comparatively short time. Limits of the spatial resolution of the presented multibeam data exist due to the distance of the hull mounted system from the seafloor.

The application of multibeam angular backscatter data enables the user to define seabed facies of different acoustic properties. The normalized, angle-invariant backscatter data serve as indicator for different acoustic facies. Because of the relation of backscatter and sediment characteristics, multibeam backscatter data provide a useful tool for seabed classification. The segmentation of the seafloor is capable to delineate structured regions. Based on the described method, seabed facies can be distinguished. Furthermore, the application of backscatter strength models can be restricted to the determined segments. The backscatter data provide first information for geological interpretations of the seabed in addition to bathymetry and sub-bottom profiles. Sampling sites selected basically on the acoustic segmentation (e.g. for sediment samples, video observation) then provide information on the characteristics of the seafloor provinces. The analysis of the angular backscatter data by means of backscatter curve parameters provides quantitative information about the seabed segments (see chapter 6). Backscatter data can be used to analyze delineated seabed segments but are also capable to map the sediment surface and its spatial variability. Sediment samples together with the angle-invariant backscatter map can be used to determine boundaries of the spatial validity of sediment properties and provide ground truth for backscatter data.

The angle-invariant backscatter map and the segmentation allow a generalization of geological analyses over the study area which are limited in practice to considerable small areas. This approach assumes that noticeable changes in the parameters

studied will be visible in the acoustic signals received (Lurton, 2002).

Segments of the channels in the Porcupine Seabight showed that the backscatter data is sensitive to variations of the sediment surface that are independent from grain size and therefore give information about the micro topography. Ground truth for backscatter data is important in these regions and the source of the backscatter variation is difficult to reveal with geological surface samples. The segments give a detailed view of the seabed and its variability and indicate optimal sample locations for ground truth.

7.5 Outstanding problems and future perspective

The results of this study were derived from the analysis of multibeam bathymetry and angular backscatter data. Not all obstacles that were detected could be solved within the frame of this thesis. In particular, issues regarding the spatial resolution, ground truth and technical aspects of the backscatter data need to be solved and form the outline of the future perspective.

7.5.1 Spatial resolution

The target areas of this study are characterized by a small spatial extension. Limits of the application of hull mounted multibeam systems are generated by their spatial resolution and frequency. For resolution enhancement, remote sensing techniques need to come closer to the target, for example by towed systems or by deploying remotely operated vehicles (e.g. Huvenne et al., 2005; Klages et al., 2004; Edy et al., 2004a). Their deployment, however, is accompanied with higher costs and increased time consumption.

Investigations based on video observations provide the highest resolution of non-destructive in situ observations. The active area of such systems is rather limited and locations designated for study need to be selected carefully beforehand. Therefore, it is advisable to use for example towed sidescan systems to pre-survey potential video observation or micro bathymetry sites selected based on ship-borne multibeam data. The deployment of towed sidescan systems then provides the transition from the ship-borne multibeam systems to detailed investigations with remotely operated vehicles.

Intense analysis of video observations and micro bathymetry are available for analysis in comparison with the multibeam bathymetry and backscatter data (Klages et al., 2004; Jerosch et al., 2004a). The link to the distribution of bacterial mats and benthic communities and their relation to gas occurrence gives new insights into the properties of the Håkon Mosby mud volcano. The data of this study cover the surroundings that were not covered by micro bathymetry and indicate areas of future studies recognized by morphologogical and backscatter characteristics (e.g. eastern part of the Håkon Mosby mud volcano). Furthermore, a combination of both bathymetry data sets provides the basis to study the level of detail obtainable with the Hydrosweep DS-2 multibeam system.

7.5.2 Ground truth for angular backscatter data

Seafloor segments that represent different sediment facies were separated in this study based on multibeam angular backscatter data and morphology information.

Ground truth is necessary to verify the classification. Sediment samples at representative locations are necessary for a detailed description of the seabed sediments (e.g. Van Walree et al., 2005). A systematic inventory of seabed types and their acoustic properties is recommended to support rough scale interpretations at unknown sites prior to further sampling. This should also consider the different levels of resolution of seabed samples and the multibeam footprint. Laboratory experiments indicated that little roughening of a smooth surface suffices to greatly increase the backscattered return (Urick, 1983).

Sediment samples were collected based on angular backscatter segmentation during RV *Polarstern* expedition ARK XIX/3a at different sites of the eastern slope of the Porcupine Seabight (Beyer et al., 2004d; Winkler, 2005). The information about sediment properties provides the basis for seabed interpretation. It is also input for the composite roughness theory which is used to determine quantitative interface and volume roughness parameters of the seabed (e.g. Jackson et al., 1986; Chakraborty et al., 2000; Beyer et al., 2003a). Sediment samples can be used to validate the backscatter models. In a next step, ground truth of the selected sites needs to be correlated to the backscatter characteristics. Based on these data it may later on be possible to predict physical properties of the seafloor (Hughes Clarke, 1994).

Future work at the Porcupine Seabight and the Håkon Mosby mud volcano should focus on the analysis of micro bathymetry and video observations to determine surface roughness of the seabed at the study sites. It contributes to the identification of the source of variable backscatter strength which is not verified by sediment samples as observed in the Gollum Channel System.

7.5.3 Approaches for angular backscatter analysis

Techniques of seafloor analysis and segmentation based on echo intensity can be adapted to a wide range of multibeam systems. Other approaches focuses mainly on image gray scale analysis based on texture analysis (e.g. Preston et al., 2004). However, high data density relatively to the target size is necessary for such analysis which is absent for ship-borne multibeam systems when focusing on small scale structures. It is, therefore, more suited for towed high resolution sidescan systems or backscatter analyses of recorded micro bathymetry.

Gas bubbles in the sediment affect the volume roughness of the seafloor and contribute to the volume backscattering at higher incidence angles. Based on sub-segments at the Håkon Mosby mud volcano, one focus of future research should lie on the quantification of the amount of gas and gas hydrate in the sediment. This also implicates the availability of representative sediment samples.

Indications of sediment slides have been found in the central part of the study area in the Porcupine Seabight. Slide areas and scarp lines are visible in the multibeam data. The quantification of moved sediments and mapping of the head scarps can be done based on the bathymetry and backscatter data providing an inventory of mass movements.

An automatic algorithm for seabed segmentation based on parameters of the angular backscatter data would provide first clues for interpretation of the seabed. Due to an objective and repeatable automatic segmentation, the approach assists first onboard interpretations with quantitative parameters. Additional software development

is required to convert the applied method into real-time processing and automatic segmentation algorithm. This also includes real-time or near real-time availability of accurate terrain models. Special attention need to be paid to seabed variability that occurs within the swath width.

Backscatter data of this study were recorded with an uncalibrated multibeam system and can be used to identify relative variations of the seafloor backscattering. Calibrated systems provide absolute units of surface scattering in addition to the depth measurement which is essential to observe possible natural or man-made changes of the seafloor over time (Foote et al., 2005). They also provide the opportunity to directly compare backscatter data with scattering models and different sonar systems, and to convert acoustic measurements to physical or biological measures (e.g. Mitchell and Somers, 1989; Foote et al., 2005)

7.5.4 Main future activities

Although some problems remain unsolved (section 7.5.1 through 7.5.3), two main directions are proposed on which future research in the field of multibeam backscatter analysis should focus:

a) Correction of the beam pattern effect and the erroneous angular characteristic of the backscatter curve in the Medium Depth mode:

The angular backscatter data of this study show increased backscatter values at incidence angle around 15°. It was found that this characteristic is correlated with the beam number (beam pattern effect). Future analysis should focus on a correction of the theoretically determined beam coefficients that are applied during the backscatter process.

Furthermore, backscatter data of the Medium Depth mode show significant differences to the Deep Sea mode data. It becomes obvious in particular at study sites that cover depth ranges shallower than 800 m. The data presented in chapter 6 are affected by the Medium Depth mode indicated by data gaps between survey lines of the Deep Sea mode. Further studies are necessary to identify the source of that error to provide homogeneous data of the entire depth range of the Hydrosweep DS-2 multibeam system. It is of particular importance because sedimentary active areas at the continental margins occur in a depth range the requires both the Deep Sea and Medium Depth mode for mapping.

b) Ground truthing of backscatter characteristics:

In order to broaden the application of angular backscatter data for geological interpretation, it is proposed to focus on the effect of sediment properties such as grain size and micro topography on the backscatter data. A diversified data set that covers a wide range of surface characteristics of the sediment comprising sediment samples, micro bathymetry and video observations was obtained during the cruise ARK XIX/3. These finding can then serve as basis for an inventory of sediment properties and backscatter characteristics.

ACKNOWLEDGEMENTS AND REFERENCES

8 Acknowledgements

Many persons have contributed to the realization of this PhD thesis. I would like to thank them all for their cooperation in the research that resulted in the various publications.

I sincerely thank my advisors and referees Prof. Dr. Heinrich Miller and Prof. Dr. Katrin Huhn who enabled me to finalize and submit this thesis at the University of Bremen. I also thank Prof. Dr. Dieter Fütterer who gave me the opportunity to start and realize my research at the Alfred Wegener Institute for Polar and Marine Research in Bremerhaven.

I convey my special thanks to Dr. Hans Werner Schenke for his engagement in bathymetric research and for organizing various opportunities for seagoing experience and continuation of this research.

To the same degree, I would like to thank Prof. Dr. Michael Schlüter for establishing the possibility for research at the Håkon Mosby Mud Volcano which gave me insight to an unknown and extraordinary marine seabed structure.

Many thanks go to all co-authors of the publications, talks and posters that developed from this research. In particular, I thank Dr. Bishwajit Chakraborty from the National Institute of Oceanography, Dona Paula, in India who gave me plenty support in the field of multibeam backscatter analysis. Dr. Bishwajit Chakraborty pushed the multibeam backscatter analysis at the Alfred Wegener Institute considerably and we shared many fruitful discussions.

I acknowledge all reviewers of my publications for their critical remarks and annotations that very much improved the quality and the language of the manuscripts.

This research was only possible by the funding of the European Commission Fifth Framework Project Geomound (contract no. EVK3-CT-1999-00016).

I sincerely acknowledge the Alfred Wegener Institute for Polar and Marine Research for the opportunity to work in the field of marine science and to realize this research. This thesis would not have been possible without the support of the Alfred Wegener Institute that realized funding during different periods in the last few years.

I enjoyed the work within the Geomound and Ecomound community and I would like to thank in particular Prof. Dr. Jean-Pierre Henriet, Prof. Dr. Wolf-Christian Dullo, Dr. Veerle Huvenne, Dr. David van Rooij and Dr. Andy Wheeler for discussing data and improving my understanding of carbonate mounds and cold-water coral communities. I also thank the shipboard parties of the RV *Polarstern* expeditions ANT XVII/4 and ARK XIX/3.

I would like to thank Dr. Catalina Gebhardt for motivation, fruitful discussions, for pushing the finalizing of the manuscript and improving of the English language of this thesis. Many thanks also go to Dr. Angela Schäfer, Kerstin Jerosch, Christina Morchner and Ulrich Fritsche for their support in the field of geo-data modelling and analysis. I thank Dr. Christopher Cogan for his effort to correct the English language of the final manuscript.

I enjoyed very much the friendly and cooperative atmosphere within the Bathymetry and Geodesy group at the Alfred Wegener Institute. I would like to thank my colleagues for inspiring discussions and for help in various computer software and hardware matters. In particular I acknowledge Fred Niederjasper, Dr. Martin Klenke, Ralf Krocker, Daniel Schulte, Jörn Hatzky, Merijn Jacops, Andreas Winkler, Rike Rathlau and Tanja Kohls.

I also sincerely thank my parents who gave me the opportunity to start my studies in Geodesy which forms the basis of my recent work.

9 References

Anonymous, 1993. Atlas Hydrosweep DS, Data for backscattering analysis, GE6017F101SB, internal report, STN Atlas Elektronik, Bremen.

Anonymous, 1994. Atlas Hydrosweep DS-2 Software-Paket zur Bestimmung des Rückstreumaßes nach de Moustier, BL1039G192, system description, internal report.

Anonymous, 1999. The Mound Factory: Internal Controls, Geomound. Project description, 14 June 1999, proposal # EVK3-1999-00080.

Bergmann, M., 2004. Mapping of (fish) habitats at the Håkon Mosby Mud Volcano. In: Klages M., Thiede J. and J.-P. Foucher, 2004. The expedition ARK XIX/3 of RV ‘‘Polarstern’’. Reports on Polar and Marine Research, 488, 220-224.

Beyer, A., 2002. Seafloor analyses based on multibeam backscatter strength. EGS 27th General Assembly 2002, Nice, France, 21-26 April 2002.

Beyer, A., Chakraborty, B., Schenke, H. W, 2003a. Multi-beam backscatter data to characterize the mound and channel provinces of the Porcupine Seabight - northeast Atlantic margin, EGS Meeting 2003, Nice, France, 6-11 April 2003.

Beyer, A., Schenke, H. W., Klenke, M. and Niederjasper, F., 2003b. High resolution bathymetry of the eastern slope of the Porcupine Seabight, Marine Geology 198, 27-54, doi:10.1016/S0025-3227(03)00093-8.

Beyer, A., Rathlau, R., Schenke, H. W, 2004a. Haakon Mosby Mud Volcano: Terrain model and multibeam backscatter analyses. EGU General Assembly 2004, Nice, France, 25-30 April 2004.

Beyer, A., Rathlau, R., Schenke, H. W, 2004b. Bathymetrie und Rückstreueigenschaften das Haakon Mosby Schlammvulkans. Dokumentation 19. Hydrographentag 2004, Stralsund, 7.-9. Juni 2004, Deutsche Hydrographische Gesellschaft, Stade.

Beyer, A., Chakraborty, B., Schenke, H. W., 2004c. Seafloor characterization based on multibeam backscatter data. In: Simons, D. G. (Editor), Proceedings of the Seventh European Conference on Underwater Acoustics, ECUA 2004, Delft, The Netherlands, 5-8 July 2004, Vol. 2, 769-774.

Beyer, A., Krocker, R., Pokorna, M., Rathlau, R., Dabrowski, P., 2004d. Microbathymetry surveys along deep-water canyons (Gollum Channel) in the Porcupine Seabight. In: Klages M., Thiede J. and J.-P. Foucher, 2004. The expedition ARK XIX/3 of RV ‘‘Polarstern’’. Reports on Polar and Marine Research 488, 33-43.

Beyer, A., Chakraborty, B., Schenke, H. W., 2005a. Seafloor classification of the mound and channel provinces of the Porcupine Seabight: an application of the multibeam angular backscatter data, International Journal of Earth Sciences (Geologische Rundschau), doi:10.1007/s00531-005-0022-1.

Beyer, A., Rathlau, R., Schenke, H. W., 2005b. Multibeam bathymetry of the Håkon Mosby Mud Volcano. Marine Geophysical Researches 26, 61-75, doi:10.1007/s11001-005-1131-8.

Blondel, P., Murton, B. J., 1997. Handbook of Seafloor sonar imagery, John Wiley & Sons, Praxis Publishing, Chichester.

Boetius, A., Ravenschlag, K., Schubert, C. J., Rickert, D., Widdel, F., Gieseke, A., Amann, R., Jørgensen, B. B., Witte, U., and Pfannkuche, O., 2000. Microscopic identification of a microbial consortium apparently mediating anaerobic methane oxidation above marine gas hydrate. Nature 407, 623-626.

Boetius, A., de Beer, D., Foucher, J.-P., Kaul, N., Schlüter, M., Witte, U., Usbeck, R., shipboard scientific party, 2004. Cruise leg ARK XIX/3b: An introduction into multidisciplinary investigations on methane fluxes and related processes at the Håkon Mosby Mud Volcano. In: Klages, M., Thiede, J. and Foucher, J.-P. 2004. The expedition ARK XIX/3 of RV ‘‘Polarstern’’. Reports on Polar and Marine Research 488, 153-157.

Bohrmann, G., Ivanov, M., Foucher, J.-P., Spiess, V., Bialas, J., Greinert, J., Weinrebe, W., Abegg, F., Aloisi, G., Artemov, Y., Blinova, V., Drews, M., Heidersdorf, F., Krabbenhöft, A., Klaucke, I. Krastel, S. Leder, T., Polikarpov, I., Saburova, M., Schmale, O., Seifert, R., Volkonskaya, A., Zillmer, M., 2003. Mud volcanoes and gas hydrates in the Black Sea: new data from Dvurechenskii and Odessa mud volcanoes, Geo-Marine Letters, Volume 23, Issue 3-4, 239-249.

CARIS, 1998. Hydrographic Information Processing System, User’s guide. Universal Systems Ltd., Fredericton, NB.

Caruthers, J. W., 1979. Fundamentals of Marine Acoustics. Second impression, Elsevier, Amsterdam.

Carter, D. J. T., Matthews, D. J., 1980. Echo-Sounding Correction Tables, Formerly Matthews' Tables. Third edition, Hydrographic Department, Ministry of Defence, Taunton.

Chakraborty, B., Schenke, H. W., Kodagali, V, Hagen, R., 2000. Seabottom characterization using multibeam echosounder angular backscatter: An application of the Composite Roughness Theory. IEEE Transactions on geoscience and remote sensing, Volume 38, No. 5, 1-4.

Chen, C.-T., Millero, F. J., 1977, Speed of sound in seawater at high pressures, Journal of the Acoustical Society of America 62, 1129-1135.

Crane, K., Herrington, S. and Egorov, A. V., 1997, High heat flow and warm water-methane enriched plumes above the Håkon Mosby mud volcano. Eos 78, 187.

Colladon, J. D., Sturm, J. K. F., 1827. The compression of Liquids (in French). Annales de Chimie et de la Physique, Series 2 (36), part IV, Speed of Sound in Liquids, 236-257.

Clennell, M. B., 2000. Submarine gas hydrates: Nature, occurrence & perspectives for exploration in the Brazilian continental margin. Brazilian Journal of Geophysics, Vol. 18 (3), 397-410.

Cohen, P. M., 1970. Bathymetric navigation and charting. United States Naval Institute, Annapolis, Maryland.

Cook, P. J., Carleton, C. M., 2000. Continental shelf limits, The scientific and legal interface. Oxford University Press, New York.

Croker, P. F., Shannon, P. M., 1987. The evolution and hydrocarbon prospectivity of the Porcupine Basin, offshore Ireland. In: Brooks, J., Glennie, K. W. (Editors), Petroleum Geology of North West Europe. Graham and Trotman, London, 633-642.

Croker, P. F., Klemperer, S. L., 1989. Structure and stratigraphy of the Porcupine Basin: relationship to deep crustal structure and the opening of the North Atlantic. In: Tankard, A. J., Balkwill, H. R. (Editors), 1998. Extensional Tectonics and Stratigraphy of the North Atlantic margins. American Association of Petroleum Geologists, No. 46, 445-459.

Croker, P. F. and O'Loughlin, O., 1998. A Catalogue of Irish offshore carbonate mounds. In: De Mol, B. (Editor), 1998. Geosphere-biosphere coupling: Carbonate Mud Mounds and Cold Water Reefs. IOC-UNESCO Workshop Report 142, 11.

De Mol, B., Friend, P., Akhmetzhanov, A., Ivanov, M., de Haas, H., Belenkaya, I., Stadnitskaya, A., 1999. Porcupine Seabight: Short visit. In: Kenyon, N. H., Ivanov, M. K., Akhmetzhanov, A. M. (Editors), 1999. Geological Processes on the Northeast Atlantic Margin. IOC Technical Series 54, UNESCO, 34-47.

De Mol, B., Van Rensbergen, P., Pillen, S., Van Herreweghe, K., Van Rooij, D., McDonnell, A., Huvenne, V., Ivanov, M, Swennen, R., Henriet, J.-P., 2002. Large deep-water coral banks in the Porcupine Basin, southwest of Ireland. Marine Geology 188, 193-231.

De Mol, B., Henriet, J.-P., Canals, M., 2005. Development of coral banks in Porcupine Seabight : do they have Mediterranean ancestors? In: Freiwald, A. and Roberts, J. M. (Editors), 2005. Cold-water corals and Ecosystems. Springer, Berlin, Heidelberg, 515-533.

Dimitrov, L. I., 2002. Mud volcanoes – the most important pathway for degassing deeply buried sediments. Earth-Science Reviews 59, 49-76.

Edy, C., Bisquay, H. and shipboard scientific party, 2004a. Microbathymetry on ROV "Victor 6000". In: Klages M., Thiede J. and J.-P. Foucher, 2004. The expedition ARK XIX/3 of RV ''Polarstern''. Reports on Polar and Marine Research 488, 158-163.

Edy, C., Bisquay, H., Foucher, J.-P., Opderbecke, J., Simeoni, P., Allais, A.-G., Beyer, A., Jerosch, K., Rathlau, R., 2004b. Microbathymetry of the Hakon Mosby Mud Volcano off Northern Norway: Results of a ROV-born multibeam survey. EGU General Assembly 2004, Nice, France, 25-30 April 2004, Geophysical Research Abstracts, Vol. 6, 04619.

Eldholm, O., Sundvor, E., Vogt, P. R., Hjelstuen, B. O., Crane, K., Nilsen, A. K. and Gladczenko, T. P., 1999. SW Barents Sea continental margin heat flow and Håkon Mosby Mud Volcano, Geo-Marine Letters 19, 29–37.

Expedition Scientists, 2005. Modern carbonate mounds: Porcupine drilling. IODP Preliminary Report 307, doi:10.2204/iodp.pr.307.2005.

Fosså, J. H., Lindberg, B., Christensen, O., Lundälv, T., Svellingen, I., Mortensen, P. B., Alvsvåg, 2005. Mapping of *Lophelia* reefs in Norway: experiences and survey methods. In: Freiwald, A. and Roberts, J. M. (Editors), 2005. Cold-water corals and Ecosystems. Springer, Berlin, Heidelberg, 359-391.

Foote, K. G., Chu, D., Hammar, T. R, Baldwin, K. C., Mayer, L. A., Hufnagle Jr., L. C., Jech, J. M., 2005. Protocols for calibrating multibeam sonar. Journal of the Acoustical Society of America 117 (4), 2013-2027.

Freiwald, A. and Roberts, J. M. (Editors), 2005. Cold-water corals and Ecosystems. Springer, Berlin, Heidelberg.

GEBCO, 1997. General Bathymetric Chart of the Oceans (Data from GEBCO Digital Atlas), Sheet 97.3, bathymetric contours. IOC, IHO and BODC, 'Supporting Volume to the GEBCO Digital Atlas' , published on behalf of the Intergovernmental Oceanographic Commission (of UNESCO) and the International Hydrographic Organization as part to the General Bathymetric Chart of the Oceans (GEBCO), British Oceanographic Data Centre, Birkenhead.

Gebruk, A. V., Krylova, E. M., Lein, A. Y., Vinogradov, G. M., Anderson, E., Pimenov, N. V., Cherkashev, G. A., Crane, K., 2003. Methane seep community of the Håkon Mosby mud volcano (the Norwegian Sea): composition and trophic aspects. Sarsia 88, 394-403.

Ginsburg, G. D., Milkov, A. V., Soloviev, V. A., Egorov, A. V., Cherkashev, G. A., Vogt, P. R., Crane, K., Lorenson, Khutorskoy, M. D., 1999. Gas hydrate accumulation at the Håkon Mosby Mud Volcano, Geo-Marine Letters 19, 57-67.

Grant, J. A., Schreiber, R., 1990. Modern swathe sounding and sub-bottom profiling technology for research applications: The Atlas Hydrosweep and Parasound Systems. Marine Geophysical Researches 12, 9-19.

Grehan, A., Unnithan, V., Guinan, J., Wilson, M, 2004. Fisheries Impact Studies on the Porcupine Seabight and Bank. In: Klages M., Thiede J. and J.-P. Foucher, 2004. The expedition ARK XIX/3 of RV ''Polarstern''. Reports on Polar and Marine Research 488, 143-146.

Gutberlet, M., Schenke, H. W. 1989. Hydrosweep: New era in high precision bathymetric surveying in deep and shallow water. Marine Geodesy 13, 1-23.

Hagen, R., Chakraborty, B., Schenke, H. W., 1994a. Preliminary backscatter results from the Hydrosweep multibeam system. Summary report of the research work accomplished on international scientific cooperation initiatives – Marie Curie Fellowship (application number: 930290), Appendix 2.

Hagen, R. A., Hinze, H., Monk, J., Niederjasper, F., Schenke, H. W., Schöne, T., 1994b. Applied Marine Geodetic Research in Polar Regions. Marine Geodesy 17, 81-94.

Henriet, J.-P., De Mol, B., Pillen, S., Vanneste, M., Van Rooij, D., Versteeg, W., 1998. Gas hydrates crystals may help build reefs. Nature 391, 648-649.

Henriet, J.-P., De Mol, B., Dullo, W., Freiwald, A., Jørgensen, B., Parkes, J., Patching, J., 2000. Modern carbonate mounds on Europe's margin: Preparing the Porcupine Scientific Drilling Project. Eos transactions AGU 81 (48), Fall Meeting 2000, Abstract OS52-H04.

Henriet, J.-P., Guidard, S., and the ODP Proposal 573 Team, 2003. Carbonate Mounds as a possible Example for Microbial Activity in Geological Processes. In: Wefer, G., Billett, D., Hebbeln, D., Jørgensen, B. B., Van Weering, T. C. E., Ocean Margin Systems. Springer, Heidelberg, 439-455.

Hjelstuen, B. O., Eldholm, O., Faleide, J. I. and Vogt, P. R., 1999. Regional setting of Håkon Mosby Mud Volcano, SW Barents Sea margin. Geo-Marine Letters 19, 22-28.

Hovland, M., 2000. Are there commercial deposits of marine hydrates in ocean sediments? Energy Exploration & Exploitation 18, 339-347.

Hovland, M., 2002. On the self-sealing nature of marine seeps. Continental Shelf Research 22, 2387-2394.

Hovland, M., 2005 Pockmark-associated coral reefs at the Kristin field off Mid-Norway. In: Freiwald, A., and Roberts, J. M. (Editors), Cold-water corals and Ecosystems. Springer, Berlin, Heidelberg, 623-632.

Hovland, M., Judd, A., G., 1988. Seabed pockmarks and seepages: impact on geology, biology and the marine environment. Graham & Trotman, London.

Hovland, M., Thomsen, E., 1997. Cold-water corals-are they hydrocarbon seep related? Marine Geology 137, 159-164.

Hovland, M., Risk, M., 2003. Do Norwegian deep-water coral reefs rely on seeping fluids? Marine Geology 198, 83-96.

Hovland, M., Crocker, P. F., Martin, M., 1994. Fault associated sea bed mounds (carbonate knolls) off western Ireland and north-west Australia. Marine and Petroleum Geology 11, 232-246.

Hughes Clarke J. E., 1993. The potential for seabed classification using backscatter from shallow water multibeam sonars. Proceedings of the Institute of Acoustics 15 (part 2), 381-387.

Hughes Clarke, J. E. 1994, Toward remote seafloor classification using the angular response of acoustic backscattering: a case study from multiple overlapping GLORIA data. IEEE Journal of Oceanic Engineering 19, No. 1, 112-127.

Huguen, C., Mascle, J., Chaumillon, E., Kopf, A., Woodside, J., Zitter, T., 2004. Structural setting and tectonic control of mud volcanoes from the Central Mediterranean Ridge (Eastern Mediterranean). Marine Geology 209, Issues 1-4, 245-263.

Huvenne, V. A. I., Blondel, P., Henriet, J.-P., 2002. Textural analyses of sidescan sonar imagery from two mound provinces in the Porcupine Seabight. Marine Geology 189, 323-341.

Huvenne, V. A. I., De Mol, B., Henriet, J.-P., 2003. A 3D seismic study of the morphology and spatial distribution of buried coral banks in the Porcupine Basin, SW of Ireland. Marine Geology, 5-25.

Huvenne, V. A. I., Beyer, A., de Haas, H., Dekindt, K., Henriet, J.-P., Kozachenko, M., Olu-Le Roy, K., Wheeler, A. J., TOBI/Pelogia 197 and CARACOLE cruise participants, 2005. The seabed appearance of different coral bank provinces in the Porcupine Seabight, NE Atlantic: results from sidescan sonar and ROV seabed mapping. In: Freiwald, A. and Roberts, J. M. (Editors), 2005. Cold-water corals and Ecosystems. Springer, Berlin, Heidelberg, 535-569.

Jackson, D. R., Winebrenner, D. P., Ishimary, A., 1986. Application of the composite roughness model to high-frequency bottom backscattering, Journal of the Acoustical Society of America 79 (5), 1410-1422.

Jacops, M., 2002. Analyses of high resolution bathymetric data in the Eltanin Impact Area, Master thesis, Alfred Wegener Institute for Polar and Marine Research, Bremerhaven.

Jerosch, K., Schlüter, M., Foucher, J.-P., 2004a. Geo-Referenced Video-Mosaicking as a Means to GIS-supported Sea Floor Community Mapping at Håkon Mosby Mud Volcano. EGU General Assembly 2004, Nice, France, 25-30 April 2004.

Jerosch, K., Vincent, A. G., Schlüter, M., 2004b. Video Mosaicking on Håkon Mosby Mud Volcano. In: Klages M., Thiede J. and J.-P. Foucher, 2004. The expedition ARK XIX/3 of RV ‘‘Polarstern’’. Reports on Polar and Marine Research 488, 215-220.

Jerosch, K., Schlüter, M., Foucher, J.-P., Allais, A.-G., Klages, M., Edy, C., submitted. Spatial distribution of mud flows and chemoautotrophic communities affecting the methane cycle at Håkon Mosby Mud Volcano. Marine Geology.

Kenyon, N. H., Belderson, R. H., Stride, A. H., 1978. Channels, canyons and slump folds on the continental slope between South-West Ireland and Spain. Oceanologica Acta 1, 369-379.

Kenyon, N. H., Ivanov, M. K., Akhmetzhanov, A. M. (Editors), 1998. Cold water carbonate mounds and sediment transport on the Northeast Atlantic margin. IOC Technical Series 52. UNESCO.

Kenyon, N. H., Ivanov, M. K., Akhmetzhanov, A. M. (Editors), 1999. Geological Processes on the Northeast Atlantic margin. IOC Technical Series 54. UNESCO.

Kenyon, N. H., Akhmetzhanov, A. M., Wheeler, A. J., Van Weering, T. C. E, de Haas, H., Ivanov, M. K., 2003. Giant carbonate mud mounds in the southern Rockall Trough. Marine Geology 195, 5-30.

Klages M., Thiede J. and J.-P. Foucher, 2004. The expedition ARK XIX/3 of RV ‘‘Polarstern’’. Reports on Polar and Marine Research 488.

Kohl, B. and Roberts, H. H., 1994. Fossil foraminifera from four active mud volcanoes in the Gulf of Mexico. Geo-Marine Letters 14, 126-134.

Kopf, A. K., 2002. Significance of mud volcanism, Reviews of Geophysics 40(2), 1005, doi: 10.1029/2000RG000093.

Kozachenko, M., Wheeler, A., Beyer, A., Blamart, D., Masson, D., Olu-Le Roy, K., 2002. A four dimensional perspective of the sedimentary processes and their interactions with Ireland’s deep-water coral carbonate mound ecosystems: Belgica Carbonate Mound province, eastern Porcupine Seabight, NE Atlantic. Geophysical Research Abstracts, Vol. 4, EGS 27th General Assembly, Abstract EGS02-A-02529.

Kuhn, G., in preparation. The Expedition ANTARKTIS-XVII/4 of RV „Polarstern“ 2000. Reports on Polar and Marine Research.

Kuhn, G., Weber, M. E., 1993. Acoustical characterization of sediments by Parasound and 3.5 kHz systems: Related sedimentary processes on the southeastern Weddell Sea continental slope, Antarctica. Marine Geology 113, 201-217.

Kulm, L. D., Suess, E., Moore, J. C., Carson, B., Lewis, B. T., Ritger, S. D., Kadko, D. C., Thornburg, T. M., Embley, R. W., Rugh, W. D., Massoth, G. J., Langseth, M. G., Cochrane, G. R., and

Scamman, R. L., 1986. Oregon subduction zone: venting, fauna, and carbonates. Science 231, 561-566.

Lampitt, R. S., 1985. Evidence for the seasonal deposition of detritus to the deep-sea floor and its subsequent resuspension. Deep Sea Research 32(8), 885-897.

Lemke, P., 2003. The Expedition ARKTIS XVIII/1 a, b of the Research Vessel „Polarstern“ in 2002. Reports on Polar and Marine Research 446.

Levin, L. A., Ziebis, W., Mendoza, G. F., Growney, V. A., Tryon, M. D., Brown, K. M., Mahn, C., Gieskes, J. M., Rathburn, A. E., 2003. Spatial heterogeneity of macrofauna at northern California methane seeps: influence of sulphide concentration and fluid flow. Marine Ecology Progress Series 265, 123-139.

Lurton, X., 2002. An introduction to underwater acoustics, principles and applications. Springer, Praxis Publishing.

MacDonald, I. R., Boland, G. S., Baker, J. S., Brooks, J. M., Kennicutt II, M. C., Bidigare, R. R., 1989. Gulf of Mexico hydrocarbon seep communities: II. Spatial distribution of seep organisms and hydrocarbons at Bush Hill. Marine Biology 101, 235-247.

Masson, D. G., Miles, P. R., 1986. Structure and development of Porcupine Seabight Sedimentary Basin, offshore southwest Ireland. The American Association of Petroleum Geologists Bulletin 70, No. 5, 536-548.

Medwin, H., Clay, C. S., 1998. Fundamentals of Acoustical Oceanography. Academic Press, London.

Mienert, J., Berndt, C., Laberg, J. S., Vorren, T. O., 2003. Slope Instability of Continental Margins. In: Wefer, G., Billett, D., Hebbeln, D., Jørgensen, B. B., Van Weering, T. C. E., 2003. Ocean Margin Systems. Springer, Heidelberg, 179-193.

Milkov, A. V., 2000. Worldwide distribution of submarine mud volcanoes and associated gas hydrates. Marine Geology 167, 29-42.

Milkov, A. V., Vogt, P., Cherkashev, G., Ginsburg, G., Chernova, N. and Andriashev, A., 1999. Sea floor terrains of Håkon Mosby Mud Volcano as surveyed by deep-tow video and still photography. Geo-Marine Letters 19, 38–47.

Milkov, A. V., Sassen, R., Apanasovich, T. V., Dadashev, F. G., 2003. Global gas flux from mud volcanoes: A significant source of fossil methane in the atmosphere and the ocean. Geophysical Research Letters 30 (2), 1037, doi:10.1029/2002GL016358.

Milkov, A. V., Vogt, P. R., Crane, K., Lein, A. Y., Sassen, R. and Cherkashev, G. A., 2004. Geological, geochemical, and microbial processes at the hydrate-bearing Håkon Mosby mud volcano: a review. Chemical Geology 205, 347-366.

Millero, F. J., Chen, C-T., Bradshaw, A. and Schleicher, K., 1980. A new high pressure equation of state for seawater. Deep Sea Research 27A, 255-264.

Mitchell, N. C., Somers, M. L., 1989. Quantitative measurements with a long-range side-scan sonar. IEEE Journal of Oceanic Engineering 14, No. 4, 368-374.

de Moustier, C., 1986. Beyond bathymetry : Mapping acoustic backscattering from deep seafloor with Sea Beam. Journal of the Acoustical Society of America 79 (2), 316-331.

de Moustier, C., Kleinrock, M. C., 1986. Bathymetric artifacts in Sea Beam data: How to recognize them and what causes them. Journal of Geophysical Research 91, 3407-3424.

de Moustier, C., Alexandrou, D., 1991. Angular dependence of 12-kHz seafloor acoustic backscatter. Journal of the Acoustical Society of America 90 (1), 522-531.

de Moustier, C., Matsumoto, H., 1993. Seafloor acoustic remote sensing with multibeam echo-sounders and bathymetric sidescan sonar systems. Marine Geophysical Researches 15, 27-42.

MPL, 1991. Derivation of seafloor acoustic backscatter strength from data recorded with the Hydrosweep DS echo-sounder using the NRGCOR software package. Marine Physical Laboratory, Scripps Institution of Oceanography, La Jolly, CA 92093-0205, internal report.

Pimenov, N., Savvichev, A., Rusanov, I., Lein, A., Egorov, A., Gebruk, A., Moskalev, L. and Vogt, P., 1999. Microbial processes of carbon cycle as the base of food chain of Håkon Mosby Mud Volcano benthic community. Geo-Marine Letters 19, 89-96.

Pimenov, N. V., Savvichev, A. S., Rusanov, I. I., Lein, A. Y., Ivanov, M. V., 2000. Microbiological processes of the carbon and sulphur cycles at cold methane seeps of the North Atlantic. Microbiology 69, 709-720.

Preston, J. M., Christney, A. C., Beran, L. S., Collins, W. T., 2004. Statistical seabed segmentation – from images and echoes to objective clustering. In: Simons, D. G. (Editor), 2004. Proceedings of the

Seventh European Conference on Underwater Acoustics. ECUA 2004, Delft, The Netherlands, 5-8 July 2004, Vol. 2, 813-818.

Rice, A. L., Billet, D. S. M., Thurston, M. H., Lampitt, R. S., 1991. The Institute of Oceanographic Sciences biology programme in the Porcupine Seabight: background and general introduction. Journal of the Marine Biological Association of the UK 71, 281-310.

Sauter, E., Baumann, L., Harms, Hohmann, C., Kolar, Queric, Schewe, I., Soltwedel, T., Wegner, J. and Wisotzki, 2003. Geochemical and biological investigations at Håkon Mosby Mud Volcano, in: Lemke, P. (Editor), 2003. The Expedition ARKTIS XVIII/1 a, b of the Research Vessel ‘‘Polarstern’’ in 2002. Reports on Polars and Marine Research 466, 75-80.

Sauter, E. J., Muyakshin, S. I., Charlou, J.-L., Schlüter, M., Boetius, A., Jerosch, K., Damm, E., Foucher, J.-P., Klages, M., 2006. Methane discharge from a deep-sea submarine mud volcano into the upper water column by gas hydrate-coated methane bubbles. Earth and Planetary Science Letters, doi:10.1016/j.epsl.2006.01.041.

Schlitzer, R., 2003. Ocean Data View, http://www.awi-bremerhaven.de/GEO/ODV.

Sea-Bird. General Specification. Sea-Bird Electronics Inc., Washington, DC.

Sea-Bird, 2001. Users Manual. Sea-Bird Electronics Inc., Washington, DC.

Shilov, V. V., Druzhinina, N. I., Vasilenko, L. V. and Krupskaya, V. V., 1999. Stratigraphy of sediments from the Håkon Mosby Mud Volcano Area. Geo-Marine Letters 19, 48-56.

Sibuet, M., Olu, K., 1998. Biogeography, biodiversity and fluid dependence of deep-sea cold-seep communities at active and passive margins. Deep-Sea Research II 45, 517-567.

Simons, D. G., 2004. Proceedings of the Seventh European Conference on Underwater Acoustics. ECUA 2004, Delft, The Netherlands, 5-8 July 2004.

Smith, W. H. F., Sandwell, D. T., 1997. Global Sea Floor Topography from Satellite Altimetry and Ship Depth Soundings. Science Magazine 277, issue 5334, 1956-1962.

Shannon, P.M., 1991a. The development of Irish offshore sedimentary basins. Journal of the Geological Society, London, 148, 181-189.

Shannon, P. M., 1991b. Irish offshore basins: geological development and petroleum plays. In: Spencer, A. M. (Editor), 1991. Generation, accumulation, and production of Europe’s hydrocarbons. Special Publication of the European Association of Petroleum Geoscientists, No. 1, 99-109, Oxford University press, Oxford.

Suess, E. M., Torres, M. E., Bohrmann, G., Collier, R. W., Greinter, J., Linke, P., Rehter, G., Trehu, A. M., Wallmann, K., Winckler, G., and Zulegger, E., 1999. Gas hydrate destabilization: enhanced dewatering, benthic material turnover, and large methane plumes at the Cascadia convergent margin. Earth and Planetary Science Letters 170, 1-15.

Sumida, P., Kennedy, R., 1998. Porcupine Seabight – biological data. In: Kenyon, N. H., Ivanov, M. K., Akhmetzhanov, A. M. (Editors), 1998. Cold water carbonate mounds and sediment transport on the Northeast Atlantic margin. IOC Technical Series 52. UNESCO, 102-106.

Swennen, R., Cronin, B., Ivanov, M., Kozlova, E., Wheeler, A. J., Akhmetzhanov, A., Sautkin, A., Van Rooij, D., Zaragosi, S., Mazurenko, L., Degryse, C., Sumida, P., Satur, N., Kennedy, R., Akhmanov, G., Belenkaya, I., Pillen, S., Naumov, Y., Stadtnitskaya, A., De Mol, B., Balashova, A., Saprykina, A., 1998. Bottom sampling results. In: Kenyon, N. H., Ivanov, M. K., Akhmetzhanov, A. M. (Editors), 1998. Cold water carbonate mounds and sediment transport on the Northeast Atlantic margin. IOC Technical Series 52. UNESCO, 59-97.

Thissot, B. P., Welte, D. H., 1984. Petroleum formation and occurrence. Second revised and enlarged edition, Springer, Berlin, Heidelberg, New York, Tokyo.

Thomson, C.W., 1873. The Depths of the Sea. MacMillan, London.

Tudhope, A. W., Scoffin, T. P., 1995. Processes of sedimentation in Gollum Channel Porcupine Seabight: Submersible observations and sediment analyses. Transactions of the Royal Society of Edinburgh: Earth Sciences 86, 49-55.

Urick, R.J., 1983, Principles of Underwater Sound. Third edition, McGraw-Hill, New York.

Urban, H. G., 2002. Handbuch der Wasserschalltechnik. 2. Auflage, STN Atlas Elektronik GmbH, Bremen.

Van Rooij, D., De Mol, B., Huvenne, V., Ivanov, M., Henriet, J.-P., 2003. Seismic evidence of current-controlled sedimentation in the Belgica mound province, upper Porcupine slope, southwest of Ireland. Marine Geology 195, 31-53.

Van Walree, P. A., Tegowski, J., Laban, C., Simons, D. G., 2005. Acoustic seafloor discrimination with echo shape parameters: A comparison with the ground truth. Contionental Shelf Research 25, 2273-2293, doi:10.1016/j.csr.2005.09.002

Van Weering, T. C. E, Dullo, C., Henriet, J.-P., 2003a. An introduction to geosphere-biosphere coupling; cold seep related carbonate and mound formation and ecology. Marine Geology, 198, 1–3.

Van Weering, T. C. E., de Haas, H., de Stigter, H. C., Lykke-Andersen, H., Kouvaev, I., 2003b. Structure and development of giant carbonate mounds at the SW and SE Rockall Trough margis, NE Atlantic Ocean. Marine Geology 198, 67-81.

Vogt, P. R., Crane, K., Pfirman, S., Sundvor, E., Cherkis, N., Fleming, H., Nishimura, C. and Shor, A., 1991. SeaMARC II sidescan sonar imagery and swath bathymetry in the Nordic Basin, Eos 72, 486.

Vogt, P. R., Cherkashev, G., Ginsburg, G., Ivanov, G., Milkov, A., Crane, K., Lein, A., Sundvor, E., Pimenov, N. and Egorov, A., 1997, Håkon Mosby mud volcano provides unusual example of venting, Eos 78, 549–557.

Vogt, P. R., Crane, K., Sundvor, E., Hjelstuen, B. O., Gardner, J., Bowles, F. and Cherkashev, G., 1999a, Ground-truthing 11 to 12 kHz side-scan imagery in the Norwegian-Greenland Sea: Part II: Probable diapirs on the Bear Island fan slide valley margins and the Vøring Plateau. Geo-Marine Letters 19, 111-130.

Vogt, P. R., Gardner, J. and Crane, K., 1999b. The Norwegian-Barents-Svalbard (NBS) continental margin: introducing a natural laboratory of mass wasting, hydrates, and ascent of sediment, pore water, and methane. Geo-Marine Letters 19, 2-21.

Welte, D. H., Horsfield, B., Baker, D. R. (Editors), 1996. Petroleum and basin Evolution – Insights from Petroleum Geochemistry, Geology and basin Modeling. Springer, Berlin.

Wheeler, A. J., Degryse, C., Limonov, A., Kenyon, N. H., 1998. OREtech sidescan sonar data. In: Kenyon, N. H., Ivanov, M. K., Akhmetzhanov, A. M. (Editors), 1998. Cold water carbonate mounds and sediment transport on the Northeast Atlantic margin. IOC Technical Series 52. UNESCO, 40-58.

Wheeler, A. J., Bett, B. J., Billet, D. S. M., Masson, D. G., 2000. High resolution side-scan mapping of deep-water coral mounds: surface morphology and processes affecting growth. Eos transactions AGU, 81 (48), Fall Meeting 2000, Abstract OS61B-16.

Wheeler, A. J., Kenyon, N. H., Ivanov, M. K., Beyer, A., Cronin, B. T., McDonnell, A., Schenke, H. W., Akhmetzhanov, A. M., Satur, N., Zaragosi, S., 2003. Canyon heads and channel architecture of the Gollum Channel, Porcupine Seabight. In: Mienert, J. & Weaver, P. (Editors), European margin sediment dynamics: side-scan sonar and seismic images. Springer, Berlin, 183-186.

Wheeler, A. J., Kozachenko, M., Beyer, A., Foubert, A., Huvenne, V. A. I., Klages, M., Masson, D. G., Olu-Le Roy, K., Thiede, J., 2005. Sedimentary processes and carbonate mounds in the Belgica Mound province, Porcupine Seabight, NE Atlantic. In: Freiwald, A. and Roberts, J. M. (Editors), 2005. Cold-water corals and Ecosystems. Springer, Berlin, Heidelberg, 571-603.

Wheeler, A. J., Beyer, A., Crocker, P., Freiwald, A., Geogheghan, M., de Haas, H., Huvenne, V. A. I., Kozachenko, M., Masson, D. S. M., Schenke, H. W., White, M., submitted. The environmental context of carbonate mounds on the NW European Margin. International Journal of Earth Sciences.

Winkler, A., 2005. Analyse der physikalischen Eigenschaften von Multicorer-Sedimentproben aus dem Gebiet der Porcupine Bucht und deren Einfluss auf die akustische Rückstreuung. Diploma thesis, Alfred Wegener Institute for Polar and Marine Research, Bremerhaven.